Remarks

Claims 18 and 26 are pending. Support for the amendment to claim 18 can be found in canceled claim 25.

In the Office Action dated March 10, 2005, the Examiner states that claims 18 and 25-26 are rejected under 35 U.S.C. 112, first paragraph, as failing to comply with the written description requirement. The Examiner objects to the phrase "wherein the subject is not a rat." The applicant respectfully traverses this rejection. However, in an effort to forward prosecution, applicant has removed this phrase from the claim. Therefore, Applicant respectfully requests withdrawal of this rejection.

The Examiner has rejected claims 18 and 25-26 under 35 U.S.C. 103(a) as being unpatentable over Luo et al. in view of Zhang et al. The applicant respectfully traverse this rejection, and offer the following arguments in response.

The Luo publication demonstrates that galanin inhibits spinal cord electrical hyper-excitability for 60 minutes following nerve section (see Figure 3), at which point the animals were sacrificed. Galanin was administered 30 minutes before the nerve injury as a single bolus injection of 2.4nM (low dose) directly into the space surrounding the bottom part of the spinal cord (intrathecal (IT) administration into the lumbar enlargement, see page 163, paragraph headed "Effect of galanin" and Figure 3 of Luo et al.). That is, the galanin is delivered into the cerebrospinal fluid (CSF). The Luo publication deals exclusively with neuropathic pain and spinal cord excitability, not with peripheral nerve regeneration as claimed in the patent application. In fact, there is no evidence of any nerve regeneration in the method and publication

of Luo et al. The mechanism by which the galanin rapidly alters pain activity is most likely by direct modulation of spinal cord neuronal firing rather than at the level of the dorsal root ganglion (DRG).

When damage or injury to sensory or motor nerves (in Luo et al. in the sciatic nerve) occurs, this triggers a cascade of molecular events within the cell bodies of that nerve, the DRG, which in turn attempts to repair the damage and restore the normal function of the nerve, so-called nerve regeneration. The Protein Kinase C (PKC) and MAP Kinase (MAPK) intra-cellular signalling cascades have both been shown to up-regulate after nerve injury and are essential for nerve regeneration (Klinz & Heumann (1995) J. Neurochem. 65:1046-53; Kiryu et al. (1995) Brain Res. Mol. Brain Res. 29:147-56; attached). At the 1996 priority date of the current patent application, no published literature existed to indicate that galanin speeded up nerve regeneration, nor that it activated PKC or MAPK.

It is the Examiner's contention that, in the 90 minutes following the intrathecal administration of galanin into the lumbar enlargement and before the animal was sacrificed, that "...the preliminary beginnings of regeneration..." could have begun and that this is encompassed by claim 18 (page 4 of Office Action, last sentence). The scientific facts do not support this contention. For regeneration to have occurred in the animals used in the experiments of Luo et al. during the 90 minute period before the animals were sacrificed, the galanin would have had to gain access to the cell bodies in the DRG, since this is where the intra-cellular pro-regenerative machinery resides (Terenghi (1994) J. Anatomy (Pt I) 1-14; attached). The only way that galanin, when applied to the space surrounding the bottom part of the spinal cord, could have

reached the cell bodies of the sensory neurons in the DRG which is where "...the preliminary beginnings of regeneration..." would have occurred, is by direct uptake of the galanin by the nerve terminals in the dorsal horn of the spinal cord. It should be noted that the cell bodies of the sensory neurons of the DRG lie outside the central nervous system (CNS), whilst the spinal cord is part of the CNS. The cerebrospinal fluid (CSF) that bathes the spinal cord is not in contact with the DRG and thus galanin could not have reached the DRG by passive diffusion.

There are well documented and active transport mechanisms in sensory neurons that move proteins from the nerve terminals of the spinal cord or the ends of the peripheral axons of the sciatic nerve to the cell bodies in the DRG, termed retrograde transport. A number of these retrograde transport mechanisms for Nerve Growth Factor (NGF) and Horseradish Peroxidase (HRP) have been extensively studied and characterized. There is good agreement between these published papers that the rate at which these retrograde transport processes move proteins from the rat dorsal horn of the spinal cord to the cell body in the DRG is a maximum rate of 7.5 mm/hour (range 2.5 – 7.5 mm/hr, Yip and Johnson, Jr. (1986) J. Neurocytol. 15:789-98; Richardson and Riopelle. (1984) J. Neurosci. 4:1683-9; attached).

The applicant has measured the length of the nerve root (i.e. the part of the nerve that connects the cell bodies of the DRG to the dorsal horn of the spinal cord) from a total of 21 nerve roots which were harvested from the lumbar region of 5 female Sprague-Dawley rats weighing 200-250g (as used in the experiments of Luo et al.). The length of the nerve root was then measured using a calibrated graticule and a dissecting microscope and the mean length was found to be 18.5±0.9 mm (see Declaration from Professor Wynick, attached). This figure is in

good agreement with the findings of Michael et al. (Michael et al. (1997) J. Neurosci. 17:8476-8490; attached) who found the nerve root of adult male Wistar rats (200-400g body weight) to be 17 mm in length. Similarly, Baba et al. (Baba et al. (1999) J. Neurosci. 2:859-867; attached) found the dorsal root to be between 18-20 mm in length in adult male Sprague-Dawley rats weighing 300-350g.

Based on the above findings, assuming the maximum rate of retrograde transport of galanin from the dorsal horn of the spinal cord to the DRG is 7.5 mm/hr and the length of the nerve root between the dorsal horn of the spinal cord and the DRG is at least 17mm in length (Declaration, attached), then the galanin would only have been transported 11.25 mm in the 90 minutes after galanin was administered before the animals were sacrificed (i.e. about two thirds of the way to the DRG). Galanin could not, therefore, have even begun to affect regeneration in the DRG cell bodies by the time the experiment was terminated.

It should also be noted that the concentration of galanin would have immediately and rapidly begun to fall after the administration of the bolus injection of 2.4nM galanin into the lumbar enlargement of the spinal cord. This would have occurred within seconds, as the galanin would immediately be diluted by the CSF and almost immediately would also have started to be degraded by proteolytic enzymes in the CSF (Bedecs et al. (1995) Neuropeptides 29:137-43; attached). Therefore, even in the highly unlikely event that a small proportion of the galanin that was administered by bolus-dose to the spinal cord did reach the DRG by retrograde transport, the final dose would be substantially lower (in the sub-nanomolar range) than that originally administered IT (page 163 and Figure 3 of Luo et al.). In contrast, the dose of galanin

demonstrated to stimulate nerve outgrowth from sensory neurons by direct application in cell culture to the DRG cell body is 100nM galanin (Mahoney et al. (2003) J. Neurosci. 23:416-421; attached). In light of this, the concentration of galanin that would have reached the DRG would have been at least 100-fold lower than that necessary to stimulate regeneration, again making it nearly impossible that galanin could have even begun to affect regeneration in the DRG cell bodies by the time the experiment was terminated.

For these reasons, one of ordinary skill in the art would have no incentive, on reading the Luo publication, to imagine that galanin-induced nerve regeneration of the severed sciatic nerve would have begun during the time period utilized in the experiments of Luo et al. In addition, in light of the Luo et al. disclosure and on reading the disclosure in Zhang et al. that galanin may be suitable for use as an analgesic in humans, one of ordinary skill in the art would have no motivation to administer a galanin agonist in a method for the treatment of peripheral nerve damage, wherein the peripheral nerve damage is treated by nerve regeneration, as claimed in claim 18 as amended.

The applicant therefore requests removal of this basis for rejection and allowance of claims 18 and 26 to issue.

Pursuant to the above amendments and remarks, consideration and allowance of the pending application is believed warranted. The Examiner is invited and encouraged to directly contact the undersigned if such contact may enhance the efficient prosecution of this application to issue.

Credit Card Payment Form PTO-2038 authorizing payment in the amount of $395.00 (Filing Fee)is enclosed. This amount is believed to be correct; however, the Commissioner is hereby authorized to charge any additional fees which may be required, or credit any overpayment to Deposit Account No. 14-0629.

Respectfully submitted,

NEEDLE & ROSENBERG, P.C.

Janell T. Cleveland
Registration No. 53,843

NEEDLE & ROSENBERG, P.C.
Customer Number 23859
(404) 688-0770
(404) 688-9880 (fax)

CERTIFICATE OF EXPRESS MAILING UNDER 37 C.F.R. § 1.8

I hereby certify that this correspondence, including any items indicated as attached or included, is being deposited with the United States Postal Service as First Class Mail in an envelope addressed to: Mail Stop RCE, Commissioner for Patents, P.O. Box 1450, Alexandria, VA 22313-1450 on the date indicated below.

Janell T. Cleveland — June 23, 2005
Date

The Second Galanin Receptor GalR2 Plays a Key Role in Neurite Outgrowth from Adult Sensory Neurons

Sally-Ann Mahoney,[1] Richard Hosking,[1] Sarah Farrant,[1] Fiona E. Holmes,[1] Arie S. Jacoby,[2] John Shine,[2] Tiina P. Iismaa,[2] Malcolm K. Scott,[3] Ralf Schmidt,[4] and David Wynick[1]

[1]University Research Centre for Neuroendocrinology, Bristol University, Bristol BS2 8HW, United Kingdom, [2]The Garvan Institute of Medical Research, Sydney, NSW 2010, Australia, [3]Johnson & Johnson Pharmaceutical Research Institute, Spring House, Pennsylvania 19477-0776, and [4]AstraZeneca R&D Montreal, Montreal, Quebec H4S 1Z9, Canada

Expression of the neuropeptide galanin is markedly upregulated within the adult dorsal root ganglion (DRG) after peripheral nerve injury. We demonstrated previously that the rate of peripheral nerve regeneration is reduced in galanin knock-out mice, with similar deficits observed in neurite outgrowth from cultured mutant DRG neurons. Here, we show that the addition of galanin peptide significantly enhanced neurite outgrowth from wild-type sensory neurons and fully rescued the observed deficits in mutant cultures. Furthermore, neurite outgrowth in wild-type cultures was reduced to levels observed in the mutants by the addition of the galanin antagonist M35 [galanin(1–13)bradykinin(2–9)]. Study of the first galanin receptor (GalR1) knock-out animals demonstrated no differences in neurite outgrowth compared with wild-type animals. Similarly, use of a GalR1-specific antagonist had no effect on neuritogenesis. In contrast, use of a GalR2-specific agonist had equipotent effects on neuritogenesis to galanin peptide, and inhibition of PKC reduced neurite outgrowth from wild-type sensory neurons to that observed in galanin knock-out cultures. These results demonstrate that adult sensory neurons are dependent, in part, on galanin for neurite extension and that this crucial physiological process is mediated by activation of the GalR2 receptor in a PKC-dependent manner.

Key words: galanin; GalR2; dorsal root ganglion; neuritogenesis; nerve injury; protein kinase C

Introduction

To date, the mechanisms and factors that regulate the regeneration of sensory neurons in the adult after peripheral nerve injury remain poorly understood. Damage to a peripheral nerve causes major changes within the cell bodies of the sensory neurons [dorsal root ganglion (DRG)], which are thought to promote regeneration by stimulating neurite outgrowth and enhancing survival of the damaged neuron. Furthermore, injury alters the retrograde flow of target-derived factors to the DRG. Examples of such phenomena include (1) the 120-fold upregulation in the levels of the neuropeptide galanin in the DRG after injury (Hokfelt et al., 1987) and (2) the marked increase in expression of the cytokines leukemia inhibitory factor (LIF) (Banner and Patterson, 1994; Dowsing et al., 1999) and interleukin 6 (IL-6) (Murphy et al., 1995) within Schwann cells at the site of injury and their retrograde transport to the DRG (Curtis et al., 1994). IL-6 and LIF have both been shown to promote axonal regeneration in the adult (Cheema et al., 1994; Hirota et al., 1996; Tham et al., 1997; Cafferty et al., 2001), and IL-6 knock-out mice have deficits in peripheral nerve regeneration after a crush injury to the sciatic nerve (Zhong et al., 1999). Recent data would indicate that LIF and IL-6 (acting through the gp130 coreceptor) may play a role in both injury-induced regeneration and minimizing pathological nociceptive responses by positively regulating the expression of galanin in the DRG (Corness et al., 1996; Thompson et al., 1998).

In the adult, galanin is expressed at low levels in <5% of DRG cells, which are predominantly the small peptidergic C-fiber neurons (Hokfelt et al., 1987). After nerve injury, there is a rapid and robust upregulation of both galanin mRNA and peptide, and expression of the peptide is now observed in 40–50% of all DRG neurons (Villar et al., 1989; Hokfelt et al., 1994). Studies indicate that galanin reduces transmission of sensory information in the spinal cord after nerve injury (Wiesenfeld-Hallin et al., 1989, 1992; Verge et al., 1993). In addition, rising levels of galanin in sensory neurons may also contribute to the initiation and maintenance of axonal regeneration in the injured neurons, leading to functional recovery and restoration of function while minimizing pathological nociceptive responses.

We showed previously that cultured DRG cells from animals homozygous for a targeted mutation in the galanin gene have a 35% reduction in the length of neurites and number of cells that extend neurites (Holmes et al., 2000). In this study, we used a combination of pharmacological and genetic tools to further elucidate the mechanisms by which galanin regulates neuritogenesis. Here, we show that galanin plays a neuritogenic role in adult sensory neurons and rescues the deficits in neurite outgrowth seen in mutant cultures. Furthermore, we demonstrate that its actions are mediated by the second galanin receptor (GalR2) in a PKC-dependent manner.

Materials and Methods

Animals

Galanin knock-out mice. Experiments were performed on 8-week-old female mice homozygous for a targeted mutation in the galanin gene.

Received July 19, 2002; revised Oct. 16, 2002; accepted Oct. 30, 2002.

This work was supported by the Medical Research Council, the Wellcome Trust, National Health and Medical Research Council (Australia), and a Human Science Program short-term fellowship.

Correspondence should be addressed to Prof. David Wynick, University Research Centre for Neuroendocrinology, Bristol University, Marlborough Street, Bristol BS2 8HW, UK. E-mail: d.wynick@bristol.ac.uk.

 0270-6474/03/230416-06$15.00/0

Age-matched wild-type littermates were used as controls in all experiments. Details of the strain and breeding history have been published previously (Wynick et al., 1998; Kerr et al., 2000). In brief, galanin knock-out mice were generated using the E14 cell line. A PGK-*Neo* cassette in reverse orientation was used to replace exons 1–5, and the mutation was bred to homozygosity and has remained inbred on the 129olaHsd strain. All animals were fed standard chow and water *ad libitum*. Animal care and procedures were performed within United Kingdom Home Office protocols and guidelines.

GalR1 knock-out mice. Experiments were performed on 8-week-old female mice that carry an insertional inactivating mutation within the first exon of the gene encoding the murine GalR1. Age-matched wild-type littermates were used as controls. In brief, GalR1 knock-out mice were generated using the W9.5 cell line and have remained inbred on the 129T2/SvEmsJ strain (Jacoby et al., 2002). All animals were fed standard chow and water *ad libitum*. Animal care and procedures were performed according to the Code of Practice of the Australian National Health and Medical Research Council.

DRG culture

Cultures were performed as described previously (Holmes et al., 2000). In brief, animals were killed by cervical dislocation, and DRGs from the lumbar, thoracic, and cervical regions were removed aseptically, trimmed of connective tissue and nerve roots, and pooled in DMEM–F12 medium. Ganglia were subjected to 0.25% collagenase P for 1 hr at 37°C, washed in PBS, and treated enzymatically with trypsin–EDTA for 10 min at 37°C. Ganglia were washed in medium containing trypsin inhibitor and then mechanically dissociated by trituration using a flame-narrowed Pasteur pipette. After centrifugation, cells were resuspended in DMEM–F12 medium supplemented with 5% horse serum, 1 mM glutamine, and 10 ng/ml gentamycin. To enhance the cultures for neurons and eliminate much of the cellular debris, cells were plated on six-well plates coated with 0.5 mg/ml polyornithine and maintained overnight at 37°C in a humidified incubator with 95% air–5% CO_2 (Patrone et al., 1999). Medium was removed and discarded. The neurons were removed from the surface by squirting with a jet of fresh medium. After centrifugation, cells were plated on 24-well plates treated with 0.5 mg/ml polyornithine and 5 μg/ml laminin and maintained for 8 hr at 37°C in a humidified incubator with 95% air–5% CO_2.

Treatments

Cells were cultured in DMEM–F12-supplemented medium as described above with or without the addition of the following chemicals: 1 nM M35 [galanin(1–13)bradykinin(2–9)] (Bachem UK, Essex, UK), 100 nM galanin peptide (Bachem UK), 10 μM bisindolylmaleimide I (BIM) (Calbiochem, La Jolla, CA), 10 nM RWJ-57408 [2,3-dihydro-2-(4-methyl-phenyl)-1,4-dithiepine-1,1,4,4-tetroxide] (Johnson & Johnson, Spring House, PA), and 100 nM AR-M961 ([Sar(1), D-Ala^{12}]Gal(1–16)-NH_2) or AR-M1896 [Gal(2–11)Trp-Thr-Leu-Asn-Ser-Ala-Gly-Tyr-Leu-Leu-NH_2] (AstraZeneca, Montreal, Quebec, Canada).

Data analysis

Cultures were washed with PBS and fixed with 4% paraformaldehyde for 20 min at room temperature. Cells were visualized by phase-contrast microscopy. The percentage of cells bearing neurites and neurite length were both measured using NIH Image (Scion, Frederick, MD). Data are presented as mean ± SEM.

Results

Galanin signaling mediates neurite outgrowth

The addition of 100 nM galanin to wild-type adult DRG cells significantly increased the length of neurites (Fig. 1*B*), whereas the percentage of cells producing neurites was unchanged (Fig. 1*A*), suggesting that the number of cells capable of extending neurites was already at maximum under these culture conditions. Addition of 100 nM galanin peptide to mutant cultures fully rescued the deficits in the percentage of cells producing neurites and restored neurite length to wild-type levels.

We substantiated this putative neuritogenic role in the adult further by using the potent galanin antagonist M35 (Bartfai et al., 1992), which acts at all known galanin receptor subtypes (Wiesenfeld-Hallin et al., 1993). The addition of 1 nM M35 to wild-type cultures produced a significant 35% reduction in both the percentage of cells bearing neurites (Fig. 2*A*) and neurite length (Fig. 2*B*) to levels observed in mutant cultures. No effect was seen on either parameter in mutant cultures. This dose of M35 has been shown previously to have purely antagonistic effects (Wiesenfeld-Hallin et al., 1992; Ogren et al., 1993).

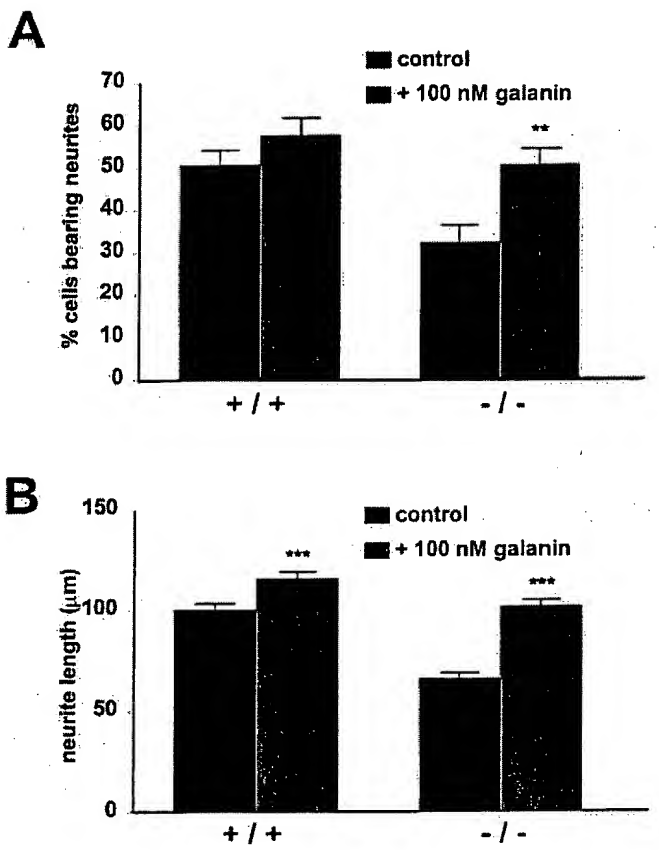

Figure 1. The percentage of cells bearing neurites (*A*) and length of neurite outgrowth (*B*) from dissociated DRG cultures isolated from wild-type and galanin knock-out animals in the presence and absence of 100 nM galanin peptide 8 hr after plating. Addition of 100 nM galanin to wild-type cultures significantly increased neurite length, whereas there was no significant difference in the percentage of cells producing neurites. However, addition of 100 nM galanin to galanin knock-out cultures significantly increased both the percentage of cells producing neurites and the length of neurites. Data are presented as percentage of cells bearing neurites or mean ± SEM length (*t* test; $^{**}p < 0.01$; $^{***}p < 0.001$; $n = 5$).

The neuritogenic role of galanin is not mediated by GalR1

To determine whether the GalR1 receptor subtype is important in mediating the neuritogenic effects of galanin, we first used the small-molecule, nonpeptide GalR1-specific antagonist RWJ-57408 (Scott et al., 2000). The addition of 10 nM RWJ-57408 had no effect on the percentage of cells bearing neurites in either wild-type or mutant cultures (Fig. 3*A*). Similar results were seen with the addition of 1 nM RWJ-57408 (data not shown).

To study the role of GalR1 in mediating neuritogenesis further, we studied neurite outgrowth in GalR1 knock-out mouse dissociated DRG cultures (Jacoby et al., 2002). No differences were observed in the percentage of GalR1 mutant cells bearing neurites compared with those from wild-type controls (Fig. 3*B*).

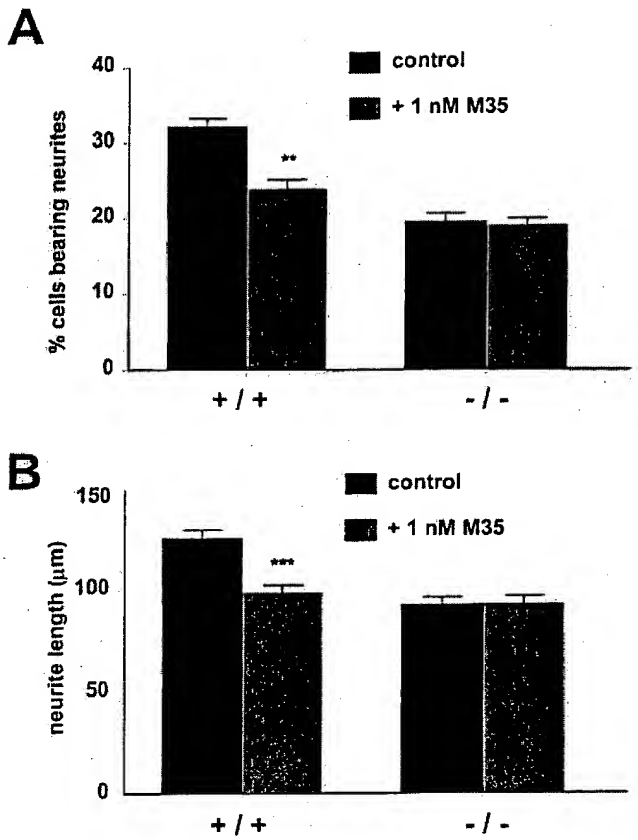

Figure 2. The percentage of cells bearing neurites (*A*) and length of neurite outgrowth (*B*) from dissociated DRG cultures isolated from wild-type and galanin knock-out animals in the presence and absence of 1 nM M35 8 hr after plating. In both cases, significant deficits were noted in the wild-type cultures, whereas no effect was seen in the knock-out cultures. Data are presented as percentage of cells bearing neurites or mean ± SEM length (*t* test; $^{**}p < 0.01$; $^{***}p < 0.001$; $n = 5$).

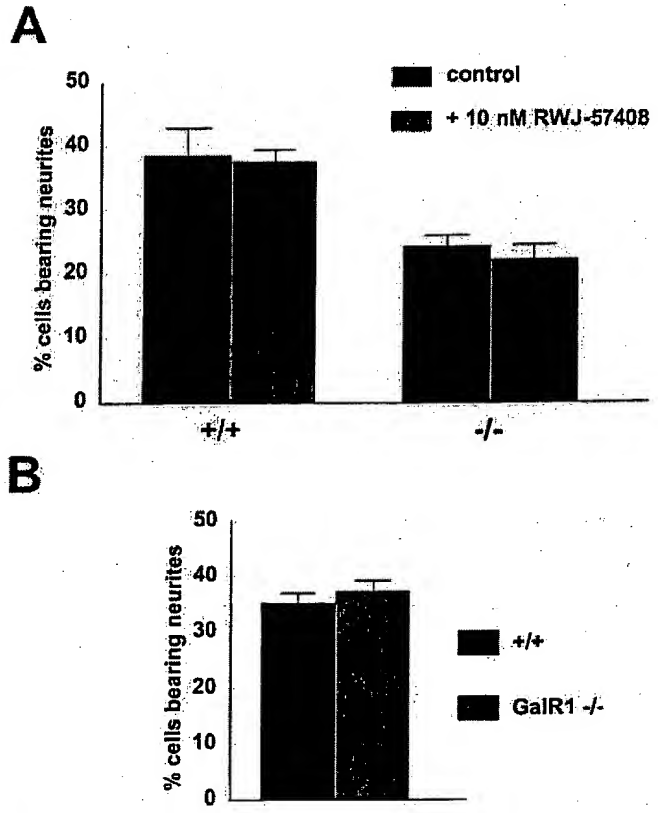

Figure 3. *A*, The percentage of cells bearing neurites from dissociated DRG cultures isolated from wild-type and galanin knock-out animals in the presence and absence of 10 nM RWJ-57408 8 hr after plating. *B*, The percentage of cells bearing neurites from dissociated DRG cultures isolated from wild-type and GalR1 knock-out animals 8 hr after plating. Data are presented as percentage of cells bearing neurites ± SEM ($n = 5$).

Furthermore, there was no significant difference in neurite length between cells from wild-type controls (140.8 ± 9 μm) and GalR1 mutant cells (161.6 ± 8 μm).

The neuritogenic role of galanin is mediated by GalR2 in a PKC-dependent manner

We next studied whether GalR2 might be responsible for transducing the neuritogenic actions of galanin by using the newly described peptide analog AR-M1896, a selective GalR2 agonist (Liu et al., 2001). In addition, we studied the actions of AR-M961, which has been shown to have agonistic actions at both GalR1 and GalR2 subtypes (Liu et al., 2001). The addition of 100 nM AR-M1896 or AR-M961 fully rescued the deficits in percentage outgrowth seen in the mutant cultures to wild-type levels (Fig. 4*A*) and appeared to be equipotent to galanin (Fig. 1*A*). Similarly, the addition of either AR-M961 or AR-M1896 to wild-type cultures increased both the percentage of cells bearing neurites and neurite length to the same extent as that observed with galanin peptide (Fig. 4*A*,*B*).

To investigate whether the neuritogenic role of galanin was PKC dependent, we used the PKC-specific inhibitor bisindolylmaleimide I (GF109203X) (Rivera-Bermudez et al., 2002). Addition of 10 μM BIM to wild-type cultures significantly reduced the percentage of cells bearing neurites to the levels observed in galanin knock-out cultures; similar results were seen using 1 μM BIM (data not shown). Furthermore, 10 μM BIM completely abolished the stimulatory neuritogenic actions of 100 nM AR-M1896 on both wild-type and mutant cultures (Fig. 4*C*).

Discussion

Damage to a peripheral nerve induces major and long-lasting changes in the expression of many secreted ligands and their receptors within the sensory neurons of the DRG. One of the most striking changes that occurs is the 120-fold increase in the expression of the neuropeptide galanin. We showed recently that galanin plays an important role in the survival of a subset of DRG neurons (Holmes et al., 2000), with a 2.8- and 2.6-fold increase in the number of apoptotic cells in the DRG of galanin knock-out mice at postnatal day 3 (P3) and P4, respectively, compared with wild-type controls. This wave of apoptosis at P3 is associated with a 13% decrease in total cell number within the DRG (Holmes et al., 2000). The role of galanin in cell survival is further substantiated by the finding that galanin is essential for the developmental survival of one-third of the cholinergic neurons of the basal forebrain (O'Meara et al., 2000).

The role played by galanin in the survival of this subset of DRG neurons seems to be preferentially biased toward the small peptidergic neurons, which are most likely to be nociceptors (Holmes et al., 2000). The loss of these small unmyelinated neurons may provide an explanation for the finding that galanin knock-out animals demonstrate a decrease in chronic neuropathic pain behavior after nerve injury (Kerr et al., 2000). Many of the animal models of peripheral nerve injury that induce neuropathic pain behavior are also associated with an upregulation

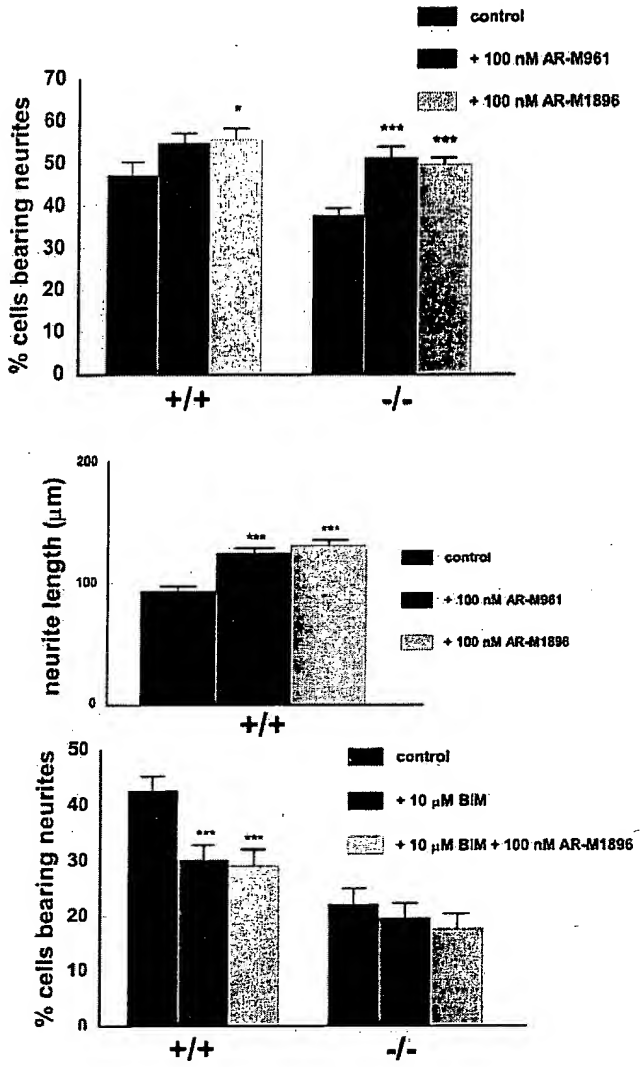

Figure 4. *A*, The percentage of cells bearing neurites from dissociated DRG cultures isolated from wild-type and galanin knock-out animals in the presence and absence of 100 nM AR-M961 or AR-M1896 8 hr after plating. The addition of either AR-M961 or AR-M1896 rescued the deficits in percentages of cells producing neurites seen in galanin knock-out cultures to near wild-type levels. Addition of AR-M1896 to wild-type cultures significantly increased the percentage of cells bearing neurites compared with controls. Although addition of AR-M961 increased the percentage, this was not significant. *B*, The length of neurite outgrowth from dissociated DRG cultures isolated from wild-type animals in the presence and absence of 100 nM AR-M961 or AR-M1896 8 hr after plating. Addition of either AR-M961 or AR-M1896 significantly increased neurite length. *C*, The percentage of cells bearing neurites from dissociated DRG cultures isolated from wild-type and galanin knock-out animals in the presence and absence of 10 μM BIM or 10 μM BIM plus AR-M1896. Significant deficits are seen in the number of cells producing neurites in wild-type cultures in the presence of 10 μM BIM, which was not rescued by the addition of 100 nM AR-M1896. Addition of 10 μM BIM had no effect on mutant cultures. Data are presented as percentage of cells bearing neurites or mean ± SEM length (*t* test; $*p < 0.05$; $***p < 0.001$; $n = 5$).

in galanin within the DRG neurons (Hokfelt et al., 1987; Villar et al., 1989; Nahin et al., 1994; Ma and Bisby, 1997). Furthermore, there appears to be a direct correlation between the extent and duration of pain behavior and the level of galanin upregulation (Ma and Bisby, 1997; Murphy et al., 1999).

The data presented here using galanin peptide or the potent galanin antagonist M35, which acts at all known galanin receptor subtypes (Wiesenfeld-Hallin et al., 1993), demonstrates that galanin is acting as a neuritogenic factor in the adult. Approximately one-third of neurite outgrowth in DRG cultures is dependent on the tonic release of galanin, implying that the developmental trophic–survival role is recapitulated in the adult after injury. At present, it is not possible to state whether there is a definite relationship between the early postnatal loss of a subset of small peptidergic neurons in the galanin knock-out animals and the reduced rate of neurite outgrowth in dispersed DRG cultures isolated from adult galanin knock-out animals. However, the finding that the deficits in neurite outgrowth that we identified in the adult galanin knock-outs are fully rescued by the addition of exogenous galanin would imply that the effects in the adult are independent of the developmental loss.

To date, three G-protein-coupled galanin receptor subtypes have been identified. GalR1 is expressed in the large-diameter neurons of the DRG, and GalR2 is expressed predominantly by the small- and medium-sized neurons. Only 5% of DRG neurons appear to express both receptor subtypes (Sten Shi et al., 1997). There have been contradictory reports as to whether GalR3 is expressed at all within the DRG. Studies using solution hybridization–RNase protection assays suggested that GalR3 is expressed at very low levels (Waters and Krause, 2000). However, other studies, again using solution hybridization–RNase protection assay (Smith et al., 1998), show no GalR3 present within the DRG; furthermore, no GalR3 has been detected in the DRG using riboprobe *in situ* hybridization (Mennicken et al., 2001). It is therefore unlikely that GalR3 plays a major role in neuritogenesis in the DRG.

Here, we demonstrate that addition of the small-molecule, nonpeptide GalR1-specific antagonist RWJ-57408 had no effect on neurite outgrowth in either wild-type or mutant cultures, suggesting that the role of galanin in neuritogenesis is not mediated via the GalR1 receptor subtype. This finding was substantiated by the finding that there was no difference in neurite outgrowth from GalR1 knock-out mice compared with wild-type controls. Furthermore, recent data using two separate *in vivo* models show that peripheral nerve regeneration is unaffected in GalR1 knock-out animals (Jacoby et al., 2002). These data therefore suggest that GalR1 does not mediate the neuritogenic or proregenerative effects of galanin in the DRG, implying that GalR2 is the predominant effector.

In this study, we used the galanin receptor agonists AR-M1896 and AR-M961 (Liu et al., 2001; Ma et al., 2001). AR-M1896 is a GalR2-specific agonist with an IC_{50} of 1.76 nM at rat GalR2 and 879 nM at human GalR1, whereas AR-M961 has been shown to have agonistic activity at both GalR2 and GalR1, with an IC_{50} of 1.74 nM and 0.403 nM, respectively (Liu et al., 2001). The data presented here demonstrate that both AR-M961 and AR-M1896 have positive effects on neuritogenesis and fully rescued deficits seen in the mutant cultures. Because our experiments using RWJ-57408 and GalR1 knock-out animals indicate that neurite outgrowth is not mediated via the GalR1 receptor, the agonistic action of AR-M961 on neurite outgrowth must be caused by activation of the GalR2 subtype, which is confirmed by the actions of the GalR2-specific agonist AR-M1896 (Liu et al., 2001).

The binding of galanin to GalR1 and GalR3 inhibits adenylyl cyclase (Habert-Ortoli et al., 1994; Smith et al., 1998; Wang et al., 1998), whereas binding to GalR2 stimulates principally phospholipase C activity (Fathi et al., 1997; Howard et al., 1997; Wang et al., 1997). Studies have shown that the G-protein-coupling profiles of GalR1 and GalR2 are distinct. GalR1 couples only to G_i, whereas GalR2 couples to G_i, G_o, and G_q (Wang et al., 1998). The G_i-mediated pathway is independent of PKC activity. In contrast, both the G_o- and G_q-mediated mitogen-activated protein kinase

signaling pathways are dependent on PKC activity (Hawes et al., 1996). Here, we demonstrate by use of the PKC-specific inhibitor BIM that the neuritogenic action of galanin is PKC dependent, which is consistent with activation of either the G_o- or G_q-mediated signaling pathways.

In summary, these results show that galanin is an important factor in neurite extension of adult sensory neurons and that this process is mediated by activation of GalR2 in a PKC-dependent manner. The role of GalR2 as a mediator of the proliferative effect of galanin is substantiated by previous findings in small-cell lung cancer cells (Wittau et al., 2000) and the pituitary (Wynick et al., 1993, 1998). Furthermore, previous studies have shown that the antiallodynic effect of galanin on neuropathic pain is mediated via GalR1 (Liu et al., 2001), whereas here we show that the neuritogenic role of galanin is mediated via GalR2. These results suggest that different receptor subtypes may be responsible for mediating the differing physiological roles of galanin in the adaptive response of the PNS to injury. Although few data are available on human galanin expression, it appears to have an expression pattern in the DRG similar to that of the rodent (Marti et al., 1987; Suburo et al., 1992). These findings have important implications for the potential therapeutic treatment of some peripheral sensory neuropathies by the use of selective GalR2 agonists.

References

Banner LR, Patterson PH (1994) Major changes in the expression of the mRNAs for cholinergic differentiation factor/leukemia inhibitory factor and its receptor after injury to adult peripheral nerves and ganglia. Proc Natl Acad Sci USA 91:7109–7113.

Bartfai T, Fisone G, Langel U (1992) Galanin and galanin antagonists: molecular and biochemical perspectives. Trends Pharmacol Sci 13:312–317.

Cafferty WB, Gardiner NJ, Gavazzi I, Powell J, McMahon SB, Heath JK, Munson J, Cohen J, Thompson SW (2001) Leukemia inhibitory factor determines the growth status of injured adult sensory neurons. J Neurosci 21:7161–7170.

Cheema SS, Richards L, Murphy M, Bartlett PF (1994) Leukemia inhibitory factor prevents the death of axotomised sensory neurons in the dorsal root ganglia of the neonatal rat. J Neurosci Res 37:213–218.

Corness J, Shi TJ, Xu ZQ, Brulet P, Hokfelt T (1996) Influence of leukemia inhibitory factor on galanin/GMAP and neuropeptide Y expression in mouse primary sensory neurons after axotomy. Exp Brain Res 112:79–88.

Curtis R, Scherer SS, Somogyi R, Adryan KM, Ip NY, Zhu Y, Lindsay RM, DiStefano PS (1994) Retrograde axonal transport of LIF is increased by peripheral nerve injury: correlation with increased LIF expression in distal nerve. Neuron 12:191–204.

Dowsing BJ, Morrison WA, Nicola NA, Starkey GP, Bucci T, Kilpatrick TJ (1999) Leukemia inhibitory factor is an autocrine survival factor for Schwann cells. J Neurochem 73:96–104.

Fathi Z, Cunningham AM, Iben LG, Battaglino PB, Ward SA, Nichol KA, Pine KA, Wang J, Goldstein ME, Iismaa TP, Zimanyi IA (1997) Cloning, pharmacological characterization and distribution of a novel galanin receptor. Brain Res Mol Brain Res 51:49–59.

Habert-Ortoli E, Amiranoff B, Loquet I, Laburthe M, Mayaux JF (1994) Molecular cloning of a functional human galanin receptor. Proc Natl Acad Sci USA 91:9780–9783.

Hawes BE, Luttrell LM, van Biesen T, Lefkowitz RJ (1996) Phosphatidylinositol 3-kinase is an early intermediate in the G beta gamma-mediated mitogen-activated protein kinase signaling pathway. J Biol Chem 271:12133–12136.

Hirota H, Kiyama H, Kishimoto T, Taga T (1996) Accelerated nerve regeneration in mice by upregulated expression of interleukin (IL) 6 and IL-6 receptor after trauma. J Exp Med 183:2627–2634.

Hokfelt T, Wiesenfeld-Hallin Z, Villar M, Melander T (1987) Increase of galanin-like immunoreactivity in rat dorsal root ganglion cells after peripheral axotomy. Neurosci Lett 83:217–220.

Hokfelt T, Zhang X, Wiesenfeld-Hallin Z (1994) Messenger plasticity in primary sensory neurons following axotomy and its functional implications. Trends Neurosci 17:22–30.

Holmes FE, Mahoney S, King VR, Bacon A, Kerr NC, Pachnis V, Curtis R, Priestley JV, Wynick D (2000) Targeted disruption of the galanin gene reduces the number of sensory neurons and their regenerative capacity. Proc Natl Acad Sci USA 97:11563–11568.

Howard AD, Tan C, Shiao LL, Palyha OC, McKee KK, Weinberg DH, Feighner SD, Cascieri MA, Smith RG, Van Der Ploeg LH, Sullivan KA (1997) Molecular cloning and characterization of a new receptor for galanin. FEBS Lett 405:285–290.

Jacoby AS, Holmes FE, Hort YJ, Shine J, Iismaa TP (2002) Phenotypic analysis of Galr1 knockout mice reveals a role for GALR1 galanin receptor in modulating seizure activity but not nerve regeneration. Lett Pept Sci 8:139–146.

Kerr BJ, Cafferty WB, Gupta YK, Bacon A, Wynick D, McMahon SB, Thompson SW (2000) Galanin knockout mice reveal nociceptive deficits following peripheral nerve injury. Eur J Neurosci 12:793–802.

Liu HX, Brumovsky P, Schmidt R, Brown W, Payza K, Hodzic L, Pou C, Godbout C, Hokfelt T (2001) Receptor subtype-specific pronociceptive and analgesic actions of galanin in the spinal cord: selective actions via GalR1 and GalR2 receptors. Proc Natl Acad Sci USA 98:9960–9964.

Ma W, Bisby MA (1997) Differential expression of galanin immunoreactivities in the primary sensory neurons following partial and complete sciatic nerve injuries. Neuroscience 79:1183–1195.

Ma X, Tong YG, Schmidt R, Brown W, Payza K, Hodzic L, Pou C, Godbout C, Hokfelt T, Xu ZQ (2001) Effects of galanin receptor agonists on locus coeruleus neurons. Brain Res 919:169–174.

Marti E, Gibson SJ, Polak JM, Facer P, Springall DR, Van Aswegen G, Aitchison M, Koltzenburg M (1987) Ontogeny of peptide- and amine-containing neurones in motor, sensory, and autonomic regions of rat and human spinal cord, dorsal root ganglia, and rat skin. J Comp Neurol 266:332–359.

Mennicken F, Hoffert C, Pelletier M, Ahmad S, Walker P, O'Donnell D (2001) Distinct distributions of GALR1, GALR2 and GALR3 mRNAs in the adult rat CNS and their modulation in pain models. Soc Neurosci Abstr 27:148.6.

Murphy PG, Grondin J, Altares M, Richardson PM (1995) Induction of interleukin-6 in axotomized sensory neurons. J Neurosci 15:5130–5138.

Murphy PG, Ramer MS, Borthwick L, Gauldie J, Richardson PM, Bisby MA (1999) Endogenous interleukin-6 contributes to hypersensitivity to cutaneous stimuli and changes in neuropeptides associated with chronic nerve constriction in mice. Eur J Neurosci 11:2243–2253.

Nahin RL, Ren K, De Leon M, Ruda M (1994) Primary sensory neurons exhibit altered gene expression in a rat model of neuropathic pain. Pain 58:95–108.

Ogren SO, Pramanik A, Land T, Langel U (1993) Differential effects of the putative galanin receptor antagonists M15 and M35 on striatal acetylcholine release. Eur J Pharmacol 242:59–64.

O'Meara G, Coumis U, Ma SY, Kehr J, Mahoney S, Bacon A, Allen SJ, Holmes F, Kahl U, Wang FH, Kearns IR, Ove-Ogren S, Dawbarn D, Mufson EJ, Davies C, Dawson G, Wynick D (2000) Galanin regulates the postnatal survival of a subset of basal forebrain cholinergic neurons. Proc Natl Acad Sci USA 97:11569–11574.

Patrone C, Andersson S, Korhonen L, Lindholm D (1999) Estrogen receptor-dependent regulation of sensory neuron survival in developing dorsal root ganglion. Proc Natl Acad Sci USA 96:10905–10910.

Rivera-Bermudez MA, Bertics PJ, Albrecht RM, Mosavin R, Mellon WS (2002) 1,25-Dihydroxyvitamin D_3 selectively translocates PKCalpha to nuclei in ROS 17/2.8 cells. Mol Cell Endocrinol 188:227–239.

Scott MK, Ross TM, Lee DH, Wang HY, Shank RP, Wild KD, Davis CB, Crooke JJ, Potocki AC, Reitz AB (2000) 2,3-Dihydro-dithiin and -dithiepine-1,1,4,4-tetroxides: small molecule non-peptide antagonists of the human galanin hGAL-1 receptor. Bioorg Med Chem 8:1383–1391.

Smith KE, Walker MW, Artymyshyn R, Bard J, Borowsky B, Tamm JA, Yao WJ, Vaysse PJ, Branchek TA, Gerald C, Jones KA (1998) Cloned human and rat galanin GALR3 receptors: pharmacology and activation of G-protein inwardly rectifying K^+ channels. J Biol Chem 273:23321–23326.

Sten Shi TJ, Zhang X, Holmberg K, Xu ZQ, Hokfelt T (1997) Expression and regulation of galanin-R2 receptors in rat primary sensory neurons: effect of axotomy and inflammation. Neurosci Lett 237:57–60.

Suburo AM, Gu XH, Moscoso G, Ross A, Terenghi G, Polak JM (1992) Developmental pattern and distribution of nerve growth factor low-affinity receptor immunoreactivity in human spinal cord and dorsal root ganglia: comparison with synaptophysin, neurofilament and neuropeptide immunoreactivities. Neuroscience 50:467–482.

Tham S, Dowsing B, Finkelstein D, Donato R, Cheema SS, Bartlett PF, Morrison WA (1997) Leukemia inhibitory factor enhances the regeneration of transected rat sciatic nerve and the function of reinnervated muscle. J Neurosci Res 47:208–215.

Thompson SW, Priestley JV, Southall A (1998) gp130 cytokines, leukemia inhibitory factor and interleukin-6, induce neuropeptide expression in intact adult rat sensory neurons in vivo: time-course, specificity and comparison with sciatic nerve axotomy. Neuroscience 84:1247–1255.

Verge VM, Xu XJ, Langel U, Hokfelt T, Wiesenfeld-Hallin Z, Bartfai T (1993) Evidence for endogenous inhibition of autotomy by galanin in the rat after sciatic nerve section: demonstrated by chronic intrathecal infusion of a high affinity galanin receptor antagonist. Neurosci Lett 149:193–197.

Villar MJ, Cortes R, Theodorsson E, Wiesenfeld-Hallin Z, Schalling M, Fahrenkrug J, Emson PC, Hokfelt T (1989) Neuropeptide expression in rat dorsal root ganglion cells and spinal cord after peripheral nerve injury with special reference to galanin. Neuroscience 33:587–604.

Wang S, He C, Hashemi T, Bayne M (1997) Cloning and expressional characterization of a novel galanin receptor: identification of different pharmacophores within galanin for the three galanin receptor subtypes. J Biol Chem 272:31949–31952.

Wang S, Hashemi T, Fried S, Clemmons AL, Hawes BE (1998) Differential intracellular signaling of the GalR1 and GalR2 galanin receptor subtypes. Biochemistry 37:6711–6717.

Waters SM, Krause JE (2000) Distribution of galanin-1, -2 and -3 receptor messenger RNAs in central and peripheral rat tissues. Neuroscience 95:265–271.

Wiesenfeld-Hallin Z, Xu XJ, Villar MJ, Hokfelt T (1989) The effect of intrathecal galanin on the flexor reflex in rat: increased depression after sciatic nerve section. Neurosci Lett 105:149–154.

Wiesenfeld-Hallin Z, Xu XJ, Langel U, Bedecs K, Hokfelt T, Bartfai T (1992) Galanin-mediated control of pain: enhanced role after nerve injury. Proc Natl Acad Sci USA 89:3334–3337.

Wiesenfeld-Hallin Z, Xu XJ, Hao JX, Hokfelt T (1993) The behavioural effects of intrathecal galanin on tests of thermal and mechanical nociception in the rat. Acta Physiol Scand 147:457–458.

Wittau N, Grosse R, Kalkbrenner F, Gohla A, Schultz G, Gudermann T (2000) The galanin receptor type 2 initiates multiple signaling pathways in small cell lung cancer cells by coupling to G_q, G_i and G_{12} proteins. Oncogene 19:4199–4209.

Wynick D, Hammond PJ, Akinsanya KO, Bloom SR (1993) Galanin regulates basal and oestrogen-stimulated lactotroph function. Nature 364:529–532.

Wynick D, Small CJ, Bacon A, Holmes FE, Norman M, Ormandy CJ, Kilic E, Kerr NC, Ghatei M, Talamantes F, Bloom SR, Pachnis V (1998) Galanin regulates prolactin release and lactotroph proliferation. Proc Natl Acad Sci USA 95:12671–12676.

Zhong J, Dietzel ID, Wahle P, Kopf M, Heumann R (1999) Sensory impairments and delayed regeneration of sensory axons in interleukin-6-deficient mice. J Neurosci 19:4305–4313.

NEUROPEPTIDES

Neuropeptides (1995) 29, 137–143

Metabolism of Galanin and Galanin (1–16) in Isolated Cerebrospinal Fluid and Spinal Cord Membranes from Rat

K. BEDECS, Ü. LANGEL and T. BARTFAI

Department of Neurochemistry and Neurotoxicology, Stockholm University, Frescati, S-10691 Stockholm, Sweden

Abstract—The occurrence of galanin (GAL) in the spinal cord and reports suggesting that it acts as an endogenous inhibitory spinal modulator in sensory/noxious transmission, have focused interest on its metabolism in the spinal cord. The metabolic half-lives and degradation patterns of GAL(1–29) and the high affinity N-terminal fragment GAL(1–16), were determined in isolated cerebrospinal fluid (CSF) from rats, and analysed by reverse phase HPLC. The half-lives for GAL(1–29) and GAL(1–16) in isolated rat CSF at 37°C were 120 min and 60 min, respectively. The first degradation products which we could isolate and identify of GAL(1–16) were: GAL(3–16) and GAL(3–12) and for GAL(1–29): GAL(1–5) and GAL(1–4), all without affinity to spinal galanin receptors. Degradation studies of GAL(1–29) and GAL(1–16) in a spinal cord membrane preparation, in absence or presence of different protease inhibitors: E-64, pepstatin A, 3,4-DCI, bestatin, phosphoramidon, kelatorphan and thiorphan, or metal chelators: EDTA, EGTA and *o*-phenanthrolin, suggest that a phosphoramidon sensitive zinc-metalloprotease is mainly responsible for the degradation of GAL(1–29) and GAL(1–16), since both *o*-phenanthrolin (0.3 mM) and phosphoramidon (920 μM) substantially prolong their half-lives.

Introduction

Galanin (GAL)[1] a 29/30 amino acid long C-terminally amidated neuropeptide is widely distributed and exerts a variety of biological actions in the peripheral and central nervous system. In the rat spinal cord GAL is present in primary sensory neurones (DRG), local dorsal horn cells and motor neurones.[2,3] GAL is of particular interest as an endogenous inhibitory spinal modulator in sensory/noxious processing and transmission. Intrathecally (i.t.) applied GAL has a concentration dependent biphasic facilitatory and depressive effect on the spinal flexor reflex (used as a model for nociceptive and sensory transmission)[4] and dose dependently inhibits the facilitatory effect 'wind-

Date received 27 October 1994
Date accepted 26 February 1995

Correspondence to Tamas Bartfai, Department of Neurochemistry and Neurotoxicology, Stockholm University, Arrhenius Laboratories for Natural Sciences, S-10691 Stockholm, Sweden

up' of conditioning stimulation (CS) of C-afferents in skin and muscle nerves.[5] I.t. GAL also potentiates the spinal anti-nociceptive effect of morphine and a selective CCK-B antagonist at a dose which by itself does not cause analgesia.[6,7]

The occurrence of GAL in the central nervous system and the possibility that it may act as an endogenous inhibitory modulator have focused interest on its metabolism. Fast enzymatic inactivation is probably of importance in terminating the actions of the synaptically released peptide neurotransmitters. Pharmacological use of peptide receptor ligands assumes that we can adequately protect these from peptidolysis either by finding non-peptide ligands (e.g. morphine) or by synthesizing protected peptide type ligands. If the pharmacological effect of the peptide receptor agonist is desirable, inhibitors to specific degrading enzymes may also be useful. The first step toward these goals is to establish the degradation pattern for the peptide in question.

Earlier studies have shown that GAL is degraded rapidly when incubated with gastric smooth muscle membranes, although the metabolic products or half-life in this preparation were not determined.[8] Degradation of GAL(1–29) and GAL(1–16) (a high-affinity agonist) in a hypothalamic crude membrane preparation showed that the metabolic half-lives were 100 min and 28 min, respectively. The proposed peptidolytic cleavage sites in GAL(1–16) were between Trp^2-Thr^3, Thr^3-Leu^4, and Leu^4-Asn^5, yielding fragments GAL(3–16), GAL(4–16) and GAL(5–16), all without measurable affinity to the GAL receptor.[9]

During an intrathecal administration, GAL is injected into the cerebrospinal fluid (CSF), permeates the pia mater and diffuses to the superficial layers (laminae I and II) of the spinal cord, where spinal GAL receptors are expressed. The metabolism of endogenously occurring GAL(1–29) and the N-terminal biologically active GAL fragment GAL(1–16) has not yet been studied in the spinal cord or CSF. Identification of the fissile bonds in GAL(1–29) and GAL(1–16) may assist the synthesis of peptidolytically more stable, long acting analogues which could be used in pain treatment.

The present study shows the metabolism of GAL(1–29) and the GAL(1–16) in isolated rat CSF and a P_2-membrane preparation from the lumbar dorsal spinal cord.

Materials and methods

Materials

Rat GAL(1–29) and GAL(1–16) were synthesized by the *t*-Boc method, purified on a LKB HPLC apparatus (SYSTEM PREP 50) using Polygosil 60–7 C_{18} reverse phase column and characterized by plasma desorption mass spectrometry, model Bioion 20, Applied Biosystems, as described by Langel et al 1992.[10] GAL(1–29) was synthesized with a C-terminal amide corresponding to the endogenous peptide while GAL(1–16) was synthesized as a free carboxylic acid. The protease inhibitors E-64 (N-[N-(L-3-Trans-carboxyoxirane-2-carbonyl)-L-leucyl]-agmatine), 3, 4-DCI (3, 4-Dichloroisocoumarin), pepstatin A, phosphoramidon, bestatin and thiorphan were from Boehringer Mannheim. Kelatorphan was a generous gift from Prof. B. Roques (Paris). All other reagents were from Sigma (St Louis, MO, USA).

Isolation of CSF

Adult male rats (Sprague-Dawley, 350–400 g) were anaesthetised with chloral hydrate 300 mg/kg body weight (i.p.) and CSF was collected from the Cisternae cerebello medullaris through a suboccipital puncture and immediately put on ice. To remove contaminating blood cells the CSF was centrifuged for 2 min at 11 000 × g.

Control experiments were performed, with serum from blood collected through a heart puncture, and showed no degradation of either GAL(1–29) or GAL(1–16).

Preparation of membranes from lumbar dorsal spinal cord

Adult male rats (Sprague-Dawley 180–200 g) were decapitated, the lumbar spinal cord rapidly dissected and divided into dorsal and ventral parts. The tissue (10% w/v) was homogenized on ice with a tight fitting Teflon-glass homogenizer (10 strokes at 695 rpm) in 0.32 M sucrose buffered with 5 mM Hepes (pH 7.4). The homogenate was diluted 10-fold with 0.32 M sucrose buffered with 5 mM Hepes

(pH 7.4) and centrifuged at 1000 × g for 10 min. The supernatant was further centrifuged at 10 000 × g for 45 min and the pellet resuspended at a concentration of 1 mg protein/ml in Hepes (5 mM)-buffered Krebs-Ringer solution (Hepes-KR), containing 137 mM NaCl, 2.68 mM KCl, 1.8 mM $CaCl_2$, 2.05 mM $MgCl_2$ and 1 g/l glucose, pH 7.4, aliquoted and stored at −80°C.

Degradation of GAL(1–29) and GAL(1–16) in CSF or lumbar dorsal spinal cord membranes

To determine the rate of degradation of and to identify the proteolytic products, GAL(1–29) and GAL(1–16) at a concentration of 1 and 0.5 μg/μl, respectively, were incubated with isolated rat CSF or P_2-membranes from the lumbar dorsal spinal cord (0.6 mg protein/ml, GAL(1–29) and GAL(1–16): 30 μM) at 37°C, 0–210 min. The degradation was stopped by precipitation of proteins with perchloric acid (final concentration 2% (v/v)), and centrifuged for 2 min at 11 000 × g. The resulting supernatant was analysed by HPLC on C18 reverse phase analytical column (Nucleosil 120–3, 100 × 4 mm ID), eluting with a 16–56% acetonitrile/water (0.1% TFA v/v), gradient for 50 min, flowrate 0.8 ml/min.

To characterize the degradation products, the different peaks were collected, lyophilised and Phenylisothiocyanate (PITC) amino acid analysis was performed.

First order rate constants of the disappearance of GAL(1–29) and GAL(1–16) were calculated according to equation 1.

$$S_t = S_o e^{-kt} \qquad \text{(eq. 1)}$$

where S_t = area of non-degraded peptide peak, at time moment t; S_o = area of initial peptide peak at t = 0; k = first order rate constant of the degradation of the peptides.

Results

To determine the half-lives and degradation pattern of GAL(1–29) and GAL(1–16), degradation studies were performed in freshly isolated CSF from rats. The rate of disappearance of GAL(1–29) and GAL(1–16), and the appearance of degradation products were followed by HPLC-analysis. Those degradation products which appeared first were collected and further characterized by PITC amino acid analysis. In the isolated CSF preparation the metabolic half-lives for GAL(1–29) and GAL(1–16) were 120 ± 60 min (n = 6) and 60 ± 30 min (n = 6), respectively at 37°C. The first independently appearing degradation products for GAL(1–16) were GAL(3–16) and GAL(3–12) and for GAL(1–29) were GAL(1–5) and GAL(1–4). None of these peptide fragments could displace ^{125}I-GAL(1–29) binding from spinal cord membranes (Fig. 1).

To characterize the protease class which is mainly responsible for the degradation of GAL(1–16) and GAL(1–29) we used a lumbar dorsal spinal cord P_2-membrane preparation, because of the poor reproducibility of half-lives of GAL(1–29) and GAL(1–16) in isolated CSF. Degradation studies, in absence or presence of different protease inhibitors were performed.

In Figure 2 the half-lives of GAL(1–16) and GAL(1–29) in presence of the serine, cysteine and aspartate protease inhibitors 3,4-DCI (0.1 mM), E-64 (1.4 mM) and pepstatin (20 μM), respectively are listed. As shown, neither one of these inhibitors is able to prolong the half-lives of GAL(1–16) or GAL(1–29). However, the metal chelators EDTA, EGTA and *o*-phenanthrolin (1,10-phenanthrolin) significantly prolonged the half-lives of GAL(1–16) and GAL(1–29) in spinal cord membranes. Whereas the Zn^{2+} chelator *o*-phenanthrolin at 0.2 mM prolonged the half-lives of GAL(1–16) and GAL(1–29) three times, EDTA and EGTA (10 mM) could prolong the half-life of GAL(1–29) 6 times, but the half-life of GAL(1–16) only 3 times. The results presented in Figure 2 clearly indicate that GAL(1–16) and GAL(1–29) are sensitive to metalloprotease(s), probably Zn-metalloprotease(s).

To further characterize which metalloproteases are involved in the degradation of GAL(1–16) and GAL(1–29), their half-lives were measured in the presence of inhibitors to some well characterized metalloproteases, known to be present in the CSF and spinal cord. In Figure 3, the half-lives of GAL(1–16) and GAL(1–29) are shown in the presence of the peptidase inhibitors: bestatin (aminopeptidase N/M (APN/M)), phosphoramidon (neutral endopeptidase EC. 3.4.24.11 (NEP)), thior-

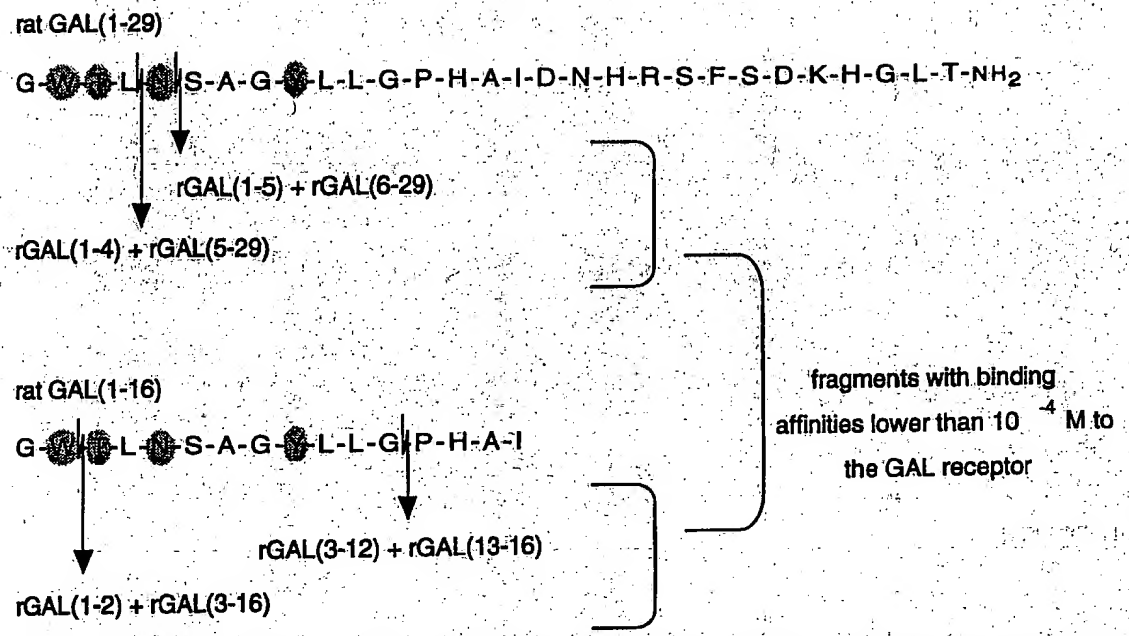

Fig. 1 Degradation patterns of GAL(1–29) and GAL(1–16) in isolated rat CSF. Encircled letters indicate main pharmacophores in binding to the GAL receptor

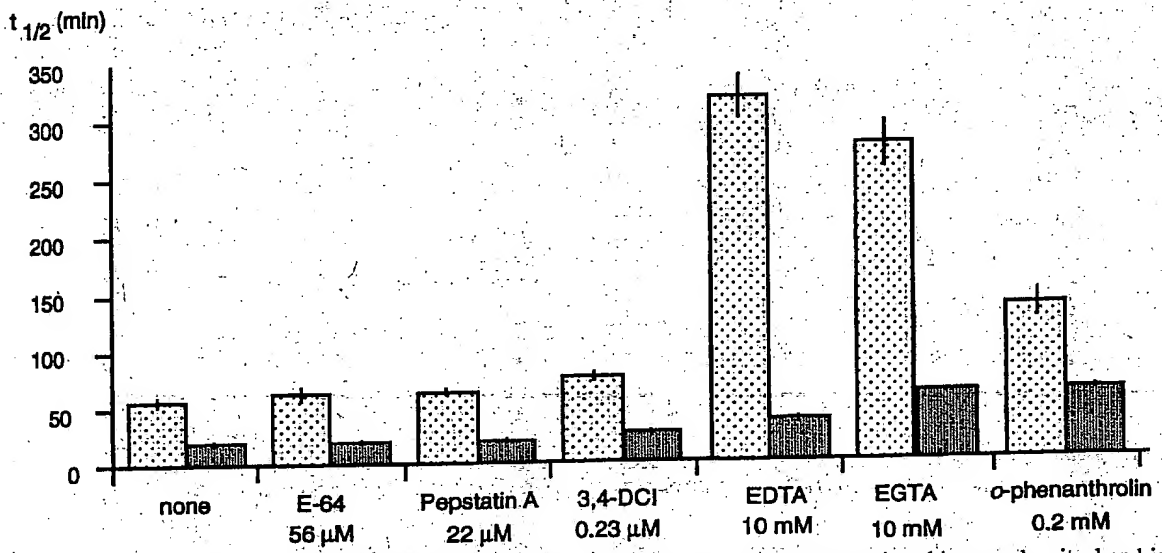

Fig. 2 The half-lives of GAL(1–16) (dark columns) and GAL(1–29) (light columns) [30 µM] incubated in a crude mitochondrial membrane preparation (P_2) [0.6 mg/ml] from LDSC, at 37°C, in presence of the protease inhibitors 3,4-DCI (serine), E-64 (cysteine), pepstatin A (aspartate) and metal-chelating agents *o*-phenanthrolin, EDTA and EGTA. The rate of peptide degradation was followed on HPLC and the half-lives were calculated according to $S_t = S_o e^{-kt}$, where S_t = area of non-degraded peptide peak at time moment t; S_o = area of initial peptide peak at t = O; k = first order rate constant of the degradation of the peptides.

phan (NEP), kelatorphan (mixed APN/M-NEP inhibitor), and a mixture of these. Of these metalloprotease inhibitors, only the endopeptidase inhibitor phosphoramidon, could significantly inhibit the degradation of GAL(1–16) and GAL(1–29).

The degradation of both GAL(1–29) and GAL(1–16) was faster when incubated with mem-

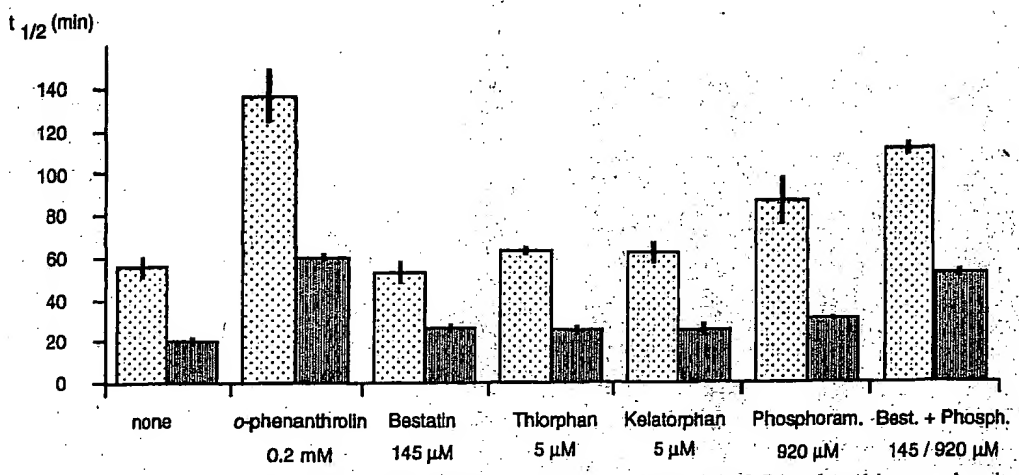

Fig. 3 The half-lives of GAL(1–16) (dark columns) and GAL(1–29) (light columns) [30 µM] incubated in a crude mitochondrial membrane preparation (P_2) [0.6 mg/ml] from LDSC, at 37°C, in presence of the protease inhibitors bestatin (APN/M), phosphoramidon (NEP), thiorphan (NEP), kelatorphan (mixed APN/M-NEP inhibitor), and a mixture of these. For calculations see legend under Figure 2.

branes from spinal cord than when incubated with isolated CSF, which can be explained by the membrane concentration used, in this case 0.6 mg protein/ml. To determine whether or not the inhibition of degradation of GAL(1–16) and GAL(1–29) by *o*-phenanthrolin was concentration-dependent, degradation of GAL(1–16) and GAL(1–29) in spinal cord membranes in the presence of increasing concentrations of *o*-phenanthrolin was studied (Fig. 4). The degradation of both GAL(1–16) and GAL(1–29) was inhibited in a concentration-dependent manner by *o*-phenanthrolin. At 0.4 mM (the highest inhibitor concentration used) the half-life of GAL(1–16) was prolonged 12-fold (from 22 to 270 min) and for GAL(1–29) the half-life was prolonged only 5-fold (from 70 to 398 min). In a preliminary study of the degradation of GAL(1–16) and GAL(1–29) in isolated human CSF (frozen) the half-lives for GAL(1–29) and GAL(1–16) were $\gg$ 180 min, probably due to inactivation of degrading activities during storage of the samples.

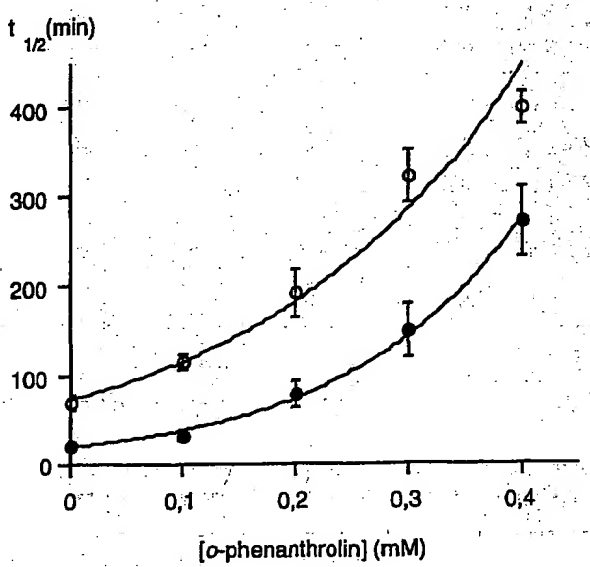

Fig. 4 Metabolic half-lives of GAL(1–16) (filled circles) and GAL(1–29) (open circles) incubated in P_2 membranes from lumbar dorsal spinal cord, 37°C, in presence of increasing concentrations of *o*-phenanthrolin.

Discussion

The present study shows that GAL(1–16) and GAL(1–29) are enzymatically degraded in isolated CSF from rat. Although GAL(1–16) has not been shown to occur endogenously, information about its metabolism is important from a pharmacological-therapeutic point of view, since it acts as a high affinity full agonist.[11] Studies on the structural requirements of the biological activity of GAL(1–29) in the spinal cord have shown that the N-terminal fragment GAL(1–16) is an equipotent agonist at the spinal GAL receptor, with a K_D value of 3 nM, but with slightly superior pharmaco-kinetic properties e.g. penetration and diffusion constants compared to GAL(1–29).[11]

The half-lives for GAL(1–16) and GAL(1–29) in

CSF were 60 ± 30 min and 120 ± 60 min, respectively, showing that GAL is a surprisingly stable peptide. The half-lives for GAL(1–16) and GAL(1–29) in the spinal cord membrane preparation were 20 ± 2 and 56 ± 5 min, respectively. An earlier study carried out in a hypothalamic membrane preparation, showed that the half-lives for GAL(1–16) and GAL(1–29) were 28 and 100 min, respectively.[9]

The higher metabolic stability of GAL(1–29) as compared to GAL(1–16), can be explained by the proposed horse-shoe like conformation of GAL(1–29) based on fluorescence energy transfer data, suggesting that the C-terminal part of the molecule can sterically protect the N-terminal and render it less susceptible for proteolytic attack.[12,13]

The first appearing degradation products for GAL(1–16) were GAL(3–16) and GAL(3–12) and for GAL(1–29) were GAL(1–4) and GAL(1–5) as determined by PITC amino acid analysis of the collected HPLC peaks/fractions. To address the question whether the formation of GAL(3–12) was secondary to a previous formation of GAL(3–16) from GAL(1–16), synthetic GAL(3–16) was incubated with isolated CSF for 90 min. No formation of GAL(3–12) was observed, indicating that GAL(3–16) and GAL(3–12) are independent degradation products of GAL(1–16). To yield the fragment GAL(3–12), GAL(1–16) is cleaved between Trp^2-Thr^3 and Pro^{12}-Gly^{13}, where the latter represents an unusual cleavage site. The degradation patterns of GAL(1–16) and GAL(1–29) in CSF showed that the cleavage sites are located mainly in the N-terminal part of the peptides. Cleavage in the N-terminal part of GAL(1–16) and GAL(1–29) represents a biologically significant degradation, as this results in fragments which no longer bind to spinal GAL receptors with high affinity, and are thus in a galaninergic perspective, inactive fragments. In order to characterize which protease class is mainly responsible for the degradation of GAL(1–16) and GAL(1–29) we changed the model system from isolated CSF to a lumbar dorsal spinal cord P_2-membrane preparation.

The degradation profile (i.e. time dependency and amount of individual degradation products) of GAL(1–16) and GAL(1–29) in spinal cord membranes were similar to that in CSF, suggesting that a similar set of peptidases is acting in the CSF and in the spinal cord membranes. The inability of the serine (3.4-DCI), cysteine (E-64) and aspartate (pepstatin) protease inhibitors to prolong the half-lives of GAL(1–16) and GAL(1–29) and the potent inhibition by *o*-phenanthrolin, EDTA and EGTA suggest that metalloproteases are active in the metabolism of GAL(1–16) and GAL(1–29) (Fig. 2). An interesting finding was that GAL(1–16) and GAL(1–29) were differently inhibited by the metal chelators *o*-phenanthrolin, EDTA and EGTA. *o*-phenanthrolin prolonged the half-lives of GAL(1–16) and GAL(1–29) three times, whereas EDTA and EGTA prolonged the half-life of GAL(1–29) six times, but the half-life of GAL(1–16) only three times. This may indicate that metalloproteases other than Zn-metalloproteases are also active in the degradation of the C-terminal part of GAL: GAL(17–29), whereas the N-terminal part is degraded mainly by Zn-metalloproteases.

In the subsequent investigation of which metalloproteases degrade GAL(1–16) and GAL(1–29), we selected inhibitors specific for NEP (thiorphan), APN/M (bestatin), mixed NEP and APN/M inhibitor (kelatorphan) and the less specific metallo-endopeptidase inhibitor phosphoramidon, which is also a potent NEP inhibitor. These studies suggest that a metallo-endopeptidase(s), other than NEP degrades GAL(1–16) and GAL(1–29) in the spinal cord membranes, since phosphoramidon but neither thiorphan nor kelatorphan significantly prolonged their half-lives. Phosphoramidon (920 μM) prolonged the half-lives of both GAL(1–16) and GAL(1–29) to the same extent(1.5-fold), indicating that the protease inhibited by phosphoramidon, is active in the GAL(1–16) part of GAL(1–29). The identification of the first appearing degradation products of GAL(1–16) i.e. GAL(3–16) and GAL(3–12) and of GAL(1–29), GAL(1–4) and GAL(1–5) in isolated CSF may suggest the involvement of (N-terminally acting) amino- and/or dipeptidyl amino peptidases. This is consistent with a study in a hypothalamic membrane preparation, where the degradation of GAL(1–29) and GAL(1–16) was shifted from the N-terminal portion to the C-terminal portion in the presence of EDTA, suggesting that the enzyme(s) responsible for the cleavage in the N-terminal part are metalloprotease(s).[9] In conclusion, degradation studies in spinal cord membranes in the presence of different protease inhibitors indicate that an *o*-phenanthrolin and

phosphoramidon sensitive zinc-metalloprotease(s) is mainly responsible for the degradation of GAL(1–16) and GAL(1–29), since both *o*-phenanthrolin in a concentration dependent manner and phosphoramidon are able to substantially prolong their half-lives.

Acknowledgement

We would like to thank Carina Palmberg who performed the PITC amino acid analysis (at the lab. of Prof. Hans Jörnvall, Department of Physiological Chemistry, Karolinska Institutet). This study was supported by the Swedish MRC (07913, 04X–2887), the Bank of Sweden Tercentenary Foundation, Marcus och Amalia Wallenbergs Minnesfond, Astra Pain Control AB, Lars Hiertas Minnes Stiftelse, Trion FUAB, Konung Gustav V:s och Drottning Victorias Stiftelse and Marianne och Marcus Wallenbergs Stiftelse, Wenner-Gren Foundation and Ivar Bendixsons Foundation.

References

1. Tatemoto, K., Rökaeus, A., Jörnvall, H., McDonald, T. J. and Mutt, V. Galanin — a novel biologically active peptide from porcine intestine. FEBS Lett. 1983; 164: 124–128.
2. Ch'ng, J. L., Christofides, N. D., Anand, P. et al. Distribution of galanin immunoreactivity in the central nervous system and the responses of galanin-containing neuronal pathways to injury. Neuroscience 1985; 16: 343–354.
3. Skofitsch, G. and Jacobowitz, D. M. Galanin-like immunoreactivity in capsaicin sensitive sensory neurons and ganglia. Brain Res. Bull. 1985; 15: 191–195.
4. Wiesenfeld-Hallin, Z., Villar, M. J. and Hökfelt, T. The effects of intrathecal galanin and C-fiber stimulation on the flexor reflex in the rat. Brain Res. 1989; 486: 205–213.
5. Xu, X. J., Wiesenfeld-Hallin, Z. and Hökfelt, T. Intrathecal galanin blocks the prolonged increase in spinal cord flexor reflex excitability induced by conditioning stimulation of unmyelinated muscle afferents in the rat. Brain Res. 1991; 541: 350–353.
6. Wiesenfeld-Hallin, Z., Xu, X. J., Villar, M. J. and Hökfelt, T. Intrathecal galanin potentiates the spinal analgesic effect of morphine: electrophysiological and behavioural studies. Neurosci. Lett. 1990; 109: 217–221.
7. Wiesenfeld-Hallin, Z., Xu, X. J., Hughes, J., Horwell, D. C. and Hökfelt, T. PD134308, a selective antagonist of cholecystokinin type B receptor, enhances the analgesic effect of morphine and synergistically interacts with intrathecal galanin to depress spinal nociceptive reflexes. Proc. Natl. Acad. Sci. U.S.A. 1990; 87: 7105–7109.
8. Rossowski, W. J., Rossowski, T. M., Zacharia, S., Ertan, A. and Coy, D. H. Galanin binding sites in rat gastric and jejunal smooth muscle membrane preparations. Peptides 1990; 11: 333–338.
9. Land, T., Langel, Ü. and Bartfai, T. Hypothalamic degradation of galanin(1–29) and galanin(1–16): identification and characterization of the peptidolytic products. Brain Res. 1991; 558: 245–250.
10. Langel, Ü., Land, T. and Bartfai, T. Design of chimeric peptide ligands to galanin receptors and substance P receptors. Int. J. Pept. Protein. Res. 1992; 39: 516–522.
11. Xu, X. J., Wiesenfeld-Hallin, Z., Fisone, G., Bartfai, T. and Hökfelt, T. The N-terminal 1–16, but not C-terminal 17–29, galanin fragment affects the flexor reflex in rats. Eur. J. Pharmacol. 1990; 182: 137–141.
12. Rigler, R., Wennerberg, A., Cooke, R. M. et al. On the solution structure of galanin. In: Hökfelt, T. (ed). Galanin: a multifunctional peptide in the neuroendocrine system. London: McMillan Press, 1991: 17–25.
13. Kulinski, T., Wennerberg, A. and Rigler, R. Side chain motions and end to end distance distribution in a-helical peptides. In: Laser Spectroscopy of Biomolecules 1992; 1921: 203–208.

The Journal of Neuroscience, January 15, 1999, 19(2):859–867

Peripheral Inflammation Facilitates Aβ Fiber-Mediated Synaptic Input to the Substantia Gelatinosa of the Adult Rat Spinal Cord

Hiroshi Baba, Timothy P. Doubell, and Clifford J. Woolf

Neural Plasticity Research Group, Department of Anesthesia and Critical Care, Massachusetts General Hospital and Harvard Medical School, Boston, Massachusetts 02129

Whole-cell patch-clamp recordings were made from substantia gelatinosa (SG) neurons in thick adult rat transverse spinal cord slices with attached dorsal roots to study changes in fast synaptic transmission induced by peripheral inflammation. In slices from naive rats, primary afferent stimulation at Aβ fiber intensity elicited polysynaptic EPSCs in only 14 of 57 (25%) SG neurons. In contrast, Aβ fiber stimulation evoked polysynaptic EPSCs in 39 of 62 (63%) SG neurons recorded in slices from rats inflamed by an intraplantar injection of complete Freund's adjuvant (CFA) 48 hr earlier ($p < 0.001$). Although the peripheral inflammation had no significant effect on the threshold and conduction velocities of Aβ, Aδ, and C fibers recorded in dorsal roots, the mean threshold intensity for eliciting EPSCs was significantly lower in cells recorded from rats with inflammation (naive: 33.2 ± 15.1 μA, $n = 57$; inflamed: 22.8 ± 11.3 μA, $n = 62$, $p < 0.001$), and the mean latency of EPSCs elicited by Aβ fiber stimulation in CFA-treated rats was significantly shorter than that recorded from naive rats (3.3 ± 1.8 msec, $n = 36$ vs 6.0 ± 3.5 msec, $n = 12$; $p = 0.010$). Aβ fiber stimulation evoked polysynaptic IPSCs in 4 of 25 (16%) cells recorded from naive rat preparations and 14 of 26 (54%) SG neurons from CFA-treated rats ($p < 0.001$). The mean threshold intensity for IPSCs was also significantly lower in CFA-treated rats (naive: 32.5 ± 15.7 μA, $n = 25$; inflamed: 21.9 ± 9.9 μA, $n = 26$, $p = 0.013$). The facilitation of Aβ fiber-mediated input into the substantia gelatinosa after peripheral inflammation may contribute to altered sensory processing.

Key words: inflammation; pain; dorsal horn; synaptic transmission; neural plasticity; substantia gelatinosa

Peripheral tissue inflammation characteristically leads to increased pain sensitivity. This is the consequence both of a peripheral sensitization of high-threshold Aδ and C nociceptor terminals on exposure to inflammatory mediators (Levine and Taiwo, 1994) and to a central facilitation of synaptic input into the dorsal horn of the spinal cord; central sensitization (Woolf, 1983; Torebjork et al., 1992). Central sensitization is initiated in noninflamed animals by brief C-fiber inputs and manifests as a modification in the receptive field properties of dorsal horn neurons caused by the recruitment of subthreshold inputs (Woolf and King, 1990), and includes the transformation of nociceptive-specific cells into multireceptive cells with a low-threshold Aβ fiber input (Simone et al., 1989; Woolf et al., 1994). In human volunteers, central sensitization induced by activation of C-fibers with chemical irritants includes the generation of a tactile pain mediated by Aβ fibers (Torebjork et al., 1992; Koltzenburg et al., 1994). In *in vitro* neonatal spinal cord preparations, repetitive brief C-fiber stimulation produces an NMDA receptor-mediated heterosynaptic facilitation of Aβ fiber inputs to deep dorsal horn and ventral horn spinal neurons (Thompson et al., 1990, 1993).

Central sensitization is likely to contribute substantially to the hypersensitivity associated with experimental inflammation as a consequence of C-fiber input from spontaneously active C-fibers or augmented peripheral activation of sensitized C-fibers. Another mechanism may, however, participate in alterations in synaptic efficacy during inflammation, a change in the synaptic drive generated by Aβ sensory neurons innervating the inflamed area. In adjuvant-inflamed but not naive rats, for example, the hamstring flexor withdrawal reflex is progressively sensitized by repetitive light mechanical stimuli applied to the inflamed tissue (progressive tactile hypersensitivity), which can be mimicked by Aβ fiber electrical stimulation (Ma and Woolf, 1996a). Aβ fiber input in inflamed animals also generates an action potential afterdischarge in dorsal horn neurons, something only Aδ and C-fibers normally evoke (Neumann et al., 1996). Finally, Aβ fiber-mediated ventral root potentials recorded from an *in vitro* spinal cord preparation from inflamed neonatal rats, show windup, a phenomenon normally only associated with C-fibers (Thompson et al., 1994). One explanation for these changes in the central action of Aβ fibers after inflammation may be the novel expression of substance P and other synaptic modulators in some of these fibers (Neumann et al., 1996), which could result in synaptic events typical of C-fibers being generated by Aβ fibers.

The central changes involved in inflammation may result in the facilitation of Aβ fiber-mediated synaptic input to neurons in the superficial dorsal horn, especially lamina II (substantia gelatinosa, SG). The direct primary afferent input into the SG is predominantly Aδ and C fiber nociceptors (Willis and Coggeshall, 1991), and the novel recruitment of low-threshold Aβ-evoked synaptic potentials in these neurons might alter sensory processing sufficiently to contribute to the abnormal hypersensitivity typical of inflammation. We have now investigated, using an *in vitro* adult

Received Aug. 3, 1998; revised Oct. 22, 1998; accepted Nov. 3, 1998.

Supported by the Human Frontier Science Program (RG73/96) and the Wellcome Trust (039631).

Correspondence should be addressed to Dr. Hiroshi Baba, Neural Plasticity Research Group, Department of Anesthesia, Massachusetts General Hospital and Harvard Medical School, MGH-East 4th Floor, 149 13th Street, Charlestown, MA 02129.

Dr Doubell's present address: University Laboratory of Physiology, University of Oxford, Oxford, OX 1 3PT UK.

 0270-6474/99/190859-09$05.00/0

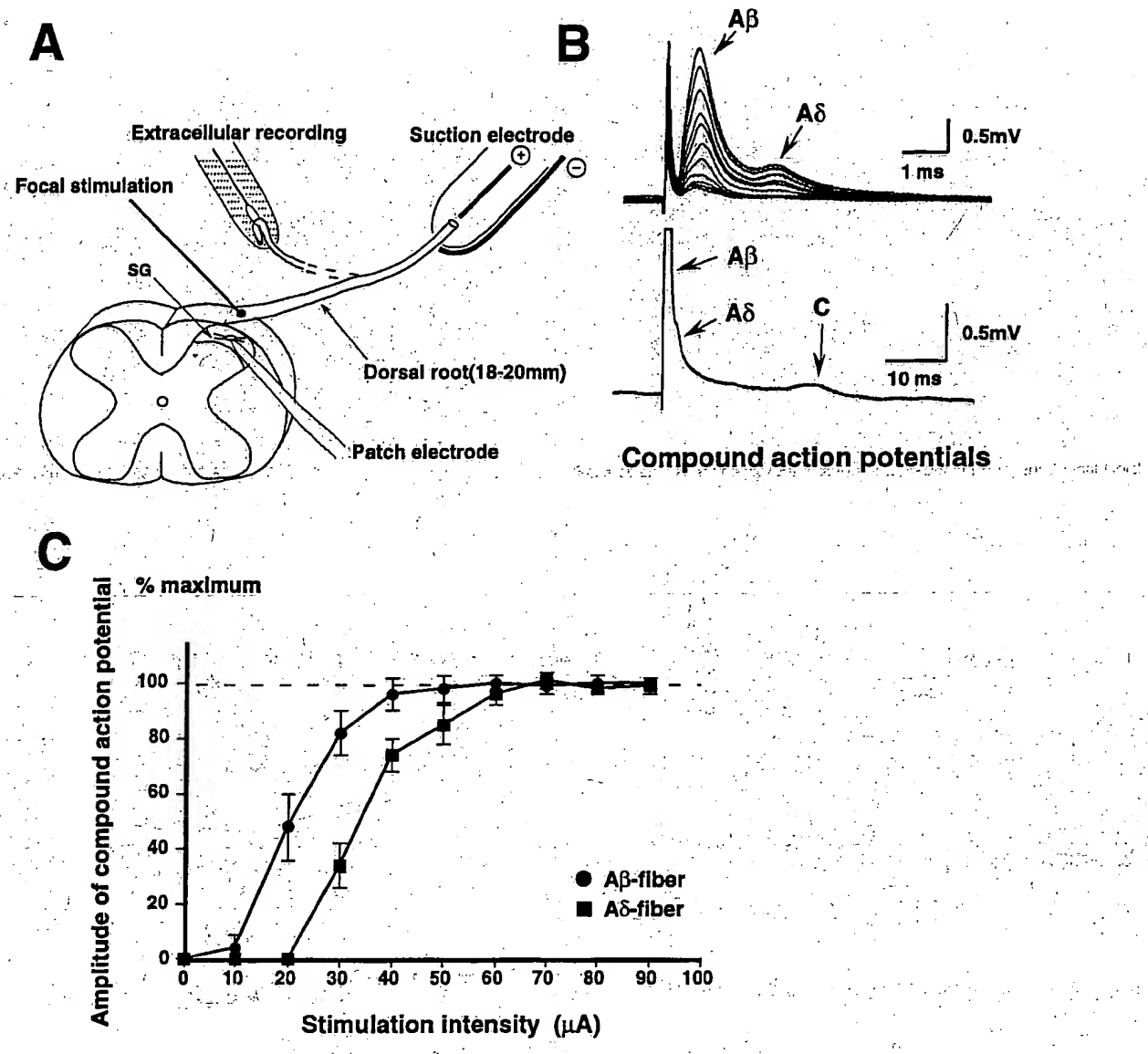

Figure 1. *A*, Schematic diagram of the experimental setup. Extracellular recordings were made from dorsal roots, and whole-cell patch-clamp recordings were made from SG neurons in adult rat spinal cord transverse slices with a long attached dorsal root. *B*, Representative extracellular recording of compound action potentials evoked at graded stimulus intensities (*top*, 12–50 μA; *bottom*, 300 μA). The threshold intensities for Aβ, Aδ, and C fibers were 12, 23, and 230 μA, respectively. The stimulus duration for Aβ and Aδ was 0.05 msec and for C fibers was 0.5 msec. Calculated conduction velocities for Aβ, Aδ, and C fibers were 27.3, 8.5, and 0.8 m/sec, respectively. *C*, The stimulus–response relationship of Aβ and Aδ compound action potentials ($n = 5$).

spinal cord preparation, the effect of inflammation on Aβ fiber-mediated fast synaptic responses in the SG.

MATERIALS AND METHODS

The methods for inducing inflammation, obtaining adult rat spinal cord slices, and blind whole-cell patch-clamp recordings from SG neurons have been described in detail previously (Yoshimura and Jessell, 1989; Yoshimura and Nishi, 1993; Ma and Woolf, 1996a). Briefly, inflammation was induced by an intraplantar injection of complete Freund's adjuvant (CFA; Sigma, St. Louis, MO; 100 μl) into the left hindpaw of adult male Sprague Dawley rats (10–11 weeks, 300–350 gm) under halothane (2.5%) anesthesia, producing an area of erythema, edema, and tenderness restricted to the hindpaw (Stein et al., 1988). Naive noninflamed animals or rats 48 hr after CFA injection were terminally anesthetized with urethane (1.5–2.0 gm/kg, i.p.), and the lumbosacral spinal cord was removed. The isolated spinal cord was then placed in preoxygenated cold Krebs' solution (2–4°C). After removal of the dura mater, all ventral and dorsal roots, except the L5 dorsal root on the left side, were cut, and the pia-arachnoid was removed. The spinal cord was placed in a shallow groove formed in an agar block and glued to the bottom of a microslicer stage with cyanoacrylate adhesive and held in place by the agar block. The spinal cord was immersed in cold Krebs' solution, and a 600-μm-thick transverse slice with attached dorsal root was cut on a vibrating microslicer (model DTK1500; Dosaka Co. Ltd., Kyoto, Japan). The spinal cord slice was then placed on a nylon mesh in the recording chamber and held in place by a titanium electron microscopy grid supported by a silver wire loop. The slice was perfused with Krebs' solution (15 ml/min) saturated with 95% O_2 and 5% CO_2 at 36 ± 1°C. The Krebs' solution contained (in mM): NaCl 117, KCl 3.6, $CaCl_2$ 2.5, $MgCl_2$ 1.2, NaH_2PO_4 1.2, $NaHCO_3$ 25, and glucose 11. The length of preserved L5 dorsal root from the cathode of the suction electrode to the dorsal root entry zone was adjusted to 18–20 mm by cutting its distal end. Orthodromic stimulation of the dorsal root was performed with a suction electrode (Fig. 1*A*) using a constant-current stimulator (Neurolog). The

Table 1. Compound action potential

	Threshold (μA)			Conduction velocity (m/sec)		
	Aβ	Aδ	C	Aβ	Aδ	C
Naive (n = 12)	13.3 ± 2.7	24.7 ± 1.9	217.9 ± 76.9	27.0 ± 3.7	8.0 ± 1.2	0.8 ± 0.1
Inflamed (n = 14)	12.6 ± 2.7	25.4 ± 2.2	198.0 ± 77.3	26.0 ± 4.3	8.1 ± 1.1	0.9 ± 0.1

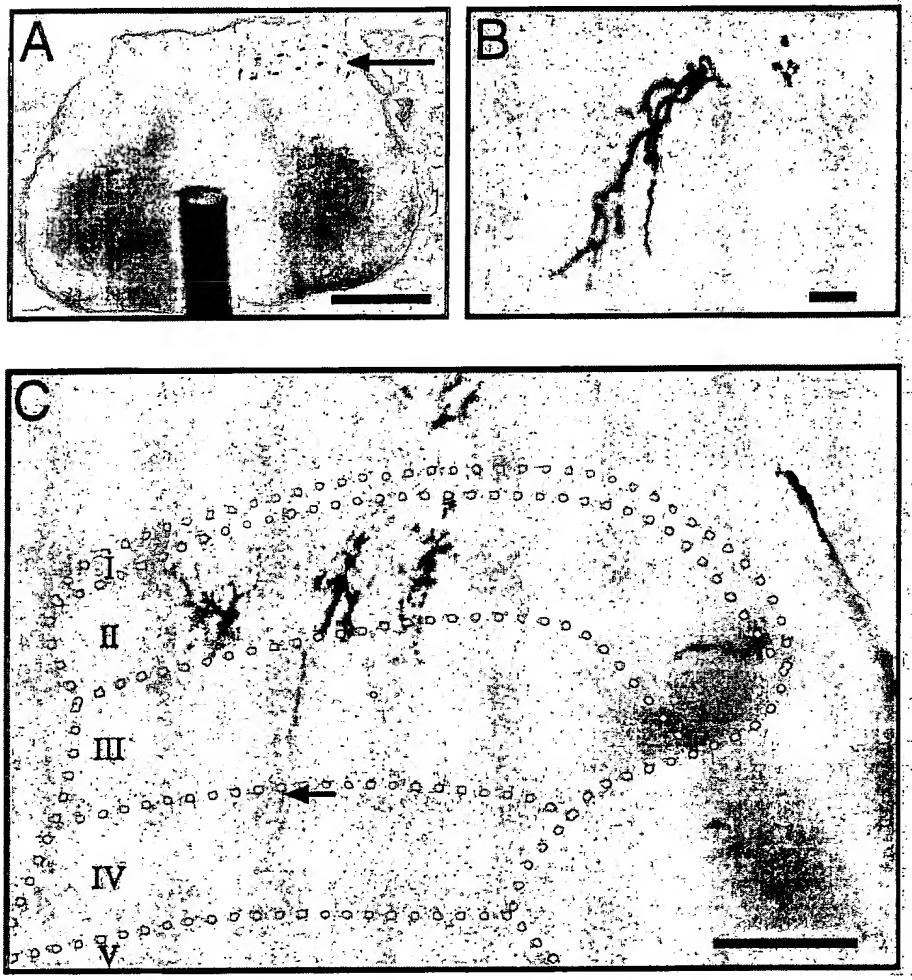

Figure 2. Identification of SG and SG neurons in the transverse spinal cord slices. *A*, Photomicrograph of the slice preparation from naive rat showing that the SG can be identified as a translucent pale area in the superficial dorsal horn (*dotted area*) enabling targeting of the recording electrode to the this region. Scale bar, 600 μm. *B*, A representative SG neuron injected with Neurobiotin. Scale bar, 20 μm. *C*, A low-power photomicrograph of a slice from naive rat showing SG neurons filled with Neurobiotin. Note all neurons lie within the middle third of the dorsoventral plane of SG and have the features typical of stalk cells. The dendrites of some cells extend ventrally into deeper laminae as indicated by the *arrow*. Scale bar, 150 μm.

stimulus intensity necessary to activate Aα/β, Aδ, and C fibers and the afferent fiber conduction velocity was determined by extracellular recording of compound action potentials from the dorsal root near the dorsal root entry zone in each experiment. The minimum stimulus intensities and duration to activate Aα/β, Aδ, and C fibers were ~10 μA (0.05 msec), 25 μA (0.05 msec), and 200 μA (0.5 msec), respectively (Fig. 1*A*,*B*; Table 1). In some experiments, focal stimulation was performed with a monopolar silver wire electrode (50 μm diameter), insulated except at the tip, positioned just distal to the dorsal root entry zone to estimate conduction velocity of the fibers responsible for particular synaptic responses.

Blind whole-cell patch-clamp recordings were made from neurons located in SG (Figs. 1*A*, 2*A*). With a light source directed under the slice, the SG, because of its relative lack of myelin is readily identifiable as a distinct translucent region in the superficial dorsal horn (Fig. 2*A*) (Yoshimura and Nishi, 1993). The recording electrodes were positioned, in all cases, under direct visual control into the middle third of SG, identified as above, in the dorsoventral plane and within its medial half in the mediolateral plane. The location of recorded neurons was confirmed in selected instances by the intrasomatic injection of Neurobiotin (0.3%; Vector Laboratories, Burlingame, CA).

Two pipette solutions were used in this study, the first, which was used in most cases with TEA and Cs, contained (in mM): Cs-sulfate 110, $CaCl_2$ 0.5, $MgCl_2$ 2, EGTA 5, HEPES 5, TEA 5, and ATP-Mg salt 5, and the second, without Cs and TEA, contained (in mM): potassium gluconate 135, KCl 5, $CaCl_2$ 0.5, $MgCl_2$ 2, EGTA 5, HEPES 5, ATP-Mg salt 5, and Na-GTP 0.5. The resistance of a typical patch pipette was 5–10 MΩ. Voltage-clamped neurons were held at a membrane potential of −70 mV for recording EPSCs and at 0 mV for recording IPSCs. At 0 mV, only IPSCs produce upward deflections (Baba et al., 1998), because the reversal potentials of EPSCs are ~0 mV (Yoshimura and Jessell, 1990).

Membrane currents were amplified with an Axopatch 200A amplifier (Axon Instruments, Foster City, CA) in voltage-clamp mode. Signals were filtered at 2 kHz and digitized at 5 kHz. Data were analyzed using pClamp 6 (Axon Instruments). Membrane potential and input resistance were measured shortly after establishing whole-cell clamp.

In preliminary experiments in 15 SG cells recorded in the absence of TEA/Cs in the pipette solution, no indication of an augmentation of K^+ channel-associated slow synaptic currents after inflammation was detected. Because the Cs/TEA-containing pipette solution, although obscuring such K^+ currents, improved space clamp and the capacity to

Table 2. Criteria for the classification of synaptic responses

Classification	Threshold	Monosynaptic (Fixed latency)	Polysynaptic (Variable latency)	Latency
Aβ mono	<50 μA	+		<2.2 msec
Aβ poly	<25 μA		+	
Aδ mono	>25 μA	+		2.2–10 msec
Aβ/Aδ poly	25–50 μA		+	
Aδ poly	>50 μA		+	
C mono	>200 μA	+		20–40 msec

record IPSCs, we used it to record the fast A fiber-mediated synaptic responses that were under investigation in this study.

Statistical analysis on differences in threshold and latencies of neurons recorded in control and inflamed tissue was performed using a nested ANOVA and on the proportions of cells with particular synaptic response by logistic regression with GEE techniques. Results presented are mean ± SD.

RESULTS

Identification of SG neurons

The neurons recovered after intrasomatic injection of Neurobiotin showed that targeting the electrode into the SG resulted in recordings from neurons with cell bodies in lamina II in all cases (n = 21) (Fig. 2*C*). These cells had, moreover, morphological features and cell body diameters similar to those described previously in the rat SG using Golgi (Beal and Bicknell, 1985) and intracellular HRP (Woolf and Fitzgerald, 1983)-labeling techniques and included stalked and islet cells, the most common cell types of the region. A distinctive feature in several cells was dendrites extending ventrally into the deeper laminae of the dorsal horn (Fig. 2*C*).

Membrane properties and spontaneous synaptic responses of SG neurons

The average membrane potentials of SG neurons recorded from naive preparations were −64.5 ± 6.2 mV (n = 21) and, in animals with inflammation they were −65.7 ± 7.4 mV (n = 25). Mean input resistance was 746 ± 357 MΩ (n = 11) in naive and 834 ± 453 MΩ (n = 14) in cells from inflamed animals, suggesting that similar sized cells were recorded in both cases. The frequency of spontaneous EPSCs was 35.9 ± 17.6 Hz (n = 12) from naive and 32.1 ± 24.1 Hz (n = 15) from cells recorded in preparations from inflamed animals. The frequency of spontaneous IPSCs was 23.2 ± 13.0 Hz (n = 5) in naive and 17.9 ± 10.7 Hz (n = 6) in preparations from inflamed animals. No significant differences in these passive and active membrane characteristics were detected between neurons recorded from slices prepared from naive and CFA-treated rats.

Primary afferent threshold and conduction velocity

Primary afferents could be divided into three distinct groups, corresponding to Aα/β, Aδ, and C fibers, on the basis of the threshold and conduction velocity of compound action potentials recorded extracellularly on the dorsal root (Fig. 1*B*). Figure 1*C* illustrates the stimulus response functions of Aα/β fiber and Aδ fiber volleys in the dorsal root at a pulse width of 50 μsec and shows that at <25 μA, only an Aβ wave is detectable with a maximum amplitude at 50 μA. Any new response elicited above 50 μA is likely to be, therefore, Aδ-mediated. It is possible that at thresholds below that necessary to detect an Aδ wave, a few single Aδ fibers may be activated. Table 1 shows that the stimulation thresholds and conduction velocities for the Aα/β, Aδ, and C fibers recorded in preparations from naive and rats with an inflamed hindpaw did not differ significantly. The values obtained for threshold and conduction velocity are in agreement with those found in earlier studies *in vivo* (Lynn and Carpenter, 1982; Harper and Lawson, 1985; Villiere and McLachlan, 1996).

Synaptic responses in SG neurons

Whole-cell patch-clamp recordings were made from 57 SG neurons in slices prepared from naive rats (n = 12) and 62 neurons in slices from rats inflamed 48 hr before with CFA (n = 14). All SG neurons recorded responded to orthodromic dorsal root stimulation. Table 2 shows the criteria for the classification of synaptic responses into Aβ or Aδ monosynaptic or polysynaptic in terms of threshold, response to repetitive inputs, and latency. Identification of EPSCs as monosynaptic was based on a constant latency and absence of failures with repetitive stimulation at a frequency of 20 Hz (Fig. 3*A*, *middle*, *bottom*) (Yoshimura and Jessell, 1989). Polysynaptic EPSCs, in contrast, had variable latencies and showed failures at 20 Hz (Fig. 3*A*, *top*; see Fig. 6*B*). At stimulus thresholds between 25 and 50 μA, it was not possible because of the stimulus response profile of the afferent volleys (Fig. 1*C*) to differentiate unambiguously any polysynaptic responses elicited into Aβ or Aδ, and we have classified these, therefore, as Aβ/Aδ (Table 2).

Most SG neurons recorded from naive rat slices exhibited either monosynaptic or polysynaptic Aδ fiber-mediated EPSCs. A small proportion of cells (25%) from the control preparations had Aβ fiber-mediated polysynaptic input, but none had a monosynaptic Aβ fiber input (Table 3), in agreement with earlier findings (Yoshimura and Nishi, 1993). No cells with an input exclusively from C-fibers were found. Polysynaptic IPSCs were recorded in some neurons at a holding membrane potential of 0 mV (Fig. 3*B*) and were mediated by $GABA_A$ and/or glycine receptors, as evidenced by the antagonism with bicuculline and strychnine (Fig. 3*C*). As for the EPSCs, the IPSCs in most SG neurons in naive rats were mediated by Aδ fibers, confirming the previous study (Yoshimura and Nishi, 1995), and only a small proportion of cells had Aβ fiber-mediated polysynaptic IPSCs (16%) (Table 3).

Synaptic responses in SG neurons recorded from rats with an inflamed hindpaw

In contrast to the naive situation, SG neurons recorded from slices obtained from rats with an inflamed hindpaw exhibited Aβ fiber-evoked polysynaptic EPSCs in the majority of cases (39 of 62; 63%; Table 3) ($p < 0.001$). No Aβ fiber-mediated monosynaptic EPSCs could be detected in these rats. Figure 4*A* shows the distribution of the minimum stimulus intensity threshold for eliciting EPSCs in slices from naive and rats with

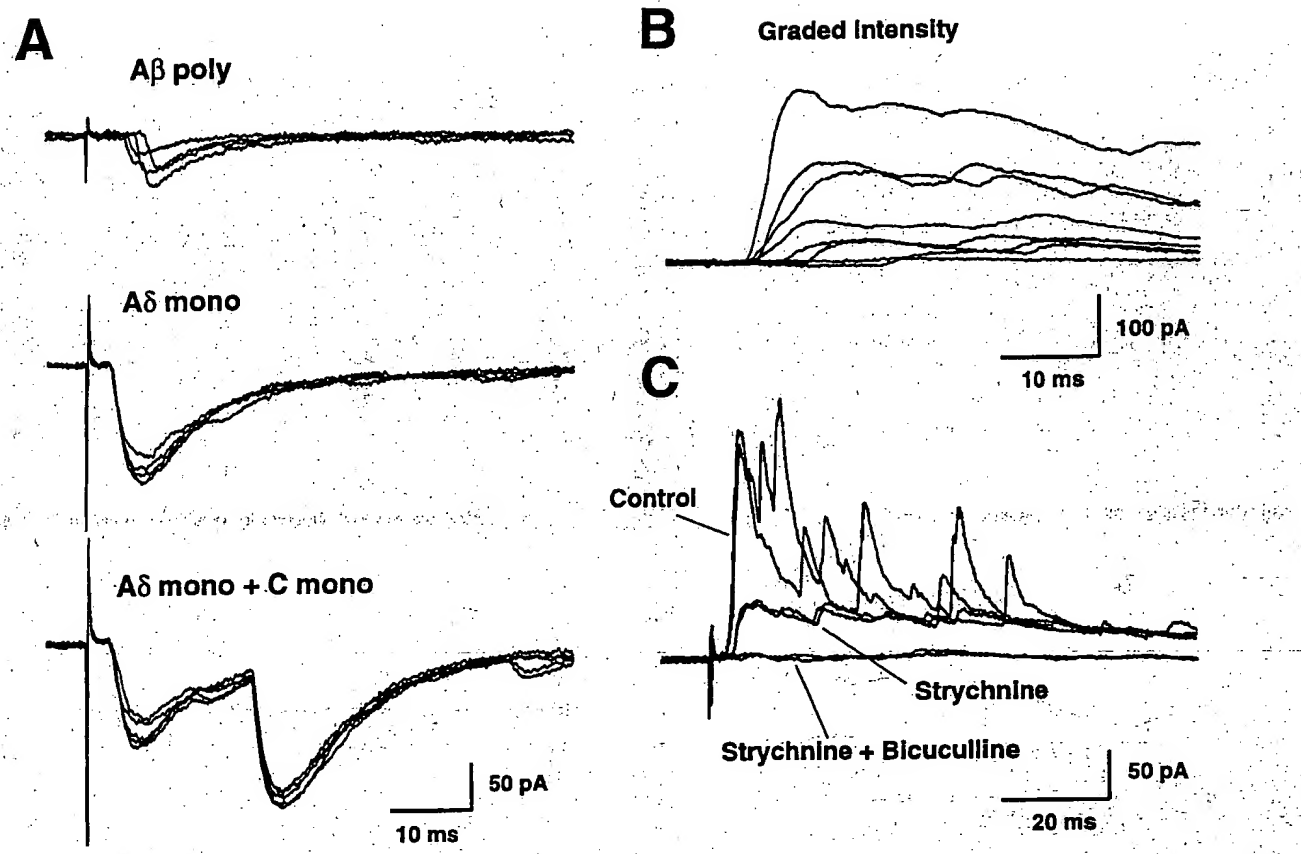

Figure 3. *A*, The *top*, *middle*, and *bottom* show respectively, EPSCs evoked by Aβ (14–20 μA, 0.05 msec), Aδ (32–50 μA, 0.05 msec), and C (200–500 μA, 0.5 msec) fiber intensities. Four to five traces are superimposed in each panel. *Top*, Aβ fiber-evoked polysynaptic EPSCs. *Middle*, Aδ fiber-evoked monosynaptic EPSCs. *Bottom*, Aδ and C fibers evoked monosynaptic EPSCs. Note that the latencies were constant for the monosynaptic EPSCs and variable in the polysynaptic responses. The above records were obtained from a single neuron. *B*, Polysynaptic IPSCs evoked by graded stimulation. As the intensity was increased from 15 to 40 μA, 0.05 msec, the latency of the IPSC shortened. *C*, The effects of strychnine (2 μM) and bicuculline (20 μM) on IPSCs. Strychnine eliminated the short-latency component of the IPSC, whereas bicuculline reduced the longer latency component.

Table 3. Classification of synaptic responses

	Aβ-mono	Aβ-poly	Aδ-mono	Aβ/Aδ poly	Aδ-poly	C-mono
EPSCs						
Naive (n = 57)	0 (0%)	14 (25%)	15 (26%)	25 (44%)	8 (14%)	8 (14%)
Inflamed (n = 62)	0 (0%)	39 (63%)	12 (19%)	19 (30%)	1 (2%)	6 (10%)
IPSCs						
Naive (n = 25)	0 (0%)	4 (16%)	0 (0%)	19 (76%)	2 (8%)	0 (0%)
Inflamed (n = 26)	0 (0%)	14 (54%)	0 (0%)	12 (46%)	0 (0%)	0 (0%)

inflammation. In slices from CFA-treated rats, the mean threshold intensity was 22.8 ± 11.3 μA, which was significantly lower than that in the naive preparations (33.2 ± 15.1 μA; $p <$ 0.001; n = 57 for naive rat and 62 for CFA-treated rats). The threshold in the inflamed preparations is well below that for eliciting Aδ volleys (Fig. 1*C*). This difference cannot be caused by changes in afferent fiber excitability because peripheral inflammation had no significant effect on either the thresholds or the conduction velocities of Aβ, Aδ, and C fibers (Table 1). Figure 5*A* shows the distribution of the latencies of EPSCs evoked at a stimulus intensity of 20 μA, 0.05 msec (above the threshold for Aβ but below the threshold of Aδ fibers). Mean latencies of EPSCs in naive and CFA-treated rats at this stimulus intensity were 6.0 ± 3.5 msec (n = 12) and 3.3 ± 1.8 msec (n = 36), respectively (p = 0.010). In the CFA-treated rats, Aβ fiber-mediated polysynaptic EPSCs with a very short latency (<2.0 msec), which is much shorter than that of Aδ fiber-mediated monosynaptic EPSCs (latency, 2.2–3.5 msec), could be detected (Fig. 5*A*, Fig. 6). These short-latency EPSCs were never recorded in cells from naive animals at this stimulus strength. The conduction velocity calculated by two point stimulation along the length of the dorsal root was in Aβ fiber range (>15 m/sec) (Fig. 6*C*). Stimulation at an intensity of 100 μA 0.05 msec, which is supramaximal for Aβ fibers and above the Aδ threshold (Fig. 5*B*), also resulted in a shorter mean latency of EPSC in inflamed rats (2.6 ± 1.0 msec; n = 60) than

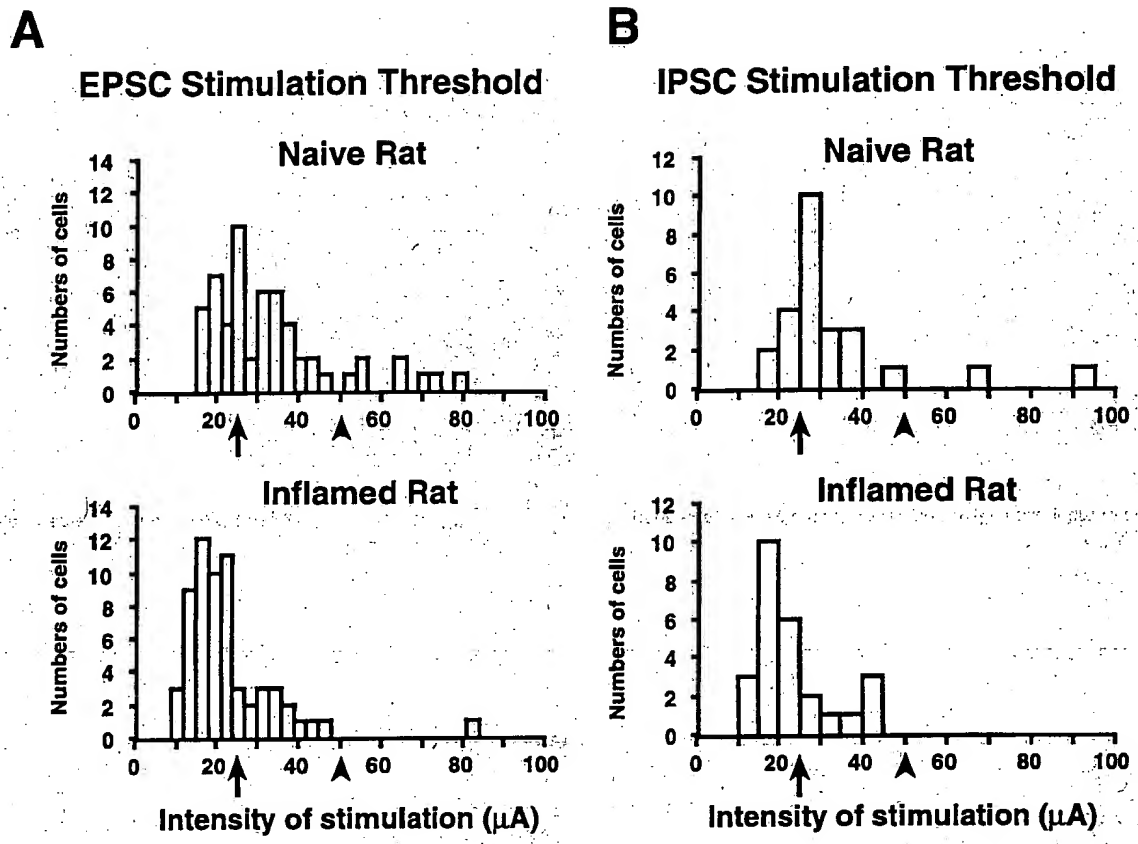

Figure 4. Distribution of the minimum stimulus threshold intensities necessary for eliciting EPSCs and IPSCs in cells recorded in the SG in slices from naive and CFA-treated rats. The mean stimulus threshold intensity required to evoke EPSCs in naive and CFA-treated rats was 33.2 ± 15.1 μA (n = 57) for naive and 22.8 ± 11.3 μA (n = 62) for CFA-treated rats ($p < 0.001$; nested ANOVA). The mean stimulus threshold intensity required to evoke IPSCs in naive and rats with an inflamed hindpaw was 32.5 ± 15.7 μA (n = 25) for naive and 21.9 ± 9.9 μA (n = 26) for the CFA-treated rats (p = 0.013; nested ANOVA). The *arrow* indicates the stimulus intensity at which an Aδ volley begins to be detected, all responses below this value are exclusively Aβ. The *arrowhead* represents the stimulus value at which a maximal Aβ volley is elicited. All responses elicited above this intensity are exclusively Aδ-evoked. For values between the *arrow* and the *arrowhead*, the responses evoked may be Aβ- and/or Aδ-evoked.

in naive rats (3.1 ± 1.1 msec; n = 53; $p < 0.05$). The suprathreshold stimulus also shortened the EPSC latency compared with the submaximal stimulus.

In SG neurons recorded from rats with inflammation, polysynaptic IPSCs were evoked by Aβ fiber intensity stimulation in about half of cells (14 of 26; 54%; Table 3), which is significantly greater than naives ($p < 0.001$). Figure 4*B* shows the distribution of the minimum stimulus intensity threshold for eliciting IPSCs in slices from naive and CFA-treated rats. In slices from rats with an inflamed hindpaw, the mean threshold intensity was 21.9 ± 9.9 μA, which was significantly lower than that in the naive preparations (32.5 ± 15.7 μA; p = 0.013; n = 25 for naive rat and 26 for inflamed group).

DISCUSSION

We have found that a localized peripheral inflammation for 48 hr results in a facilitation of short-latency fast Aβ fiber-mediated polysynaptic EPSCs and IPSCs in SG neurons that receive sensory input from sensory fibers innervating the inflamed area.

Aβ fiber-mediated synaptic input to the SG

There is substantial evidence that the primary function of neurons in the SG is to integrate noxious afferent information carried by the high-threshold Aδ and C fibers that terminate in this region of the superficial dorsal horn (Willis and Coggeshall, 1991). The SG cells, acting as inhibitory and excitatory interneurons, modify the output of projection neurons in both lamina I and the deeper layers of the dorsal horn (Willis and Coggeshall, 1991). The vast majority of SG neurons have high-threshold receptive fields, but an excitation of SG neurons by innocuous mechanical stimuli and Aβ fiber electrical stimulation has been reported in a small number of cells in *in vivo* studies (Kumazawa and Perl, 1978; Bennett et al., 1980; Woolf and Fitzgerald, 1983). Studies in adult spinal cord slices with an attached dorsal root show a similar picture. Although short-latency fast excitatory synaptic responses in SG cells in these preparations have been found to be predominantly mediated by Aδ fibers, Aβ fiber-mediated EPSCs are also detected, but only in a small proportion of SG neurons. These Aβ fiber-mediated EPSCs always have a variable and longer latency than the more common monosynaptic Aδ EPSCs (Yoshimura and Jessell, 1989; Yoshimura and Nishi, 1993). *In vitro* studies with immature young rat spinal cord preparations have not reported Aβ fiber-mediated fast EPSCs, which may reflect developmental changes or technical issues relating to the thickness of the slice and the length of dorsal root available (Bleazard et al., 1994; Randic et al., 1995; Sandkuhler et al., 1997).

Because Aβ fibers do not project directly to SG but to lamina III-VI (Brown, 1981; Woolf, 1987) and because the dendrites of many SG neurons do not leave SG (Light et al., 1979; Bennett et

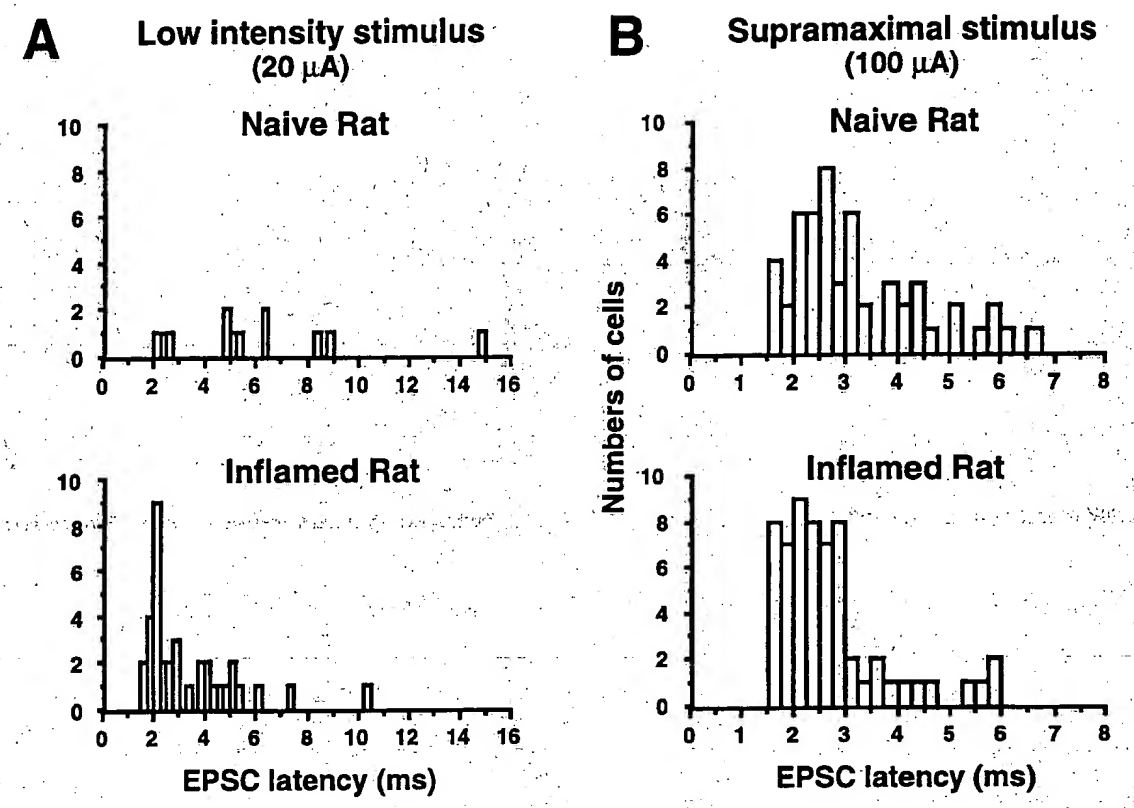

Figure 5. Distribution of the latencies of EPSCs in cells recorded in the SG in slices from naive and CFA-treated rats. *A*, The EPSC latencies evoked by Aβ fiber intensity (20 μA, 0.05 msec, below Aδ fiber threshold) were significantly shortened in the rats with an inflamed hindpaw; 3.3 ± 1.8 msec versus 6.0 ± 3.5 msec ($p = 0.010$; nested ANOVA; $n = 12$ in naive and $n = 36$ in inflamed rats). Aβ fiber-mediated EPSCs with short latencies (<2.0 msec) were only observed in the preparations from rats with an inflamed hindpaw. *B*, Distribution of the latencies of EPSCs evoked by supramaximal Aβ fiber stimulation intensity. Mean latency of EPSCs in CFA-treated rats was 2.6 ± 1.0 msec ($n = 60$), which was significantly shorter than that recorded in naive rats (3.1 ± 1.1 msec; $n = 53$; nested ANOVA; $p < 0.05$).

al., 1980), it has been commonly assumed that all responses to Aβ fiber stimulation must depend on polysynaptic pathways. In support of this is our failure ever to detect an Aβ fiber-evoked monosynaptic EPSC in the SG. However, there are some cells in the SG with dendrites that extend into the deep dorsal horn (Woolf and Fitzgerald, 1983; Fig. 2*C*). The question should be therefore, why, given this potential anatomical substrate for a direct Aβ input to some SG cells, has no such input ever been seen in naive animals or even after inflammation?

Potential mechanisms responsible for the facilitation of Aβ fiber mediated-input into SG after inflammation

There are two possible general mechanisms that could result in the recruitment of fast Aβ-evoked synaptic responses in the SG; a strengthening of pre-existing ineffective or silent synapses or the establishment of novel synapses by a structural alteration in synaptic connectivity. The former is likely to operate after inflammation, and the latter may well contribute to changes after nerve injury (Woolf et al., 1992). A functional change in synaptic connectivity could be caused by presynaptic or postsynaptic alterations, either increasing excitability or reducing inhibition and may operate at the first synapse between the afferent and dorsal horn neurons or on subsequent neurons in the polysynaptic chain that carries the Aβ fiber input to the SG from deep laminae. One example of a presynaptic change in primary afferents that could increase synaptic strength is a shift in transmitter content in A fibers. After inflammation, for example, some Aβ fibers, which are normally not substance P-immunoreactive, begin to express this peptide (Neumann et al., 1996). Aβ fibers also acquire the novel capacity to induce an NK1-mediated windup-like phenomenon (Thompson et al., 1994; Herrero and Cervero, 1996a,b). Inflammation also changes the nature of those peripheral stimuli that can evoke activity-dependent c-fos expression in the dorsal horn from predominantly nociceptors in the naive state (Hunt et al., 1987; Presley et al., 1990) to one that includes Aβ fibers (Ma and Woolf, 1996b). Other mechanisms that may potentially increase synaptic strength include increased transmitter release, increased postsynaptic receptors, reduced uptake or breakdown of transmitters, post-translational changes in receptor function, or alterations in postsynaptic membrane excitability. We found no change in the membrane potential of the SG neurons from CFA-pretreated preparations, but because the change in synaptic responsiveness was polysynaptic and not monosynaptic it is not possible to dissect out easily what is responsible and where it is acting. Nevertheless, inflammation has been shown to result in changes in the phenotype of dorsal horn neurons, including the upregulation of NK1 receptors and alterations in dynorphin expression so that postsynaptic mechanisms may be important (Ruda et al., 1988; Noguchi et al., 1991; Schafer et al., 1993; McCarson and Krause, 1994).

Although a decrease of GABAergic and glycinergic inhibition could result in an augmentation of Aβ fiber-mediated responses in the SG, this is unlikely because we found a facilitation of Aβ

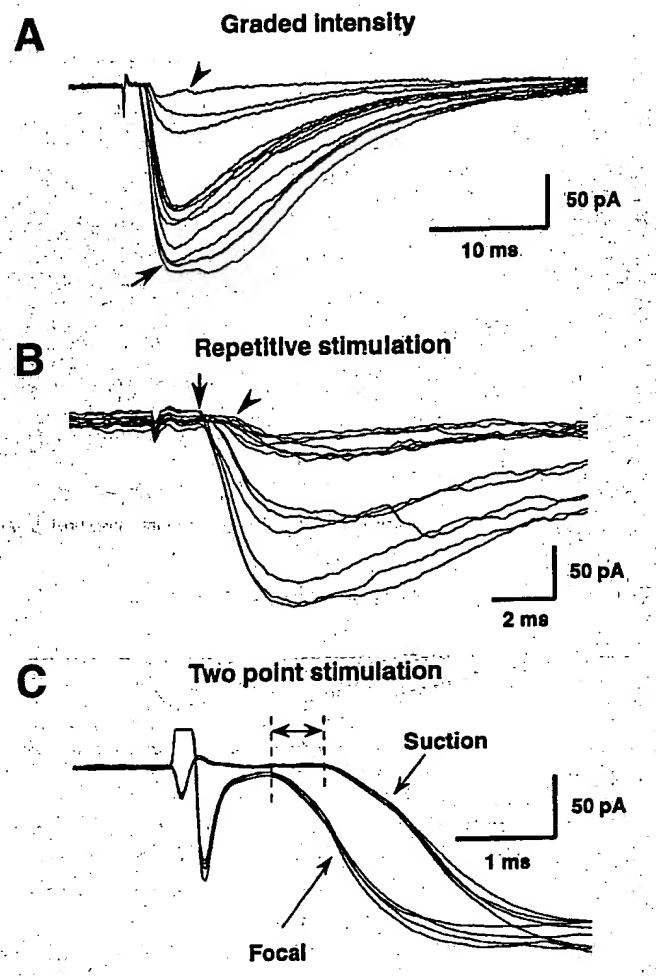

Figure 6. Aβ fiber-evoked polysynaptic EPSCs with short and variable latencies recorded in an SG cell from a slice from a rat with an inflamed hindpaw. *A*, The effect of stimulus intensity. As the intensity was increased (12–25 μA; 0.05 msec), the latency of the Aβ fiber-evoked EPSC shortened. The shortest latency was 1.6 msec at an intensity of 22–25 μA. The *arrowhead* identifies the EPSC evoked by the lowest, and the *arrow* identifies the EPSC evoked by the highest stimulus strengths. *B*, A shift in latency of the Aβ-evoked EPSCs was observed with 20 Hz repetitive stimulation at 25 μA, indicating a polysynaptic synaptic response. The *arrow* identifies the first EPSC, and the *arrowhead* identifies the last EPSC in the train. *C*, Stimulation of the dorsal root by a peripheral suction electrode and the entry zone with a focal electrode were performed to calculate the conduction velocity of fibers responsible for the evoked EPSC. Conduction velocity calculated by the difference of latencies was 32.5 m/sec (length of dorsal root, 19.5 mm).

fiber-mediated IPSCs as well as EPSCs after inflammation. We cannot exclude the possibility, however, that disinhibition occurs in laminae III or IV. This too seems unlikely, though, because both GABA and the $GABA_A$ receptor are upregulated in the dorsal horn after peripheral inflammation (Castro-Lopes et al., 1994).

After peripheral nerve injury, Aβ fibers sprout from lamina III into lamina II (Woolf et al., 1992), and Aβ fiber-mediated monosynaptic EPSCs, which are never normally observed in SG, can be detected (Okamoto et al., 1996). We have been unable, however, to detect any evidence of Aβ fiber sprouting after CFA inflammation at 48 hr (Q-P. Ma and C. Woolf, unpublished observations), which is in keeping with the lack of any monosynaptic input after this treatment.

Functional consequences of augmented Aβ input to the SG

Several studies recording from large cells in the deep dorsal horn have shown that inflammation alters receptive field size and properties (Ren et al., 1992a,b; Ren and Dubner, 1993). Synaptic input to lamina II cells is, as we show here, also modified. A recruitment of low-threshold mechanoreceptive input to nociceptive-specific neurons, including those in the superficial dorsal horn, occurs after central sensitization induced by capsaicin or mustard oil (Simone et al., 1989; Woolf et al., 1994). Central sensitization may contribute to the change in SG responsiveness to Aβ input after inflammation caused by an ongoing activity in C-fibers generated by the presence of inflammatory mediators in the inflamed tissue. Such a mechanism is unlikely, though, to be a major contributor in the present experiments, in which the sensory fibers are disconnected from the periphery, unless the inflammation-induced activity generates very long-lasting changes in membrane excitability.

The processing of sensory information in the spinal cord is dynamic, and it is this modifiability that is a major contributor to alterations in sensation after inflammation or nerve injury. The fact that an area of the spinal cord normally devoted almost exclusively to nociceptive input begins after inflammation to receive low-threshold synaptic input is a further indication of the plasticity of the system. What causes the changes and whether they contribute to inflammatory pain hypersensitivity needs now to be established.

REFERENCES

Baba H, Kohno T, Okamato M, Goldstein PA, Shimoji K, Yoshimura M (1998) Muscarinic facilitation of GABA release in substantia gelatinosa of the rat spinal dorsal horn. J Physiol (Lond) 508:83–93.

Beal JA, Bicknell HR (1985) Development and maturation of neurons in the substantia gelatinosa(SG) of the rat spinal cord. In: Development, organization and processing in somatosensory pathway (Rowe M, Willis Jr WD, eds), pp 23–30. New York: Wiley-Liss.

Bennett GJ, Abdelmoumene M, Hayashi H, Dubner R (1980) Physiology and morphology of substantia gelatinosa neurons intracellularly stained with horseradish peroxidase. J Comp Neurol 194:809–827.

Bleazard L, Hill RG, Morris R (1994) The correlation between the distribution of the NK1 receptor and the action of tachykinin agonists in the dorsal horn of the rat indicates that substance P does not have a functional role on substantia gelatinosa (lamina II) neurons. J Neurosci 14:7655–7664.

Brown AG (1981) Organization in the spinal cord: the anatomy and physiology of identified neurones. Berlin: Springer-Verlag.

Castro-Lopes JM, Tavares I, Tolle TR, Coimbra A (1994) Carragenan-induced inflammation of the hind foot provokes a rise of GABA-immunoreactive cells in the rat spinal cord that is prevented by peripheral neurectomy or neonatal capsaicin treatment. Pain 56:193–201.

Harper AA, Lawson SN (1985) Conduction velocity is related to morphological cell type in rat dorsal root ganglion neurons. J Physiol (Lond) 359:31–46.

Herrero JF, Cervero F (1996a) Changes in nociceptive reflex facilitation during carrageenan-induced arthritis. Brain Res 717:62–68.

Herrero JF, Cervero F (1996b) Supraspinal influences on the facilitation of rat nociceptive reflexes induced by carrageenan monoarthritis. Neurosci Lett 209:21–24.

Hunt SP, Pini A, Evan G (1987) Induction of c-fos-like protein in spinal cord neurones following sensory stimulation. Nature 328:632–634.

Koltzenburg M, Torebjork HE, Wahren LK (1994) Nociceptor modulated central sensitization causes mechanical hyperalgesia in acute chemogenic and chronic neuropathic pain. Brain 117:579–591.

Kumazawa T, Perl ER (1978) Excitation of marginal and substantia gelatinosa neurons in the primate spinal cord: indications of their place in dorsal horn functional organization. J Comp Neurol 177:417–434.

Levine JD, Taiwo YO (1994) Inflammatory pain. In: Textbook of pain (Wall PD, Melzack R, eds), pp 45–56. Edinburgh: Churchill Livingstone.

Light AR, Trevino DL, Perl ER (1979) Morphological features of functionally defined neurons in the marginal zone and substantia gelatinosa of the spinal dorsal horn. J Comp Neurol 186:151–172.
Lynn B, Carpenter SE (1982) Primary afferent units from the hairy skin of the rat hind limb. Brain Res 238:29–43.
Ma Q-P, Woolf CJ (1996a) Progressive tactile hypersensitivity: an inflammation-induced incremental increase in the excitability of the spinal cord. Pain 67:97–106.
Ma Q-P, Woolf CJ (1996b) Basal and touch-evoked fos-like immunoreactivity during experimental inflammation in the rat. Pain 67:307–316.
McCarson KE, Krause JE (1994) NK-1 and NK-3 type tachykinin receptor mRNA expression in the rat spinal cord dorsal horn is increased during adjuvant or formalin-induced nociception. J Neurosci 14:712–720.
Neumann S, Doubell TP, Leslie TA, Woolf CJ (1996) Inflammatory pain hypersensitivity mediated by phenotypic switch in myelinated primary sensory neurones. Nature 384:360–364.
Noguchi K, Kowalski K, Traub R, Solodkin A, Iadarola MJ, Ruda MA (1991) Dynorphin expression and fos-like immunoreactivity following inflammation induced hyperalgesia are co-localized in spinal cord neurons. Brain Res Mol Brain Res 10:227–233.
Okamoto M, Yoshimura M, Baba H, Higashi H, Shimoji K (1996) Synaptic plasticity of substantia gelatinosa neurons in the chronic pain model rat. Jpn J Physiol 46:S136.
Presley RW, Menetrey D, Levine JD, Bausbaum AI (1990) Systemic morphine suppresses noxious stimulus-evoked fos protein-like immunoreactivity in the rat spinal cord. J Neurosci 10:323–335.
Randic M, Cheng G, Kojic L (1995) k-opioid receptor agonists modulate excitatory transmission in substantia gelatinosa neurons of the rat spinal cord. J Neurosci 15:6809–6826.
Ren K, Dubner R (1993) NMDA receptor antagonists attenuate mechanical hyperalgesia in rats with unilateral inflammation of the hindpaw. Neurosci Lett 163:22–26.
Ren K, Hylden JLK, Williams GM, Ruda MA, Dubner R (1992a) The effects of a non-competitive NMDA receptor antagonist, MK-801, on behavioural hyperalgesia and dorsal horn neuronal activity in rats with unilateral inflammation. Pain 50:331–344.
Ren K, Williams GM, Hylden JLK, Ruda MA, Dubner R (1992b) The intrathecal administration of excitatory amino acid receptor antagonists selectively attenuated carrageenan-induced behavioral hyperalgesia in rats. Eur J Pharmacol 219:235–243.
Ruda MA, Iadarola MJ, Cohen LV, Young WS, III (1988) In situ hybridization histochemistry and immunocytochemistry reveal and increase in spinal dynorphin biosynthesis in a rat model of peripheral inflammation and hyperalgesia. Proc Natl Acad Sci USA 85:622–626.
Sandkuhler J, Chen JG, Cheng G, Randic M (1997) Low-frequency stimulation of afferent Aδ-fibers induces long term depression at primary afferent synapses with substantia gelatinosa neurons in the rat. J Neurosci 17:6483–6491.
Schafer MK, Nohr D, Krause JE, Weihe E (1993) Inflammation-induced upregulation of NK1 receptor mRNA in dorsal horn neurones. NeuroReport 4:1007–1010.
Simone DA, Baumann TK, Collins JG, LaMotte RH (1989) Sensitization of cat dorsal horn neurons to innocuous mechanical stimulation after intradermal injection of capsaicin. Brain Res 486:185–189.
Stein C, Millan MJ, Herz A (1988) Unilateral inflammation of the hindpaw in rats as a model of prolonged noxious stimulation: alterations in behavior and nociceptive thresholds. Pharmacol Biochem Behav 31:445–451.
Thompson SW, King AE, Woolf CJ (1990) Activity-dependent changes in rat ventral horn neurones *in vitro*: summation of prolonged afferent evoked postsynaptic depolarizations produce a D-APV sensitive windup. Eur J Neurosci 2:638–649.
Thompson SW, Woolf CJ, Sivilotti LG (1993) Small caliber afferents produce a heterosynaptic facilitation of the synaptic responses evoked by primary afferent A fibres in the neonatal rat spinal cord *in vitro*. J Neurophysiol 69:2116–2128.
Thompson SW, Dray A, Urban L (1994) Injury-induced plasticity of spinal reflex activity: NK1 neurokinin receptor activation and enhanced A- and C-fiber mediated responses in the rat spinal cord *in vitro*. J Neurosci 14:3672–3687.
Torebjork HE, Lundberg LER, LaMotte RH (1992) Central changes in processing of mechanoreceptor input in capsaicin-induced sensory hyperalgesia in humans. J Physiol (Lond) 448:765–780.
Villiere V, McLachlan EM (1996) Electrophysiological properties of neurons in intact rat dorsal root ganglia classified by conduction velocity and action potential duration. J Neurophysiol 76:1924–1941.
Willis WD, Coggeshall RE (1991) Sensory mechanisms of the spinal cord. New York: Plenum.
Woolf CJ (1983) Evidence for a central component of post-injury pain hypersensitivity. Nature 306:686–688.
Woolf CJ (1987) Central terminations of cutaneous mechanoreceptive afferents in the rat lumbar spinal cord. J Comp Neurol 261:105–119.
Woolf CJ, Fitzgerald M (1983) The properties of neurons recorded in the superficial dorsal horn of the rat spinal cord. J Comp Neurol 221:313–328.
Woolf CJ, King AE (1990) Dynamic alterations in the cutaneous mechanoreceptive fields of dorsal horn neurons in the rat spinal cord. J Neurosci 10:2717–2726.
Woolf CJ, Shortland P, Coggeshall RE (1992) Peripheral nerve injury triggers central sprouting of myelinated afferents. Nature 355:75–77.
Woolf CJ, Shortland P, Sivilotti LG (1994) Sensitization of high mechanothreshold superficial dorsal horn and flexor motor neurons following chemosensitive primary afferent activation. Pain 58:141–155.
Yoshimura M, Jessell TM (1989) Primary afferent evoked synaptic responses and slow potential generation in rat substantia gelatinosa neurons *in vitro*. J Neurophysiol 62:96–108.
Yoshimura M, Jessell TM (1990) Amino acid-mediated EPSPs at primary afferent synapses with substantia gelatinosa neurones in the rat spinal cord. J Physiol (Lond) 430:315–335.
Yoshimura M, Nishi S (1993) Blind patch-clamp recordings from substantia gelatinosa neurons in adult rat spinal cord slices: pharmacological properties of synaptic currents. Neuroscience 53:519–526.
Yoshimura M, Nishi S (1995) Primary afferent-evoked glycine- and GABA-mediated IPSPs in substantia gelatinosa neurones in the rat spinal cord *in vitro*. J Physiol (Lond) 482:29–38.

The Journal of Neuroscience, November 1, 1997, 17(21):8476–8490

Nerve Growth Factor Treatment Increases Brain-Derived Neurotrophic Factor Selectively in TrkA-Expressing Dorsal Root Ganglion Cells and in Their Central Terminations within the Spinal Cord

G. J. Michael,[1] S. Averill,[1] A. Nitkunan,[2] M. Rattray,[3] D. L. H. Bennett[2], Q. Yan,[4] and J. V. Priestley[1]

[1]Department of Anatomy, Faculty of Basic Medical Sciences, Queen Mary and Westfield College, London 31 4NS, United Kingdom, Departments of [2]Physiology and [3]Biochemistry, United Medical and Dental Schools, St. Thomas's Hospital Medical School Campus, London SE1 7EH, United Kingdom, and [4]Amgen Inc., Amgen Centre, Thousand Oaks, California 91320-1789

Using immunocytochemistry and *in situ* hybridization, we have examined the expression of brain-derived neurotrophic factor (BDNF) and of neurotrophin receptors in dorsal root ganglion cells. In the adult rat, BDNF mRNA and protein were found mainly in the subpopulation of cells that express the nerve growth factor (NGF) receptor trkA and the neuropeptide calcitonin gene-related peptide (CGRP). NGF increased BDNF within the trkA/CGRP cells to the extent that almost 90% of trkA cells contained BDNF mRNA after intrathecal NGF treatment, and 80–90% of BDNF-expressing cells contained trkA. Non-trkA cells that expressed BDNF included some trkC cells and some small cells that labeled with the lectin *Griffonia simplicifolia* IB4, a marker for cells that do not express trks. However, very few trkB cells expressed either BDNF mRNA or protein, and NGF did not increase BDNF expression in non-trkA cells. BDNF protein was anterogradely transported both peripherally and centrally. The central transport resulted in BDNF immunoreactivity in CGRP containing terminal arbors in the dorsal horn of the spinal cord, and this immunoreactivity was increased by NGF treatment. Electron microscopic analysis revealed that the BDNF immunoreactivity was present in finely myelinated and unmyelinated axons and in axon terminals, where it was most concentrated over dense-cored vesicles.

Our data do not support an autocrine or paracrine role for BDNF within normal dorsal root ganglia, but indicate that BDNF may act as an anterograde trophic messenger. NGF levels in the periphery could influence dorsal horn neurons via release of BDNF from primary afferents.

Key words: brain-derived neurotrophic factor; mRNA; trkA; trkB; NGF; dorsal root ganglion cells; primary afferent; calcitonin gene-related peptide

Brain-derived neurotrophic factor (BDNF) is a member of a small family of related molecules termed neurotrophins, the other mammalian members being nerve growth factor (NGF), neurotrophin (NT)-3, and NT-4/5. The neurotrophins exert their effects through a family of tyrosine kinase (trk) receptors comprising trkA (selective for NGF), trkB (selective for BDNF and NT-4/5), and trkC (selective for NT-3) (for review, see Maness et al., 1994).

All three trks are expressed within adult dorsal root ganglia (McMahon et al.,1994; Kashiba et al., 1995; Wright and Snider, 1995), and all members of the neurotrophin family show retrograde transport to dorsal root ganglia from peripheral nerves (DiStefano et al., 1992; Curtis et al., 1995). BDNF, however, is unusual in being also produced by adult dorsal root ganglion (DRG) cells (Ernfors et al., 1990, 1993; Wetmore and Olson, 1995; Apfel al., 1996; Cho et al., 1997), although the role of this BDNF is not known. An autocrine role has been proposed on the basis of studies of single-neuron microcultures (Acheson et al., 1995). Alternatively, BDNF protein has been suggested to be released locally to act in a paracrine manner on trkB cells (Apfel et al., 1996); however, there is little information regarding the dorsal root ganglion (DRG) subtypes that synthesize BDNF. Two studies have recently reported that NGF increases BDNF mRNA in trkA-expressing cells (Apfel et al., 1996; Cho et al., 1997), but it is not known whether trkB or trkC cells synthesize BDNF. It is also not known how the expression of BDNF protein and/or mRNA relates to subgroups of DRG cells defined according to widely used neurochemical criteria (Hunt et al., 1992; Lawson, 1992). BDNF is axonally transported by DRG cells to their central and/or peripheral processes (Zhou and Rush, 1996), but the cell type involved is not known.

The role of BDNF in DRG cells is given added importance by the fact that BDNF synthesis is greatly increased after nerve injury (Ernfors et al., 1993). Nerve damage causes the central terminals of large-diameter DRG cells to sprout within the dorsal horn (Woolf et al., 1992), and this sprouting can be prevented by NGF treatment (Bennett et al., 1996a). The stimulus for the sprouting is not known, but it has been suggested that it might be in response to BDNF released from the terminals of small-diameter DRG cells (Mannion et al., 1996). BDNF released from primary afferents might have profound effects on both spinal cord anatomy and physiology.

Received April 23, 1997; revised July 21, 1997; accepted Aug. 12, 1997.

This work was supported by the Medical Research Council (UK) and the Wellcome Trust. We thank Professor J. M. Polak and Dr. D. O. Clary for provision of rabbit CGRP and trkA antibodies. Human recombinant NGF was a generous gift of Genentech Inc.

Correspondence should be addressed to Professor J. V. Priestley, Department of Anatomy, Faculty of Basic Medical Sciences, Queen Mary and Westfield College, Mile End Road, London E1 4NS, UK.

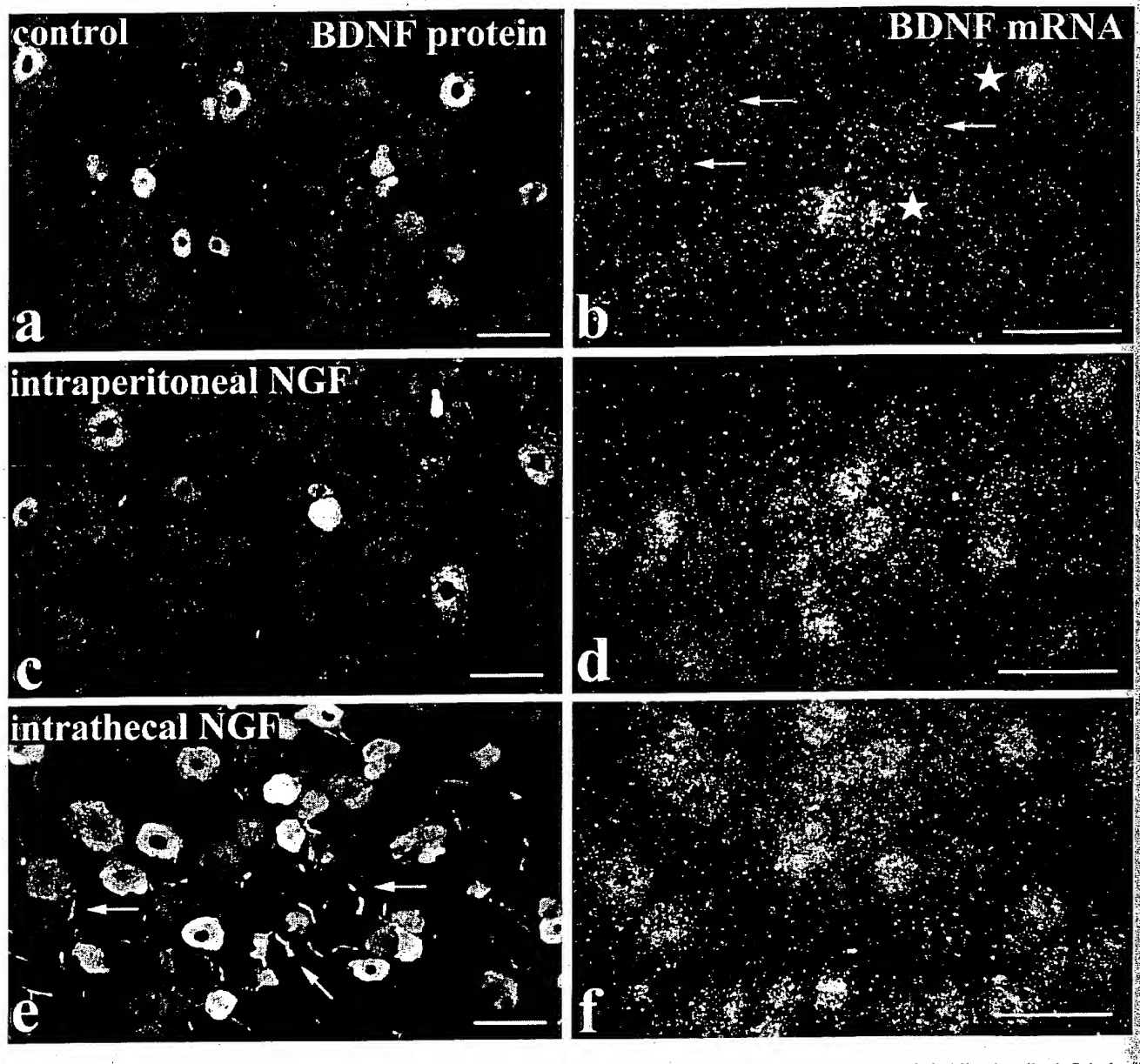

Figure 1. BDNF mRNA and protein are increased by NGF treatment. BDNF immunofluorescence (*a, c, e*) and *in situ* hybridization (*b, d, f*) in lumbar ganglia of control (*a, b*), intraperitoneal NGF-treated (*c, d*), and intrathecal NGF-treated (*e, f*) rats. BDNF immunoreactivity is present in small to medium sized DRG cells and is increased after NGF treatment. The increase is most evident after intrathecal NGF (*e*), where immunoreactivity is seen not only in a larger number of DRG cells but also in neighboring axons (*arrows*). NGF treatment also increases expression of BDNF mRNA. In control tissue (*b*), a few heavily labeled cells are seen (*stars*) together with scattered light labeling (*arrows*). The number of heavily labeled cells is increased after intraperitoneal NGF (*d*) and increased even more by intrathecal NGF (*f*). Scale bars, 100 μm.

To clarify some of these issues we have used *in situ* hybridization and immunocytochemistry to establish the DRG cell types that express BDNF and the changes that take place in response to systemic or intrathecal NGF. We have also examined axonal transport of BDNF protein, its distribution in the spinal cord, and its subcellular location within axon terminals.

A preliminary report of some of this work has been published previously in abstract form (Priestley et al., 1996).

MATERIALS AND METHODS

Tissue preparation. A total of 18 adult male Wistar rats (200–400 gm body weight) were processed for BDNF immunocytochemistry or *in situ* hybridization. Four of these had 1 mg/kg intraperitoneal injections of recombinant human NGF 13 or 24 hr before perfusion, four had intra-

Table 1. The effect of intraperitoneal NGF (IP NGF) or intrathecal NGF on the percentage of DRG cells expressing BDNF mRNA, BDNF immunoreactivity, or trkA immunoreactivity

	Control	IP NGF	Intrathecal NGF
BDNF immunoreactivity	22.3 ± 1.2% (3)	22.3 ± 3.3% (3)	40 ± 1.5% (4)**
BDNF mRNA	28.5 ± 3.3% (4)	43.7 ± 4.4% (3)*	37.8 ± 1.4% (4)*
TrkA immunoreactivity	37.8 ± 2.2% (4)	37.5 ± 2.0% (4)	42.3 ± 3.1% (3)

The figures in brackets indicate the number of animals analyzed. * indicates significantly different from controls at $p < 0.05$; ** indicates $p < 0.001$.

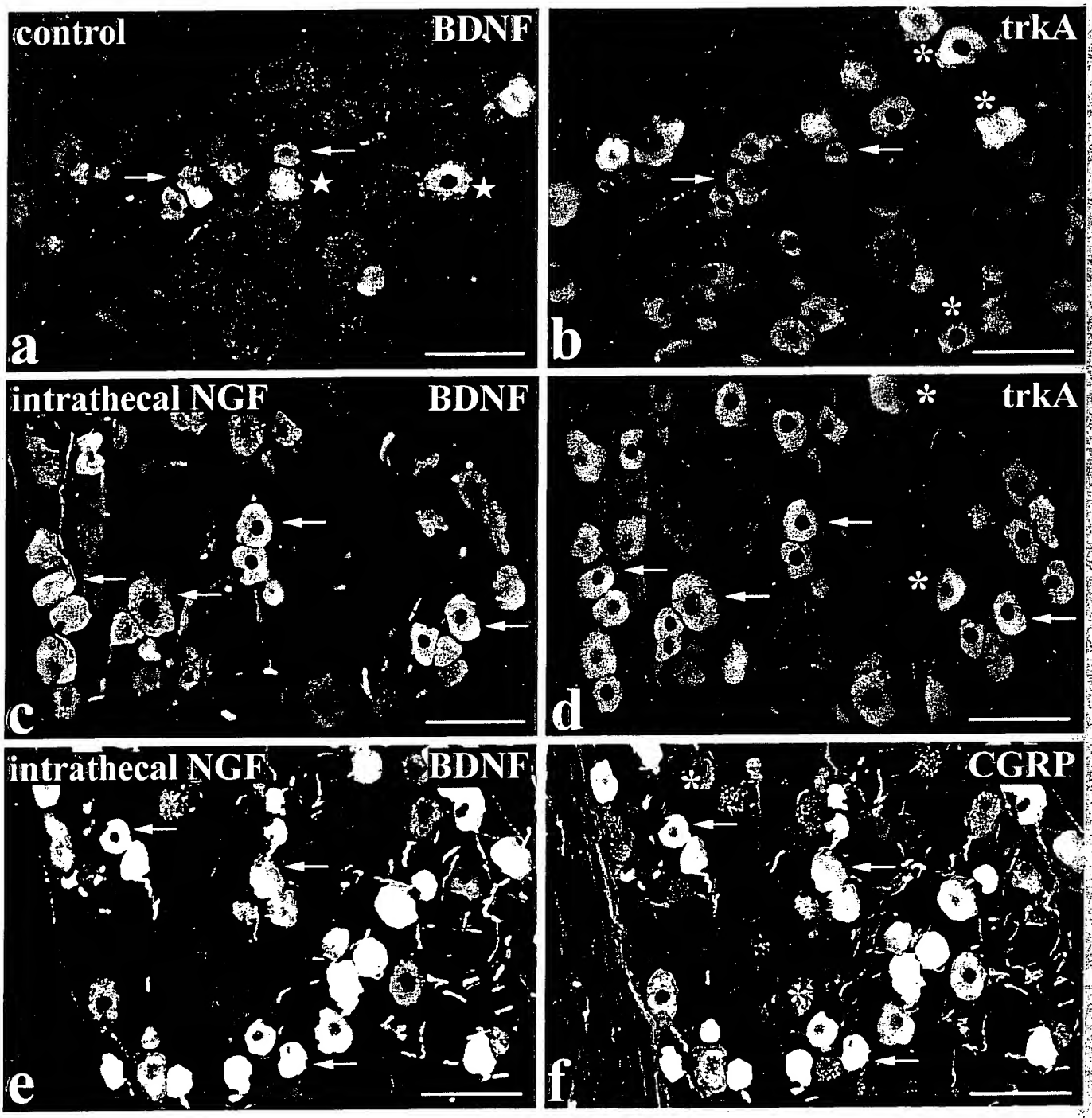

Figure 2. BDNF immunoreactivity is present in trkA/CGRP cells and is increased by NGF treatment. Double-labeling for BDNF (*a, c, e*) and either trkA (*b, d*) or CGRP (*f*) immunofluorescence in lumbar ganglia of control (*a, b*) and intrathecal NGF-treated (*c–f*) rats is shown. In both control and intrathecally treated animals, the majority of BDNF-immunoreactive DRG cells are also trkA immunoreactive (*a–d*). However, because intrathecal NGF increases the level of BDNF immunoreactivity, the number of trkA-immunoreactive cells that double-label for BDNF is increased in *c* and *d* compared with *a* and *b*. A similar situation occurs for BDNF and CGRP double-labeling, with extensive coexistence of BDNF and CGRP evident after intrathecal NGF treatment (*e, f*). *Arrows* indicate BDNF/trkA or BDNF/CGRP double-labeled cells; *asterisks* indicate cells single-labeled for trkA or CGRP; *stars* indicate cells single-labeled for BDNF. Scale bars, 100 μm.

thecal NGF, and five had unilateral ligations of dorsal roots or sciatic nerves.

Intrathecal delivery of NGF was performed basically as described previously (Bennett et al., 1996a). A laminectomy of the L5 and L6 vertebrae was performed under pentobarbitone anesthesia (Sagatal, Rhône Mérieux Ltd., UK) (40 mg/kg, i.p.). The dura was cut, and a SILASTIC tube (0.6 mm diameter) was passed intrathecally so that its tip lay over the lumbar enlargement. Alternatively, a tube was introduced through the foramen magnum and passed intrathecally to lie over the cervical cord. NGF (1 mg/ml in saline) was infused using a mini-osmotic pump (Alzet type 2002, Alza Corp., Palo Alto, CA) at a rate of 0.5 μl/hr for a period of 1–2 weeks. For ligation of dorsal roots, a laminectomy of

Table 2. The effect of intraperitoneal NGF (IP NGF) or intrathecal NGF on the percentage of BDNF-expressing DRG cells that also exhibit trkA or CGRP immunoreactivity

	Control		IP NGF		Intrathecal NGF	
	% of BDNF expressing other	% of other expressing BDNF	% of BDNF expressing other	% of other expressing BDNF	% of BDNF expressing other	% of other expressing BDNF
BDNF and trkA immunoreactivities	46% (200/434)	21% (200/931)	49% (207/421)	29% (207/721)	91% (201/221)	84% (201/268)
BDNF and CGRP immunoreactivities	68% (131/192)	20% (131/644)	44% (227/511)	21% (227/1088)	96% (322/335)	76% (322/424)
BDNF mRNA and trkA immunoreactivity	44% (301/507)	30% (301/810)	80% (900/1241)	60% (900/1311)	79% (540/685)	88% (540/603)

The figures in brackets indicate the number of cells counted.

the L2 and L3 vertebrae was performed, and the L4 and L5 roots were tied with a single or double 5/0 silk ligature. For peripheral nerve ligation, the sciatic nerve was exposed under pentobarbitone anesthesia and tied with a single or double 5/0 ligature at midthigh level. Ligation was performed on control rats and on rats that received intraperitoneal NGF 24 hr before ligation. Perfusion was performed 12–24 hr after ligation.

Rats were anesthetized with sodium pentobarbital (60 mg/kg) and perfused through the ascending aorta with 30 ml vascular rinse followed by 300 ml 4% paraformaldehyde in 0.1 M phosphate buffer. After 2.5–3.0 hr post-fixation, tissue blocks were cryoprotected in 15% sucrose, and 8–12 μm sections were cut on a cryostat. Sections were then stained using one of the following procedures: light microscopic immunocytochemistry, *in situ* hybridization, combined immunofluorescence and *in situ* hybridization, or preembedding electron microscopic immunocytochemistry.

Light microscopic immunocytochemistry. Sections were stained using standard single or dual color indirect labeled immunofluorescence or indirect tyramide signal amplification (TSA) (NEN) fluorescence procedures (Priestley, 1997). Incubations consisted of 1 hr in 10% normal serum followed by 18–36 hr in primary antibody and 3 hr in developing secondary antisera. For BDNF labeling, an affinity-purified rabbit antibody raised against recombinant human BDNF was used at 1:500 (indirect labeled procedure) or at 1:2000–1:5000 (TSA procedure). For double-labeling, this antibody was combined with one of the following: rabbit or sheep (Affiniti) CGRP polyclonal antisera (1:2000), rabbit polyclonal antiserum directed against the extracellular domain of trkA (code-labeled RTA, used at 2.5 μg/ml), or *Griffonia simplicifolia* IB4 lectin (Sigma, Poole, UK), which recognizes terminal α-galactose residues (12.5 μg/ml biotinylated IB4). The characteristics and staining specificity of all these markers have been reported previously (BDNF, Yan et al., 1997; RTA, Clary et al., 1994, Averill et al., 1995; rabbit CGRP, Merighi et al., 1988; goat CGRP and IB4, Averill et al., 1995). Controls for double-labeling included reversing the order of the primary antisera, as well as omitting the first or second primary antiserum. The two sets of antisera were applied sequentially, and this normally involved BDNF TSA followed by indirect labeled immunofluorescence. Although two primary antisera raised in rabbit were sometimes combined, nonspecific double-labeling was not observed. A similar protocol has been used by other workers (Hunyady et al., 1996; Shindler and Roth, 1996), and the lack of cross-reactivity is thought to be attributable to the fact that the TSA procedure allows the first series primary antibody to be used at a dilution that is too high to be detected by the second reagent set. Our data support this explanation. In control single-labeling using indirect labeled immunofluorescence, we were unable to visualize the BDNF antiserum at the dilutions used for the TSA procedure.

Secondary reagents used for indirect immunofluorescence included both FITC- and TRITC-labeled anti-rabbit IgG and anti-sheep IgG affinity-purified antisera (Jackson ImmunoResearch, West Grove, PA) (1:100 dilution) and 1:200 ExtrAvidin-FITC (for IB4 localization; Sigma). TSA labeling was performed using biotinylated goat anti-rabbit IgG (1:400) (Vector, Burlingame, CA) and Vectastain Elite peroxidase reagent (Vector) followed by biotinyl tyramide (NEN TSA-indirect kit) and ExtrAvidin-FITC (1:500, Sigma). After incubation in secondary reagents, sections were washed briefly in PBS and then mounted in PBS/glycerol (1:3) containing 2.5% 1,4 diazobicyclo (2,2,2) octane (antifading agent; Sigma).

In situ *hybridization.* Oligonucleotide probes complementary to bases 273–306 of the rat BDNF sequence (Timmusk et al., 1993), bases 124–157 of the rat trkA sequence (Meakin et al., 1992), bases 2213–2246 of the rat trkB sequence (Middlemas et al., 1991), and bases 1099–1132 of the rat trkC sequence (Valenzuela et al., 1993) were synthesized (Genosys) and then hybridized to cryostat sections using standard procedures (Michael and Priestley, 1995, 1996a). The trkB probe was directed against a portion of the tyrosine kinase domain and designed only to recognize full length receptors. The probes were labeled at the 3′ end with ^{35}S-dATP (Dupont NEN, Wilmington, DE) and terminal transferase (Promega, Madison, WI) to specific activities of ~5000 Ci/mmol. Sections were acetylated in 0.25 M acetic anhydride/0.1 M triethanolamine for 10 min, dehydrated in ethanols (70–100%), and delipidated with chloroform. Hybridizations were performed overnight at 37°C using probe concentrations of 2 nM. Hybridization buffer consisted of 4× SSC (1× SSC = 150 mM sodium chloride, 15 mM sodium citrate, pH 7.0), 50% deionized formamide, 0.04% Ficoll-400, 0.04% polyvinylpyrrolidone, 0.04% bovine serum albumin, 10% dextran sulfate, 0.1% SDS, 20 mM dithiothreitol (DTT), 20 μg/ml yeast tRNA, 100 μg/ml sheared salmon sperm DNA, and 10 μg/ml poly adenylate.

After hybridization, sections received two (15 min) washes at room temperature (RT) in 2× SSC, two at 50°C in 1× SSC, and one at 50°C in 0.2× SSC. Sections were washed an additional 2 hr at RT in 1× SSC, dehydrated through ethanols, dipped in autoradiographic emulsion (Amersham LM1), and exposed for 4–8 weeks. After development, slides were counterstained with toluidine blue, dehydrated, and coverslipped.

In situ *hybridization combined with immunofluorescence.* Immunofluorescence was followed by oligonucleotide *in situ* hybridization, as described previously (Priestley et al., 1993; Michael and Priestley, 1996b). Standard indirect immunofluorescence was performed as described above, except that antisera were diluted in diethylpyrocarbonate-treated PBS containing 0.5–5 mM DTT and 100 U/ml RNasin (Promega) in addition to 0.2% Triton X-100. After they were immunostained, sections were processed as for single BDNF *in situ* hybridization, except that developed sections were mounted in PBS/glycerol instead of being toluidine blue-counterstained and dehydrated. Silver grains in PBS/glycerol mounted sections were visualized using epipolarized illumination (Priestley et al., 1993).

Pre-embedding electron microscopic immunocytochemistry. Four animals were perfused with 4% paraformaldehyde, 0.1% glutaraldehyde in 0.1 M phosphate buffer and processed for electron microscopic immunocytochemistry using standard preembedding procedures (Priestley et al., 1992). The spinal cord was dissected out, post-fixed 2.5 hr in the same fixative, and immersed in PBS. Sections (40 μm) were cut using a vibratome (Oxford) and pretreated with 1% sodium borohydride in PBS for 30 min before they were immunostained. Sections were incubated for 30 min in 10% normal goat serum and then transferred to BDNF polyclonal antibody (1:1000) for 12 hr at 4°C. Primary antibody was subsequently revealed using 1:400 biotinylated goat anti-rabbit IgG (Vector) and Vectastain Elite peroxidase reagent (Vector). Sections were then developed with a solution containing 0.05% 3,3′-diaminobenzidine, 0.04% $(NH_4)_2SO_4.NiSO_4$, and 0.01% H_2O_2 in 0.1 M phosphate buffer, pH 7.3. Unless stated otherwise, incubations were performed at RT, and antisera were diluted in PBS. Stained sections were then contrasted in OsO_4 (1%) and uranyl acetate (1%), dehydrated, and flat-embedded in Durcupan (Fluka, Buchs,

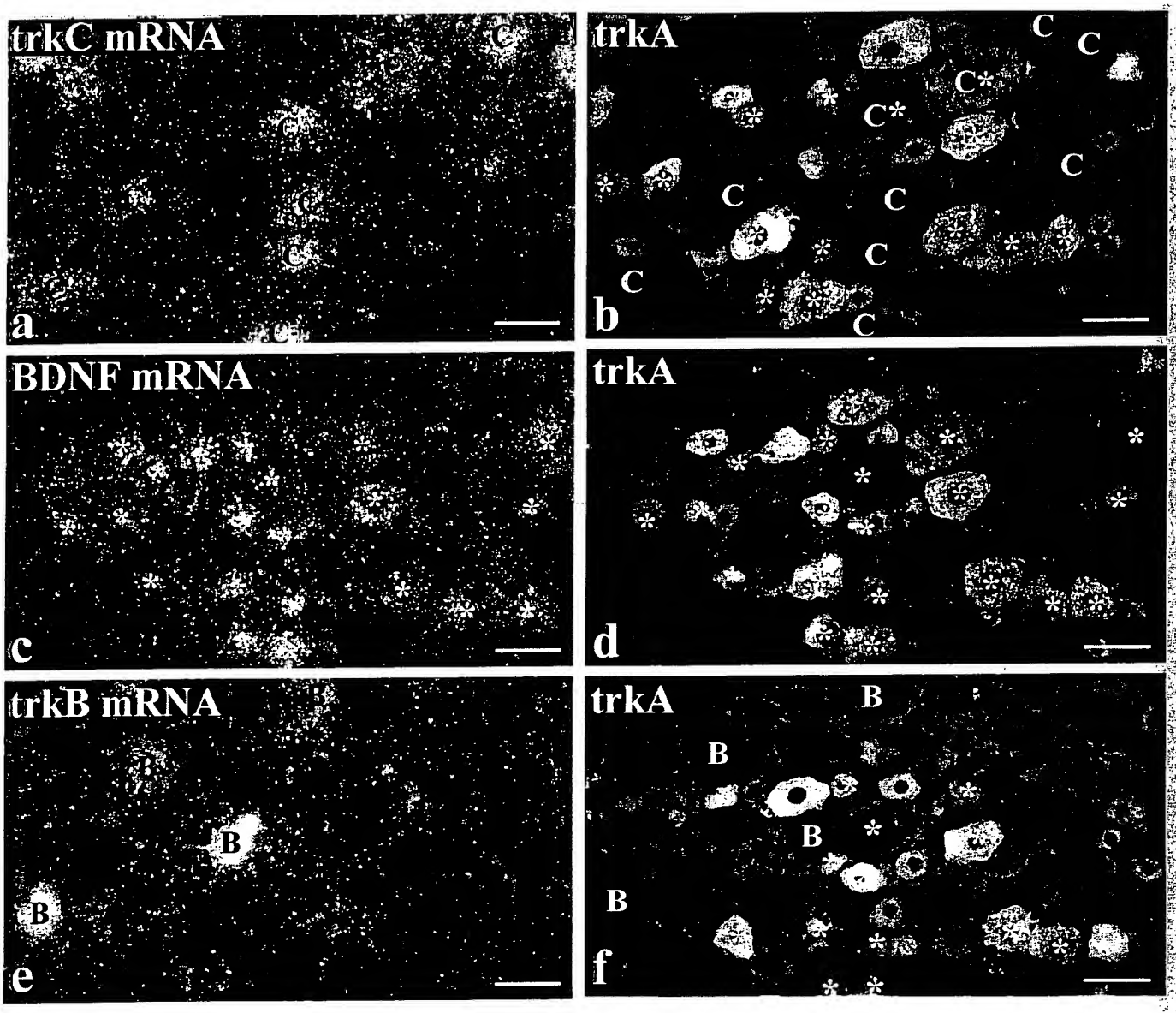

Figure 3. BDNF mRNA is expressed by numerous trkA cells but by few trkB or trkC cells. Intraperitoneal NGF treatment is shown. *a*, *c*, and *e* show three serial sections processed for trkC (*a*), BDNF (*c*), and trkB (*e*) mRNAs using *in situ* hybridization. Each section was also immunostained for trkA (*b*, *d*, *f*). Comparison of *c* and *d* shows that the majority of cells labeled for BDNF mRNA (*asterisks*) are also trkA immunoreactive. Those BDNF-labeled cells that are visible in the serial sections (*a*, *b*, *e*, *f*) are marked by *asterisks* in *b* and *f*. Comparison of *a* and *b* shows that the majority of trkC-labeled cells (marked *C*) do not express BDNF mRNA. However, two BDNF/trkC double-labeled cells are visible in *b*, one of which is trkA immunoreactive. Comparison of *e* and *f* allows the distribution of DRG cells that express trkB (marked *B*) and BDNF (*asterisks*) to be compared. They seem to form two discrete populations, and no double-labeled cells are visible. Scale bars, 50 μm.

Switzerland). After light microscopic examination, areas of interest were processed further for electron microscopy.

Imaging and quantitation. Sections were viewed on a Leica epifluorescence microscope using N2 (TRITC), L3 (FITC), and polarization filter blocks combined with bright-field and/or dark-field illumination. Immunostaining and *in situ* hybridization were documented by photography using Ilford T-MAX film. Photographs were printed by hand or were generated digitally by scanning 35 mm negatives using a Nikon LS-1000 at 900–1300 pixels/inch, by composing using Adobe Photoshop, and by printing on a Sony UP-D8800 graphics printer at 300 pixels/inch. Gray levels were stretched to optimize contrast, but images were not filtered or otherwise manipulated.

The proportion of BDNF-expressing DRG cells was determined by counting the number of immunoreactive and nonimmunoreactive neuronal profiles in sections of DRG. In double-labeled sections, the percentage of BDNF-expressing cells expressing a second marker was assessed by switching between FITC, TRITC, and/or polarization filter blocks. At least 250 labeled DRG cells were examined for each marker and counted on randomly chosen DRG sections. With use of Visilog image analysis software, the cell size and level of expression of BDNF mRNA were assessed in trkA immunoreactive and immunonegative DRG cells using previously described methodology (Priestley et al., 1991). Images were captured directly off the microscope at 25× magnification using a Grundig FA87 digital camera with integrating framestore. Cells were then outlined manually using a computer mouse, and the area within each cell that was occupied by silver grains was calculated. At least 200 cells of each type were counted. The amount of BDNF immunostaining in lamina II of the spinal cord was also quantified, basically as described previously (Bennett el al., 1996a). Images were captured as above and thresholded to reveal

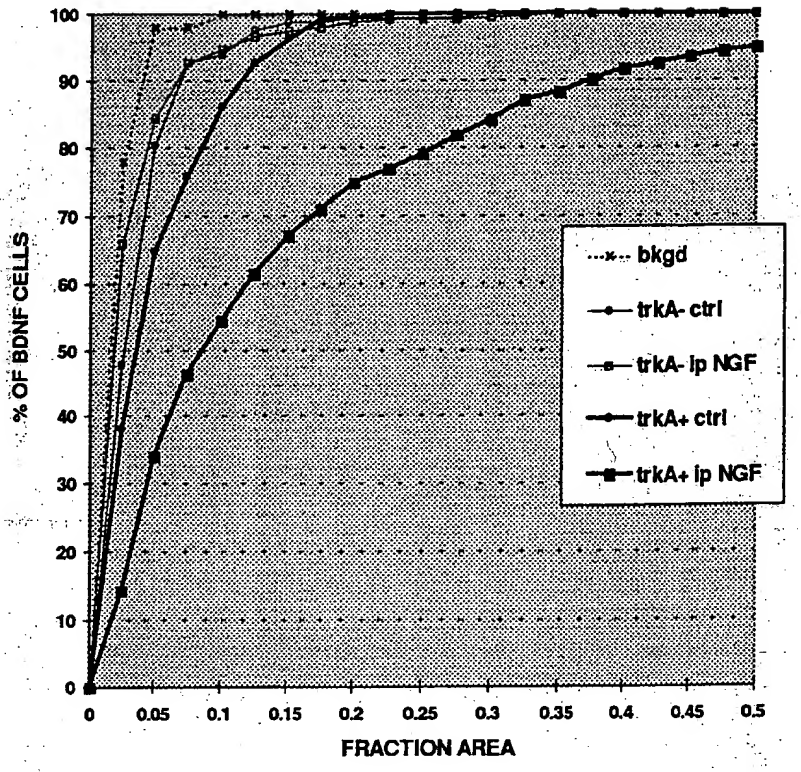

Figure 4. NGF increases BDNF mRNA expression only in trkA-immunoreactive cells as shown in Q sum plot of BDNF mRNA expression in trkA-immunoreactive (trkA+) and trkA-nonimmunoreactive (trkA−) lumbar DRG cells in control (*ctrl*) and intraperitoneal NGF-treated (*ip NGF*) animals. BDNF expression was quantified by measuring the fraction of the cell body (*FRACTION AREA*) that was covered by silver grains. Note that intraperitoneal NGF does not change the level of BDNF expression in BDNF-labeled but trkA-nonimmunoreactive cells. In contrast intraperitoneal NGF greatly increases BDNF expression in trkA immunoreactive cells, and even in control animals these cells show higher labeling than the trkA nonimmunoreactive population. *bkgd* indicates the level of background labeling in control and NGF-treated animals.

Table 3. The percentage of BDNF mRNA expressing DRG cells that also exhibit trkB mRNA, trkC mRNA, or IB4 labeling

	% of BDNF expressing other		% of other expressing BDNF	
BDNF and trkB mRNAs	1% (2/175)		2.4% (2/83)	
	trkA immunoreactive	not trkA immunoreactive	trkA immunoreactive	not trkA immunoreactive
BDNF and trkC mRNAs	8% (13/166)	7% (11/166)	10% (13/133)	8% (11/133)
BDNF mRNA and IB4 labelling	34% (71/208)	15% (31/208)	32% (71/221)	14% (31/221)

Intraperitoneal NGF treatment.

BDNF terminals, the threshold level being kept constant for both control and NGF-treated animals. Several 27 × 27 μm measuring boxes were placed over each image, and the area within each box that was occupied by immunostained terminals was calculated; 120–240 areas were sampled for each animal.

RESULTS

NGF effects on BDNF protein and BDNF mRNA in lumbar ganglia

In lumbar ganglia of control rats, BDNF immunoreactivity was evident in DRG cells and occasional axons. The quality of staining, however, varied between animals, depending on the immunocytochemical staining method. Thus few cells were stained using indirect immunofluorescence, whereas good TSA fluorescence preparations (Fig. 1*a*) showed staining in ~22% of DRG cells. Rats treated with intraperitoneal NGF showed a similar quality and range of BNDF immunostaining but little change in the number of immunoreactive DRG cells (Fig. 1*c*, Table 1). In contrast, ganglia from animals treated intrathecally with NGF showed abundant and robust BDNF immunostaining (Fig. 1*e*). As many as 40% of DRG cells showed immunoreactivity (Table 1), together with numerous axons. In all types of preparation, staining was confined to DRG cells and adjoining axons. Thus there was no indication of staining within satellite cells or Schwann cells.

In situ hybridization for BDNF mRNA showed a pattern of staining similar to that observed for BDNF protein. Thus a few heavily labeled DRG cells were observed in control animals together with numerous cells showing labeling slightly above background (Fig. 1*b*). The intraperitoneal NGF-treated animals (Fig. 1*d*) and the intrathecally treated animals (Fig. 1*f*) both showed increased labeling compared with controls. However, the total number of labeled cells increased only slightly (Table 1), suggesting that the increased *in situ* hybridization labeling represented mainly an increase in grain density per cell.

Relationship between BDNF expression and trkA expression in lumbar ganglia

The NGF effects were characterized further by combining BDNF immunocytochemistry with immunofluorescence for trkA or CGRP. BDNF immunoreactivity was present mainly in trkA cells, but the extent of double-labeling varied according to the type of NGF treatment (Fig. 2*a–d*, Table 2). For example, the percentage of trkA-immunoreactive cells that were BDNF immunoreactive increased from 21% in controls (Fig. 2*a,b*) to 84% after intrathecal NGF (Fig. 2*c,d*). NGF also increased the double-

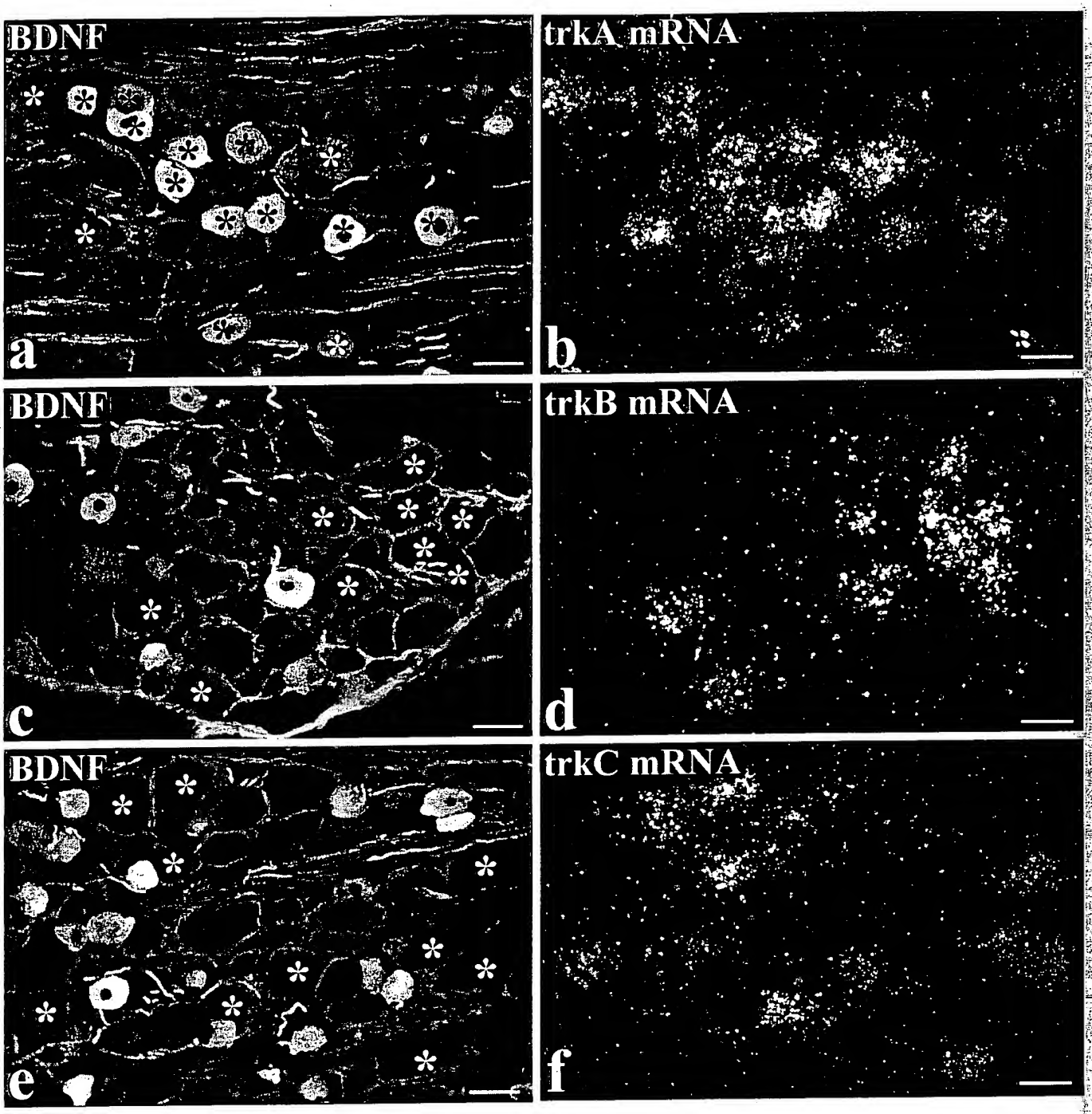

Figure 5. Intrathecal NGF treatment. BDNF immunoreactivity is present in numerous trkA cells but in few trkB or trkC cells. *a–f* show preparations double-labeled for BDNF immunoreactivity (*a, c, e*) and either trkA (*b*), trkB (*d*), or trkC (*f*) *in situ* hybridization. The *asterisks* indicate the location of trk-expressing cells, revealed by the *in situ* hybridization autoradiograms. Many BDNF-immunoreactive cells show trkA labeling (*a, b*), but the trkB- and trkC-expressing cells are distinct from the BDNF-immunoreactive ones. Scale bars, 50 μm.

labeling in terms of the percentage of BDNF cells that were trkA immunoreactive (Table 2). Very similar results were obtained for CGRP, consistent with previous studies showing that CGRP labels broadly the same DRG subpopulation as trkA (Averill et al., 1995). Thus extensive coexistence of BDNF and CGRP immunoreactivities was observed (Fig. 2*e,f*), and this coexistence varied according to the type of NGF treatment in the same way as the trkA/BDNF coexistence (Table 2).

To determine whether the BDNF protein observed in trkA/CGRP cells was locally synthesized, BDNF *in situ* hybridization was also combined with trkA immunofluorescence (Fig. 3*c,d*, Table 2). Just as with BDNF protein, extensive overlap was observed between BDNF mRNA and trkA, and the degree of coexistence increased with NGF treatment. Thus 30% of trkA-immunoreactive cells expressed BDNF mRNA in controls, whereas this figure increased to 88% after intrathecal NGF (Ta-

Table 4. The percentage of BDNF-immunoreactive DRG cells that also express trkA, trkB, or trkC mRNA

	% of BDNF expressing trk	% of trk expressing BDNF
BDNF and trkA mRNA	85% (583/684)	82% (583/706)
BDNF and trkB mRNA	2.5% (18/708)	9.5% (18/179)
BDNF and trkC mRNA	6% (53/842)	13% (53/399)

Intrathecal NGF treatment. The figures in brackets indicate the number of cells counted.

ble 2). To exclude the possibility that these changes in BDNF/trkA double-labeling were caused by changes in trkA expression, the effect of NGF on trkA immunoreactivity was also examined. The percentage of DRG cells that were trkA immunoreactive was not significantly affected by NGF treatment (Table 1).

Judged on the basis of either immunocytochemistry or *in situ* hybridization, a proportion of BDNF-expressing cells were not trkA immunoreactive (Figs. 2, 3; Table 2). Image analysis of preparations double-labeled for BDNF *in situ* hybridization and trkA immunofluorescence was performed to quantify the extent of labeling for BDNF mRNA in the trkA-immunoreactive and trkA-nonimmunoreactive cells and to quantify the effect of intraperitoneal NGF on the two populations. Consistent with the impression given by micrographs (e.g., Fig. 3*c,d*), this analysis showed that the trkA-immunoreactive cells had greater labeling for BDNF mRNA than the non-trkA cells and that intraperitoneal NGF greatly increased the degree of labeling in the trkA subpopulation (Fig. 4). In addition, it revealed that intraperitoneal NGF had no effect on the degree of BDNF mRNA labeling in the non-trkA cell population (Fig. 4) and had no effect on the cell-size distribution of the trkA subpopulation (data not shown).

Relationship between BDNF expression and trkB or trkC expression in lumbar ganglia

To determine the relationship between BDNF and trkB or trkC expression, two different methods of double-labeling were performed. The first method was used for animals treated with intraperitoneal NGF. Serial sections were processed for trkC, BDNF, and trkB *in situ* hybridization, and each section was also immunostained for trkA (Fig. 3). The trkA/BDNF double-labeled sections were also stained with the lectin *Griffonia simplicifolia* IB4, a marker that has been proposed to mainly label DRG cells that do not express any known trk (Averill et al., 1995; Molliver et al., 1995; Silos-Santiago et al., 1995). This approach allowed us to determine whether BDNF-synthesizing cells belonged to the trkB, trkC, or non-trk (IB4) populations and also revealed whether labeled cells coexpressed trkA. A small overlap was seen between BDNF and both the trkC and IB4 populations. Thus 15% of BDNF mRNA-expressing cells were labeled for trkC mRNA, of which half were also trkA immunoreactive (Fig. 3*a,b*, Table 3). In addition, 49% of BDNF mRNA-expressing cells showed IB4 labeling (not illustrated), with approximately two thirds of these also trkA immunoreactive (Table 3). In contrast to trkC or IB4, however, there was virtually no overlap between BDNF mRNA and trkB. Only 1% of BDNF mRNA-expressing cells were also labeled for trkB mRNA (Fig. 3*e,f*, Table 3).

The second method of double-labeling was applied to animals treated intrathecally with NGF and involved BDNF immunofluorescence combined with trkA, trkB, or trkC *in situ* hybridization (Fig. 5). This allowed a direct analysis of whether BDNF protein was present in trkB- or trkC-expressing cells, as well as providing an additional assessment of the degree of BDNF/trkA coexpression. Consistent with the other labeling methods, a high percentage of trkA mRNA-expressing cells were BDNF immunoreactive (82%) (Table 4). A small percentage of BDNF-immunoreactive cells expressed trkC mRNA (6%), and an even smaller percentage expressed trkB (3%) (Table 4).

BDNF axonal transport

To determine whether BDNF was axonally transported to or from lumbar dorsal root ganglia, BDNF immunoreactivity was examined at the site of dorsal root (Fig. 6*a,b*) and sciatic (Fig. 6*e,f*) ligations. The accumulation of BDNF immunoreactivity was compared with that of trkA (Fig. 6*c,d*) and CGRP (Fig. 6*g,h*) immunoreactivities. In dorsal roots, BDNF transport seemed to be mainly anterograde. BDNF immunoreactivity accumulated predominantly proximal to a dorsal root ligation (i.e., the DRG side). In contrast, both anterograde and retrograde transport of trkA was evident. TrkA immunoreactivity accumulated both proximal and distal to the ligation but with greater accumulation proximal rather than distal (Fig. 6*a–d*). In the sciatic nerve, both anterograde and retrograde transport of BDNF were detected. BDNF immunoreactivity accumulated both proximal (DRG side) and distal to a sciatic ligation (Fig. 6*e,f*). The proximal accumulation was generally greater than that distally, and on both sides of the ligation the majority of BDNF-immunoreactive axons were also CGRP immunoreactive (Fig. 6*e–h*). The BDNF accumulation in dorsal roots and sciatic nerve was greater after intraperitoneal NGF than in control animals, and in the case of double ligatures no accumulation was seen in the isolated portion of nerve between the ligatures (not illustrated). The footpad and dorsal surface of the foot were examined for peripherally transported BDNF. Immunoreactivity was present but was confined to light staining of fiber bundles in the dermis and of isolated axons in the epidermis (not illustrated).

BDNF immunoreactivity in the spinal cord

BDNF immunoreactivity was examined in the lumbar cord of control (Fig. 7*a,b*), intraperitoneal NGF-treated (not illustrated), and intrathecal NGF-treated (Figs. 7*c,d*) animals. BDNF immunoreactive axons and terminals were observed mainly in the central projections of small diameter primary afferents. Terminals were particularly abundant in the superficial dorsal horn (laminae I, II) (Figs. 7*a,c*), in patches in deep dorsal horn (Fig. 7*c,e*), and dorsolateral to the central canal (Fig. 7*g*). In all of these regions, BDNF showed extensive coexistence with CGRP (Figs. 7*e–h*), such that BDNF-immunoreactive axons that lacked CGRP immunoreactivity were rarely observed. In contrast to CGRP, BDNF-immunoreactive terminals did not coexist with IB4 (not illustrated). As with the staining in DRG, the extent of BDNF immunoreactivity in spinal cord varied, depending on whether animals had been treated with NGF. Control and intrathecal NGF-treated animals were easily distinguished. After intrathecal NGF, BDNF-immunoreactive terminals were more abundant (compare Fig. 7, *a* and *c*), and more extensive coexistence with CGRP was seen. After intrathecal delivery of NGF to the cervical cord, the BDNF immunoreactivity in primary afferents was so intense that it was possible to trace axons from the ganglion into the dorsal horn (Fig. 8). Staining in intraperitoneal NGF-treated animals was not as great as in intrathecally treated animals, and there was significant interanimal variability. In general, however,

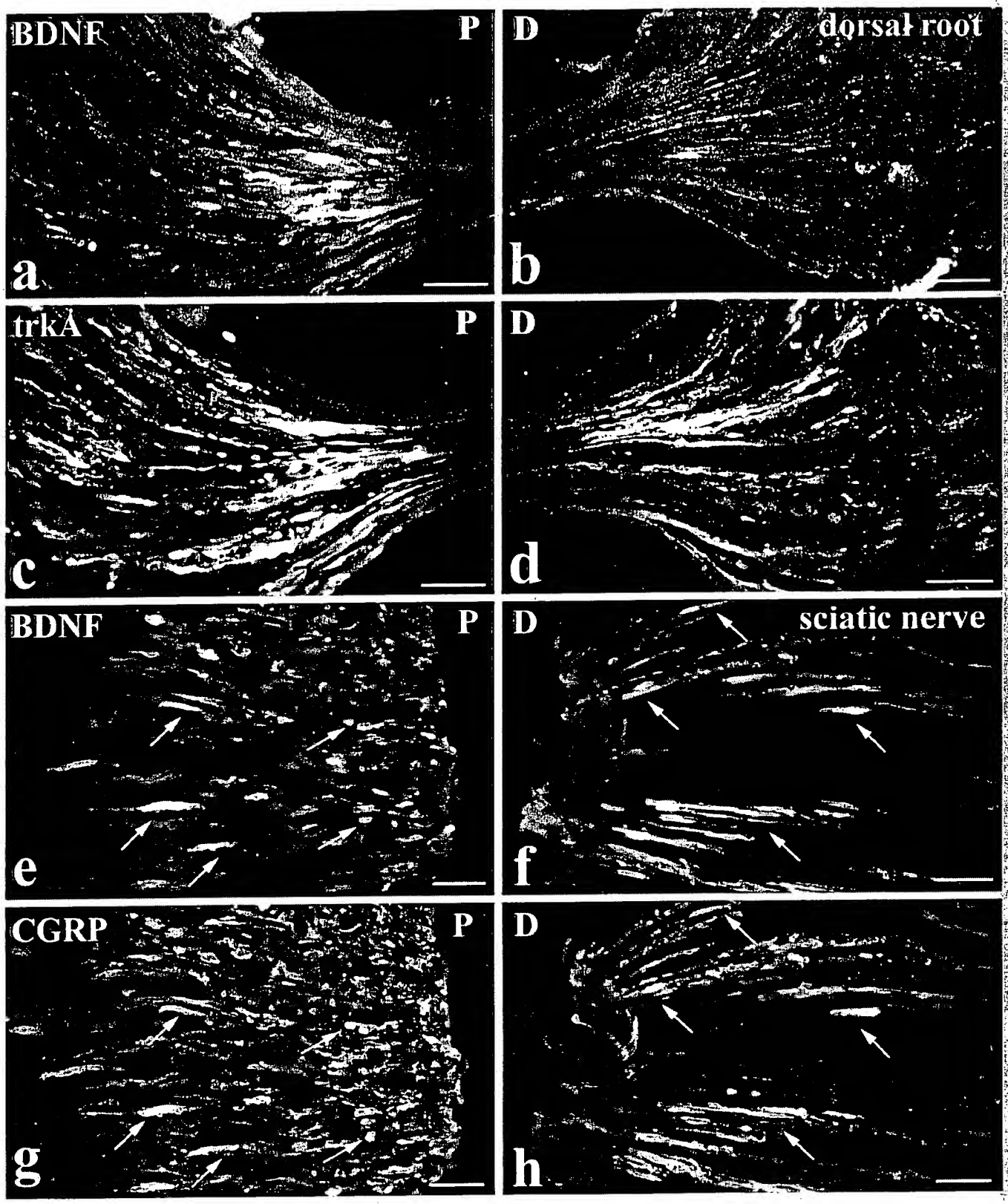

Figure 6. Intraperitoneal NGF treatment. BDNF is anterogradely transported. BDNF (*a, b, e, f*), trkA (*c, d*), and CGRP (*g, h*) immunoreactivity proximal (*P: a, c, e, g*) and distal (*D: b, d, f, h*) to lumbar dorsal root (*a–d*) or sciatic nerve (*e–h*) ligations are shown. At a dorsal root ligation, both BDNF (*a*) and trkA (*c*) accumulate proximal to the ligation (i.e., the DRG side). Distal to the ligation, trkA immunoreactivity accumulates (*d*) but only occasional BDNF-immunoreactive axons are visible (*b*). At a sciatic nerve ligation, BDNF accumulates both proximal (*e*) and distal (*f*) to the ligation. CGRP shows a similar accumulation (*g, h*), and double-staining reveals that the BDNF-immunoreactive axons are also CGRP immunoreactive (*arrows* indicate double-labeled axons). Scale bars, 50 μm.

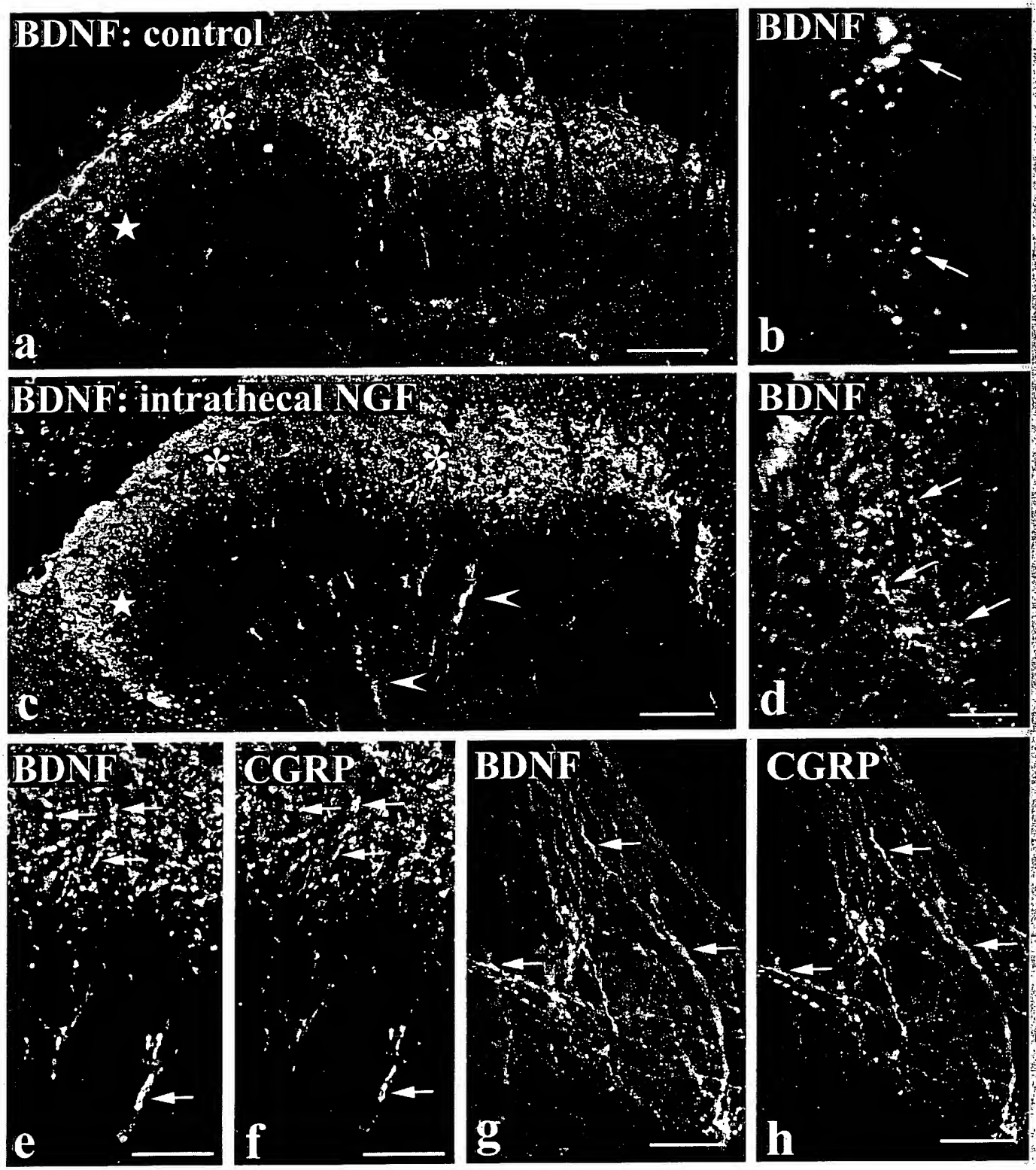

Figure 7. BDNF immunoreactivity in the spinal cord is increased by NGF treatment and is present in CGRP-immunoreactive axons. *a–d* show BDNF immunofluorescence in the dorsal horn of control tissue (*a, b*) and after intrathecal NGF treatment (*c, d*). BDNF immunoreactivity in laminae I and II (*asterisks* in *a* and *c*) and in deep dorsal horn (*arrowheads* in *c*) is increased by NGF. The increase is particularly striking in lateral lamina II (*stars* in *a* and *c*), and this region is shown at high magnification in *b* and *d*. Immunoreactive axons (*arrows* in *b* and *d*) are more abundant after NGF treatment. *e–h*, Double-labeling showing extensive coexistence of BDNF (*e, g*) and CGRP (*f, h*) after intrathecal NGF treatment. In the dorsal horn (*e, f*) and in lamina X dorsolateral to the aqueduct (*g, h*), numerous double-labeled axons and varicosities (*arrows*) are visible. Scale bars: *a, c*, 100 μm; *b, d*, 25 μm; *e–h*, 50 μm.

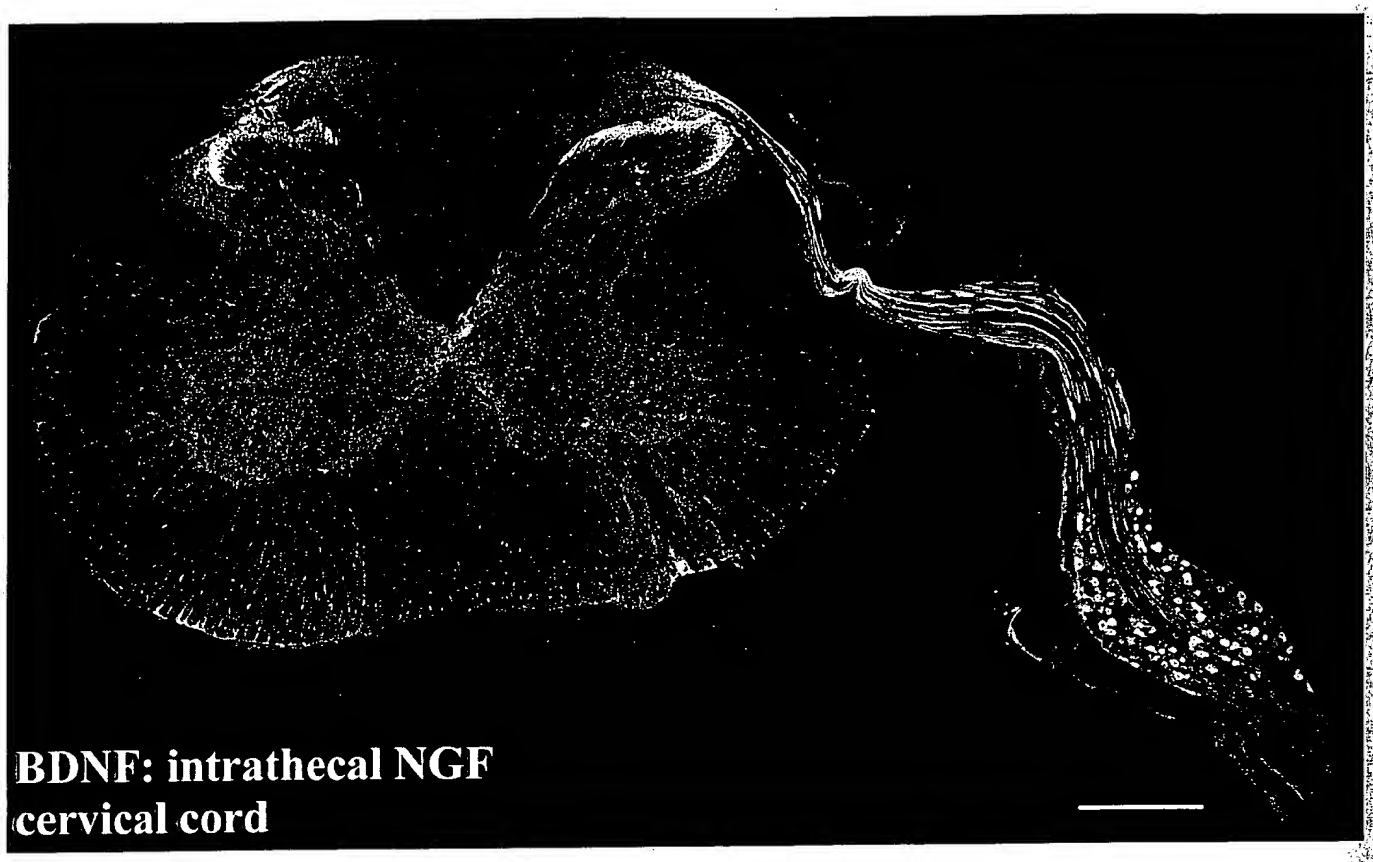

Figure 8. Photomontage of a transverse section showing the cervical spinal cord and attached DRG of an animal treated intrathecally with NGF via an upper cervical cannula. BDNF protein is transported by DRG cells along their central processes and into the spinal cord. BDNF levels have increased to such an extent that immunoreactive axons can be traced from DRG cells, along a dorsal root and into the dorsal horn of the spinal cord. Scale bar, 250 μm.

it seemed to be slightly greater than in controls, and this was confirmed by image analysis. The mean staining level of BDNF-immunoreactive terminals in lamina II of intraperitoneal NGF-treated animals was twice that obtained in control animals.

Ultrastructural localization of BDNF immunoreactivity in the dorsal horn

Immunoreactive unmyelinated axons (Fig. 9*b*), finely myelinated axons (Fig. 9*c*), and axon terminals (Fig. 9*a*) were observed in lamina II. Immunoreactive terminals included characteristic sinuous terminals that made asymmetric synapses and displayed an electron-dense axoplasm containing several large dense-cored vesicles and numerous agranular vesicles (Fig. 9*a*). In heavily stained terminals, the immunoreaction deposit filled the axoplasm and covered dense-cored vesicles and the membranes of agranular vesicles. In lightly stained terminals, the reaction deposit had a more restricted distribution and seemed to be concentrated over a subpopulation of dense-cored vesicles (Fig. 9*c*).

DISCUSSION

In this study we have shown that trkA-expressing DRG cells synthesize BDNF and anterogradely transport it to axon terminals within the spinal cord. BDNF levels are modulated by NGF, with intrathecally administered NGF having much more potent effects than systemic NGF. In addition we have shown that a small number of DRG cells that do not express trkA also synthesize BDNF but that BDNF mRNA in these cells is not increased by NGF. Such cells include trkC cells and cells that do not express any of the trks, but very few trkB cells. The expression of BDNF protein in DRG cells matches very closely the expression of BDNF mRNA. These results have profound implications for our understanding of BDNF function in sensory neurons.

DRG subgroups that synthesize BDNF

Previous studies have described BDNF mRNA (Ernfors et al., 1990, 1993; Wetmore and Olson, 1995; Apfel et al., 1996; Cho et al., 1997) or protein (Wetmore and Olson, 1995; Zhou and Rush, 1996) in adult rat DRG cells, and two studies have recently reported that some cells expressing BDNF mRNA also express trkA mRNA (Apfel et al., 1996; Cho et al., 1997). We have extended these studies by fully characterizing the expression of both BDNF mRNA and protein in relation to all of the trk-expressing subpopulations of DRG cells.

Our results show that BDNF is synthesized by several different DRG subtypes, but the biggest contribution comes from cells that express trkA and the neuropeptide CGRP (Fig. 10). TrkA-immunoreactive cells in control animals have higher levels of BDNF mRNA than non-trkA-immunoreactive cells, and after intrathecal NGF, BDNF and trkA/CGRP identify virtually identical populations. Of the BDNF-expressing cells, 80–90% belong to the trkA group, and almost 90% of trkA cells express BDNF mRNA. This close correspondence between BDNF and the trkA/CGRP group is echoed in the spinal cord, where BDNF immunoreactivity in both control and NGF-treated animals is confined to CGRP containing primary afferents. BDNF is absent

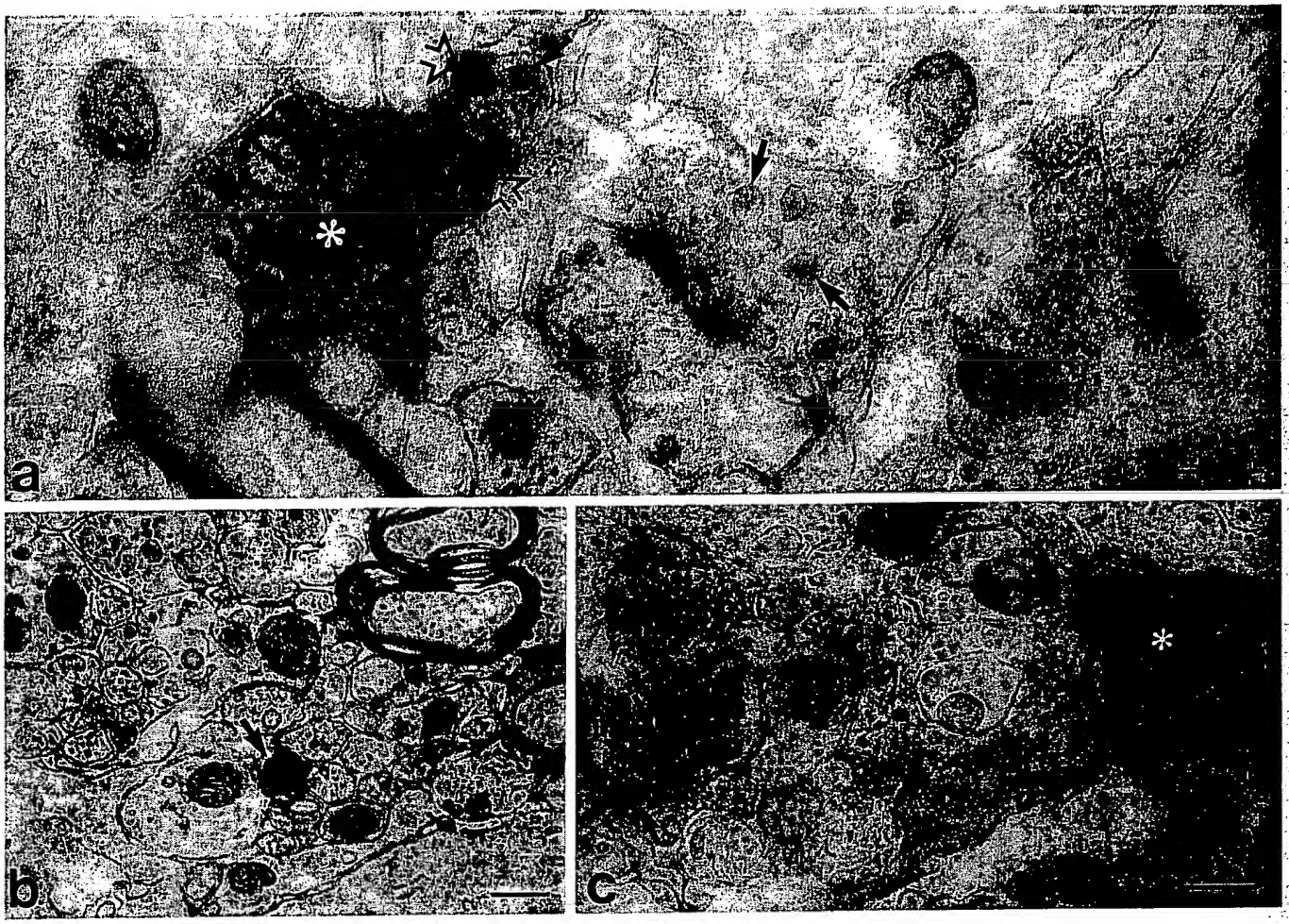

Figure 9. Preembedding ultrastructural immunocytochemistry showing BDNF immunoreactivity in axons (*b, c*) and an axon terminal (*a*) in lamina II of the lumbar spinal cord. *a*, An immunoreactive terminal (*asterisk*) shows heavy staining over a region packed with small agranular vesicles and over individual large dense-cored vesicles (*open arrows*). *Arrows* indicate dense-cored vesicles in an adjoining unstained terminal. *b*, A heavily stained unmyelinated axon (*arrow*) is visible among a group of similar, but unstained, axons. *c*, An immunostained preterminal axon and an immunostained finely myelinated axon (*asterisk*) are visible. The preterminal axon shows staining exclusively over large dense-cored vesicles (*arrows*). Scale bars, 0.25 μm.

from the termination zones of large-diameter afferents and of IB4-labeled afferents, consistent with our data showing that relatively few trkC- or IB4-labeled cells express BDNF mRNA. However, the fact that these cell types express some BDNF may be significant. NGF increases BDNF expression selectively in trkA-immunoreactive cells (discussed below), but it is possible that BDNF in the non-trkA population is affected by other factors. For example, BDNF expression in DRG cells is increased by nerve damage (Ernfors et al., 1993), and we have shown recently that this occurs at least partly in trkC cells (Averill et al., 1997). *In vitro*, a BDNF autocrine loop has been shown to mediate the survival of a subpopulation of adult DRG cells (Acheson et al., 1995). Our results, however, indicate that *in vivo* there is very little coexistence of BDNF and trkB mRNAs. Only 1% of cells expressing BDNF mRNA also expressed trkB, and only 2% of trkB cells contained BDNF mRNA. The simplest interpretation of this data is that an autocrine loop does not occur in control or NGF-supplemented adult animals. However, our data do not rule out the possibility that an autocrine loop occurs in certain circumstances. Axonal damage may upregulate BDNF in trkB cells, or BDNF may support survival of trkA cells in some way that does not involve trkB. We also cannot exclude the possibility that some BDNF cells express trkB at levels below our detection threshold. Consistent with other recent studies (Kashiba et al., 1995; Wright and Snider, 1995; McMahon et al., 1997), we observed minimal overlap between trkA and trkB cells (Fig. 10). However, extensive overlap of trkA and trkB has been described (McMahon et al., 1994) and may be attributable to low-level trkB expression in some trkA cells.

Our preparations showed good BDNF immunostaining, with BDNF mRNA and protein generally in rather similar numbers and types of cells. After NGF, BDNF mRNA was observed in more cells than BDNF protein. However, this probably simply reflects the fact that a greater increase in BDNF expression was needed to bring cells above the detection threshold for immunocytochemistry than for *in situ* hybridization. In contrast to the extensive coexistence of BDNF and trkA, we observed very little BDNF protein in trkB cells. Only 10% of trkB-labeled cells showed BDNF immunoreactivity. This is a surprising result, given that target-derived BDNF is thought to be axonally transported by trkB-expressing DRG cells (DiStefano et al., 1992). However, our studies of BDNF axonal transport support our

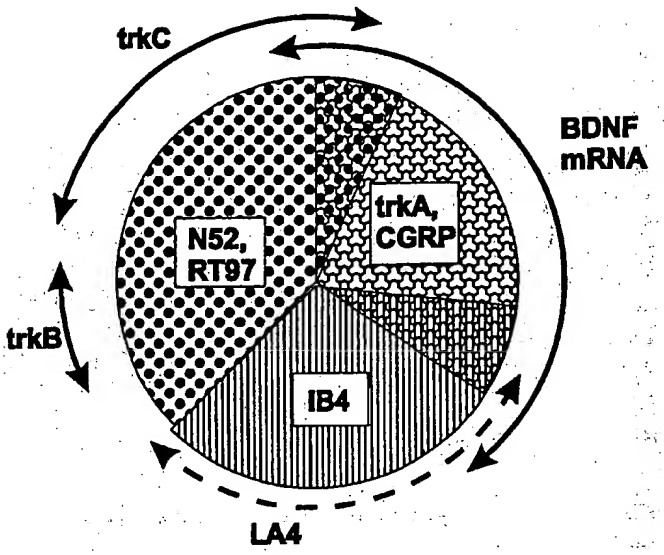

Figure 10. Pie chart summarizing the relationship between BDNF and trk expression in neurochemically defined DRG subclasses. DRG neurons can be divided broadly into large-diameter cells, which innervate low-threshold mechanoreceptors, and small-diameter cells, which innervate mainly nociceptors. BDNF mRNA is expressed by the subpopulation of small cells that contain the neuropeptide CGRP and the NGF receptor trkA. Small cells that do not express any trk receptor, and that can be labeled using the lectin *Griffonia simplicifolia* IB4 or the monoclonal antibody LA4, mainly do not express BDNF. With the exception of those trkC cells that coexpress trkA, BDNF mRNA is also largely not expressed by trkB or trkC cells. TrkC and trkB are present mainly in large-diameter cells, which can be identified using the neurofilament antisera N52 or RT97. BDNF is constitutively expressed in the cell types illustrated, but expression in trkA cells is increased further by NGF treatment.

localization data in indicating that there is little retrograde BDNF transport. BDNF immunoreactivity accumulated distal to a sciatic ligation but showed extensive colocalization with CGRP, implying that it represents mainly recycling of anterogradely transported protein. BDNF may be present in trkB cells at levels below our detection threshold, but if so it must be at levels that are much lower than those that occur in trkA cells. It thus seems that most BDNF protein in DRG cells is synthesized locally, with target-derived BDNF making only a small contribution.

Upregulation of BDNF by NGF and its functional consequences

In addition to detecting BDNF protein within trkA/CGRP immunoreactive DRG cell bodies, we observed that BDNF in these cells is (1) anterogradely transported along both their central and peripheral processes and (2) present in the spinal cord in all their terminal fields, and that (3) immunoreactivity is concentrated over dense-cored vesicles. Biochemical studies have recently shown that BDNF in cortex is enriched in a vesicular fraction of synaptosomes (Fawcett et al., 1997). Our ultrastructural results are consistent with this work and indicate that dense-cored vesicles are likely to be the primary site of BDNF storage. NGF treatment led to a massive increase of both mRNA and protein, with increased anterograde transport to central terminals. Anterograde transport of BDNF into the dorsal horn has also recently been reported by Zhou and Rush (1996), although the cell type responsible was not identified. Transport and axodendritic transfer of exogenous NT-3 has recently been reported in the developing visual system (von Bartheld et al., 1996), and BDNF-immunoreactive terminals have been described in various CNS regions (Kawamoto et al., 1996; Conner et al., 1997; Yan et al., 1997), suggesting that anterograde transport may be widespread. Goodman and colleagues (1996) have demonstrated that BDNF in cultured cells colocalizes with the secretory granule marker chromogranin A and is released from hippocampal dendrites by a regulated pathway dependent on extracellular calcium (Goodman et al., 1996). BDNF release has not been demonstrated *in vivo*, but our observations make it highly likely that BDNF can be released from primary afferent terminals in the dorsal horn.

Our data on the effects of NGF are broadly in agreement with the recent study of Apfel and colleagues (1996) in showing that NGF upregulates BDNF mRNA in trkA-expressing DRG cells; however, there are some differences of detail. They observed no effect of chronic NGF treatment and interpreted the BDNF response as an acute reaction. In contrast, we observed that a 2 week intrathecal NGF infusion had a much more potent effect, indicating not only the increased efficacy of the intrathecal route but also that the BDNF increase is maintained. Primary afferents presumably normally respond to NGF, acting at their peripheral processes, and so the intrathecal route is not like the situation *in vivo*. However, effects after intrathecal and intraperitoneal or local nerve application are qualitatively similar (this study; also see Verge et al., 1996), suggesting that the intrathecal route is appropriate for examining DRG responses to trophic factors.

Apfel and colleagues (1996) also report that BDNF mRNA is increased in non-trkA expressing cells and interpret this as a paracrine interaction. In contrast we saw no change in this cell group. Quantitative analysis of the increase in BDNF mRNA after NGF indicated that it was restricted to the trkA-immunoreactive subpopulation, as might be expected if it involves direct activation of trkA receptors. A similar analysis was not performed after intrathecal NGF, so we cannot exclude the possibility that the intrathecal route increased BDNF in some non-trkA cells. However, the extensive overlap observed between trkA and BDNF after intrathecal NGF makes it unlikely.

Our data thus support neither an autocrine nor a paracrine role for BDNF within DRG, but do support a role as an anterograde trophic messenger. Such a role has been described in late embryonic development (Robinson et al., 1996) and may be maintained, or adapted, into adult life. Many trkA-expressing DRG cells are nociceptive, and increased NGF in inflammation has both acute and chronic effects on pain processing (McMahon, 1996; Woolf, 1996). We have shown that exogenous NGF increases BDNF expression in trkA cells, and Cho et al. (1997) have recently shown that similar changes take place after peripheral inflammation. BDNF released from primary afferent terminals may therefore play a key role in chronic pain states by modulating dorsal horn activity in various ways. Full length trkB receptors are present in the dorsal horn (G. J. Michael and J. V. Priestley, unpublished observations), and BDNF applied to the spinal cord increases c-*fos* and nitric oxide synthase in dorsal horn neurons (Bennett et al., 1996b). BDNF may also have effects on spinal cord anatomy and on expression of neurotransmitter receptors. These possibilities are being investigated.

REFERENCES

Acheson A, Conover JC, Fandl JP, DeChlara TM, Russell M, Thadani A, Squinto SP, Yancopoulos GD, Lindsay RM (1995) A BDNF

autocrine loop in adult sensory neurons prevents cell death. Nature 374:450–453.

Apfel SC, Wright DE, Wiideman AM, Dormia C, Snider WD, Kessler JA (1996) Nerve growth-factor regulates the expression of brain-derived neurotrophic factor messenger RNA in the peripheral nervous system. Mol Cell Neurosci 7:134–142.

Averill S, McMahon SB, Clary DO, Reichardt LF, Priestley JV (1995) Immunocytochemical localization of trkA receptors in chemically identified subgroups of adult rat sensory neurons. Eur J Neurosci 7:1484–1494.

Averill S, Michael GJ, Shortland PJ, Priestley JV (1997) BDNF increases in large diameter dorsal root ganglion cells and in their central projections following peripheral axotomy. Soc Neurosci Abstr 23:134.8.

Bennett DLH, French J, Priestley JV, McMahon SB (1996a) NGF but not NT-3 or BDNF prevents the A fibre sprouting into lamina II of the spinal cord that occurs following axotomy. Mol Cell Neurosci 8:211–220.

Bennett DLH, French JS, Priestley JV, McMahon SB (1996b) The effects of BDNF on c-fos and NOS expression in dorsal horn neurones of the adult rat spinal cord. Soc Neurosci Abstr 22:396.15.

Cho HJ, Kim SY, Park MJ, Kim DS, Kim JK, Chu MY (1997) Expression of mRNA for brain-derived neurotrophic factor in the dorsal root ganglion following peripheral inflammation. Brain Res 749:358–362.

Clary DO, Weskamp G, Austin LAR, Reichardt LF (1994) TrkA cross-linking mimics neuronal responses to nerve growth factor. Mol Biol Cell 5:549–563.

Conner JM, Lauterborn JC, Yan Q, Gall CM, Varon S (1997) Distribution of brain-derived neurotrophic factor (BDNF) protein and mRNA in the normal adult rat CNS: evidence for anterograde axonal transport. J Neurosci 17:2295–2313.

Curtis R, Adryan KM, Stark JL, Park JS, Compton DL, Weskamp G, Huber LJ, Chao MV, Jaenisch R, Lee KF, Lindsay RM, DiStefano PS (1995) Differential role of the low-affinity neurotrophin receptor (p75) in retrograde axonal-transport of the neurotrophins. Neuron 14:1201–1211.

DiStefano PS, Friedman B, Radziejewski C, Alexander C, Boland P, Schick CM, Lindsay RM, Wiegand SJ (1992) The neurotrophins BDNF, NT-3, and NGF display distinct patterns of retrograde axonal transport in peripheral and central neurons. Neuron 8:983–993.

Ernfors P, Wetmore C, Olson L, Persson H (1990) Identification of cells in rat brain and peripheral tissues expressing mRNA for members of the nerve growth factor family. Neuron 5:511–526.

Ernfors P, Rosario CM, Merlio JP, Grant G, Aldskogius H, Persson H (1993) Expression of mRNAs for neurotrophin receptors in the dorsal root ganglion and spinal cord during development and following peripheral or central axotomy. Mol Brain Res 17:217–226.

Fawcett JP, Aloyz R, Mclean JH, Pareek S, Miller FD, McPherson PS, Murphy RA (1997) Detection of brain-derived neurotrophic factor in a vesicular fraction of brain synaptosomes. J Biol Chem 272: 8837–8840.

Goodman LJ, Valverde J, Lim F, Geschwind MD, Federoff HJ, Geller AI, Hefti F (1996) Regulated release and polarized localization of brain-derived neurotrophic factor in hippocampal neurons. Mol Cell Neurosci 7:222–238.

Hunt SP, Mantyh PW, Priestley JV (1992) The organization of biochemically characterized sensory neurons. In: Sensory neurons. Diversity, development, and plasticity (Scott SA, ed), pp 60–76. New York: Oxford UP.

Hunyady B, Krempels K, Harta G, Mezey E (1996) Immunohistochemical signal amplification by catalyzed reporter deposition and its application in double immunostaining. J Histochem Cytochem 44:1353–1362.

Kashiba H, Noguchi K, Ueda Y, Senba E (1995) Coexpression of trk family members and low-affinity neurotrophin receptors in rat dorsal-root ganglion neurons. Mol Brain Res 30:158–164.

Kawamoto Y, Nakamura S, Nakano S, Oka N, Akiguchi I, Kimura J (1996) Immunohistochemical localization of brain-derived neurotrophic factor in adult rat brain. Neuroscience 74:1209–1226.

Lawson SN (1992) Morphological and biochemical cell types of sensory neurons. In: Sensory neurons. Diversity, development, and plasticity (Scott SA, ed), pp 27–59. New York: Oxford UP.

Maness LM, Kastin AJ, Weber JT, Banks WA, Beckman BS, Zadina JE (1994) The neurotrophins and their receptors: structure, function, and neuropathology. Neurosci Biobehav Rev 18:143–159.

Mannion RJ, Doubell TP, Coggeshall RE, Woolf CJ (1996) Collateral sprouting of uninjured primary afferent A-fibers into the superficial dorsal horn of the adult rat spinal cord after topical capsaicin treatment to the sciatic-nerve. J Neurosci 16:5189–5195.

McMahon SB (1996) NGF as a mediator of inflammatory pain. Philos Trans R Soc Lond [Biol] 351:431–440.

McMahon SB, Armanini MP, Ling LH, Phillips HS (1994) Expression and coexpression of trk receptors in subpopulations of adult primary sensory neurons projecting to identified peripheral targets. Neuron 12:1161–1171.

McMahon SB, Bennett DLH, Michael GJ, Priestley JV (1997) Neurotrophic factors and pain. In: Progress in pain research and management, Vol 8 (Jensen TS, Turner JA, Wiesenfeld-Hallin Z, eds). Seattle: IASP Press, in press.

Meakin SO, Suter U, Drinkwater CC, Welcher AA, Shooter EM (1992) The rat trk protooncogene product exhibits properties characteristic of the slow nerve growth factor receptor. Proc Natl Acad Sci USA 89:2374–2378.

Merighi A, Polak JM, Gibson SJ, Gulbenkian S, Valentino KL, Peirone SM (1988) Ultrastructural studies on calcitonin gene-related peptide-immunoreactive, tachykinin-immunoreactive and somatostatin-immunoreactive neurons in rat dorsal root ganglia: evidence for the colocalization of different peptides in single secretory granules. Cell Tissue Res 254:101–109.

Michael GJ, Priestley JV (1995) Expression of GAP-43 messenger-RNA in preganglionic sympathetic neurons of the adult rat spinal cord. NeuroReport 7:338–342.

Michael GJ, Priestley JV (1996a) Expression of trkA and p75 low affinity nerve growth factor receptors in the adrenal gland. NeuroReport 7:1617–1622.

Michael GJ, Priestley JV (1996b) Combined immunocytochemistry and in situ hybridization. In: In situ hybridization techniques for the brain (Henderson Z, ed), pp. 111–118. Chichester: Wiley.

Middlemas DS, Lindberg RA, Hunter T (1991) TrkB, a neural receptor protein-tyrosine kinase: evidence for a full-length and two truncated receptors. Mol Cell Biol 11:143–153.

Molliver DC, Radeke MJ, Feinstein SC, Snider WD (1995) Presence or absence of trkA protein distinguishes subsets of small sensory neurons with unique cytochemical characteristics and dorsal horn projections. J Comp Neurol 361:404–416.

Priestley JV (1997) Immunocytochemical techniques for the study of the nervous system. In: Neurochemistry: a practical approach, 2nd ed (Bachelard H, Turner A, eds), pp 71–120. Oxford: Oxford UP.

Priestley JV, Réthelyi M, Lund PK (1991) Semi-quantitative analysis of somatostatin mRNA distribution in the rat central nervous system using in situ hybridization. J Chem Neuroanat 4:131–153.

Priestley JV, Alvarez FJ, Averill S (1992) Pre-embedding electron microscopic immunocytochemistry. In: Electron microscopic immunocytochemistry (Polak JM, Priestley JV, eds), pp 89–121. Oxford: Oxford UP.

Priestley JV, Wotherspoon G, Savery D, Averill S, Rattray M (1993) A combined in situ hybridization and immunofluorescence procedure allowing visualisation of peptide mRNA and serotonin in single sections. J Neurosci Methods 48:99–110.

Priestley JV, Michael GJ, Averill S, Nitkunan A, Wotherspoon G, Rattray M, Bennett DLH, Yan Q, McMahon SB (1996) NGF treatment increases BDNF expression in trkA immunoreactive dorsal root ganglion cells and in their central terminations within the spinal cord. Soc Neurosci Abstr 22:223.8.

Robinson M, Bujbello A, Davies AM (1996) Paracrine interactions of BDNF involving NGF-dependent embryonic sensory neurons. Mol Cell Neurosci 7:143–151.

Shindler KS, Roth KA (1996) Double immunofluorescent staining using two unconjugated primary antisera raised in the same species. J Histochem Cytochem 44:1331–1335.

Silos-Santiago I, Molliver DC, Ozaki S, Smeyne RJ, Fagan AM, Barbacid M, Snider WD (1995) Non-trkA-expressing small DRG neurons are lost in trkA deficient mice. J Neurosci 15:5929–5942.

Timmusk T, Palm K, Metsis M, Reintam T, Paalme V, Saarma M, Persson H (1993) Multiple promoters direct tissue-specific expression of the rat BDNF gene. Neuron 10:475–489.

Valenzuela DM, Maisonpierre PC, Glass DJ, Rojas E, Nunez L, Kong Y, Stitt TN, Ip NY, Yancopoulos GD (1993) Alternative forms of rat TrkC with different functional capabilities. Neuron 10:963–974.

Verge VMK, Gratto KA, Karchewski LA, Richardson PM (1996) Neu-

rotrophins and nerve injury. Philos Trans R Soc Lond [Biol] 351:423–430.

von Bartheld CS, Byers MR, Williams R, Bothwell M (1996) Anterograde transport of neurotrophins and axodendritic transfer in the developing visual system. Nature 379:830–833.

Wetmore C, Olson L (1995) Neuronal and nonneuronal expression of neurotrophins and their receptors in sensory and sympathetic ganglia suggest new intercellular trophic interactions. J Comp Neurol 353:143–159.

Woolf CJ (1996) Phenotypic modification of primary sensory neurons: the role of nerve growth factor in the production of persistent pain. Philos Trans R Soc Lond [Biol] 351:441–448.

Woolf CJ, Shortland P, Coggeshall RE (1992) Peripheral nerve injury triggers central sprouting of myelinated afferents. Nature 355:75–78.

Wright DE, Snider WD (1995) Neurotrophin receptor mRNA expression defines distinct populations of neurons in rat dorsal root ganglia. J Comp Neurol 351:329–338.

Yan Q, Rosenfeld RD, Matheson CR, Hawkins N, Lopez OT, Bennett L, Welcher AA (1997) Expression of brain-derived neurotrophic factor (BDNF) protein in the adult rat central nervous system. Neuroscience 78:431–448.

Zhou X-F, Rush RA (1996) Endogenous brain-derived neurotrophic factor is anterogradely transported in primary sensory neurons. Neuroscience 74:945–951.

0270-6474/84/0407-1683$02.00/0

The Journal of Neuroscience
Vol. 4, No. 7, pp. 1683–1689
July 1984

UPTAKE OF NERVE GROWTH FACTOR ALONG PERIPHERAL AND SPINAL AXONS OF PRIMARY SENSORY NEURONS[1]

P. M. RICHARDSON[2] AND R. J. RIOPELLE

Division of Neurosurgery, McGill University, Montreal, Canada, and Division of Neurology, Queen's University, Kingston, Canada

Received August 22, 1983; Revised January 13, 1984; Accepted January 13, 1984

Abstract

To investigate the distribution of nerve growth factor (NGF) receptors on peripheral and central axons, [^{125}I]NGF was injected into the sciatic nerve or spinal cord of adult rats. Accumulation of [^{125}I]NGF in lumbar dorsal root ganglia was monitored by gamma emission counting and radioautography.

[^{125}I]NGF, injected endoneurially in small quantities, was taken into sensory axons by a saturable process and was transported retrogradely to their cell bodies at a maximal rate of 2.5 to 7.5 mm/hr. Because very little [^{125}I]NGF reached peripheral terminals, the results were interpreted to indicate that receptors for NGF are present on nonterminal segments of sensory axons. The specificity and high affinity of NGF uptake were illustrated by observations that negligible amounts of gamma activity accumulated in lumbar dorsal root ganglia after comparable intraneural injection of [^{125}I] cytochrome C or [^{125}I]oxidized NGF.

Similar techniques were used to demonstrate avid internalization and retrograde transport of [^{125}I]NGF by intraspinal axons arising from dorsal root ganglia. Following injection of [^{125}I]NGF into lumbar or cervical regions of the spinal cord, neuronal perikarya were clearly labeled in radioautographs of lumbar dorsal root ganglia.

Sites for NGF uptake on primary sensory neurons in the adult rat are not restricted to peripheral axon terminals but are extensively distributed along both peripheral and central axons. Receptors on axons provide a mechanism whereby NGF supplied by glia could influence neuronal maintenance or axonal regeneration.

Nerve growth factor (NGF) is necessary for the development and function of sensory neurons (Gorin and Johnson, 1979, 1980; Kessler and Black, 1980; Goedert et al., 1981; Schwartz et al., 1982; Otten and Lorez, 1983); NGF, or a similar molecule, is released by Schwann cells or other cells that are present within peripheral nerve trunks (Burnham et al., 1972; Riopelle et al., 1981; Richardson and Ebendal, 1982). If NGF-like activity of endoneurial origin is physiologically important (Varon and Bunge, 1978), receptors for NGF are to be expected in axonal membrane along the course of peripheral sensory fibers. In previous studies of axonal internalization and retrograde transport of [^{125}I]NGF *in vivo* (Hendry et al., 1974; Stoeckel et al., 1975; Johnson et al., 1978; Dumas et al., 1979), uptake has been demonstrated at or near peripheral sympathetic and sensory terminals, but the possible existence of receptors on more proximal axonal segments has not been examined systematically. *In vitro*, [^{125}I]NGF has been shown by radioautography to bind to cell bodies, neurites, and neurite terminals of cultured sympathetic and dorsal root ganglion neurons (Kim et al., 1979; Carbonetto and Stach, 1982; Rohrer and Barde, 1982). From observations of [^{125}I]NGF uptake and transport in adult rats, we conclude that specific receptors for NGF are found on peripheral sensory axons within the sciatic nerve and also on spinal axons of primary sensory neurons.

Materials and Methods

Preparation of [^{125}I]NGF. NGF was prepared from submandibular glands of male Swiss-Webster mice (Jackson Laboratories) according to the method of Mobley et al. (1976) with substitution of a continuous gradient of NaCl concentration for the last elution (Chapman et al., 1981). In bioassay with dissociated chick

[1] This work was supported by the Medical Research Council of Canada and the Multiple Sclerosis Society of Canada. We wish to thank Valerie Issa, Monica Altares, and Shizuye Faulkner for technical assistance and Evelyn Domond for secretarial assistance.

[2] To whom correspondence should be addressed, at Division of Neurosurgery, Montreal General Hospital, 1650 Cedar Avenue, Montreal, Canada, H3G 1A4.

sensory neurons (Riopelle and Cameron, 1981), maximal neurite outgrowth was obtained at approximately 70 pg/ml of NGF. For radioiodination (Sutter et al., 1979), a mixture of NaI (5 μCi, Amersham Searle), NGF (5 μg), hydrogen peroxide (5 μl of a 0.003% solution at 0 and 30 min), and phosphate buffer (0.1 M, pH 7.4 to a total volume of 50 μl) were incubated for 1 hr at room temperature. Fifty microliters of cold 0.4% acetic acid and 200 to 400 μl of acetate buffer (0.5 M, pH 4.0) with bovine serum albumin (1 mg/ml) and protamine sulfate (1 mg/ml) were then added, and the mixture was dialyzed for 36 to 48 hr against two or three changes of 0.05 M acetate buffer (pH 4.0). The efficiency of labeling was 50 to 65%, and after dialysis >95% of gamma activity was precipitable with 10% trichloroacetic acid. Six preparations of [^{125}I]NGF from two batches of NGF were used with final concentrations of 10 to 38 ng/μl and specific activities of 34 to 84 cpm/pg (approximately 30 to 80 μCi/μg). For dose-response curves, [^{125}I]NGF was diluted with saline or mixed with unlabeled NGF, and final concentrations were verified with gamma counting. Cytochrome C (Sigma Chemical Co.) and NGF with two oxidized tryptophan residues (Cohen et al., 1980) were also radioiodinated by the lactoperoxidase technique. The final concentrations and specific activities were 12 ng/μl and 18 cpm/pg for [^{125}I]cytochrome C and 11 ng/μl and 14 cpm/pg for [^{125}I]oxidized NGF. Iodinated proteins were injected within 2 weeks of preparation.

Injections. Female Sprague-Dawley rats weighing 150 to 200 gm (Charles River Breeding Labs) were anesthetized with pentobarbital, and the sciatic nerve was exposed in the thigh. Through a glass micropipette connected to a Hamilton syringe and filled with mineral oil (Beitz and King, 1976), 1 μl of a given solution was injected into the sciatic nerve near the origin of the nerve to biceps femoris. In control experiments, injection was, if necessary, further distal, and the sciatic nerve was crushed with jeweller's forceps either at the site of injection or 1.0 to 2.0 cm proximally. In two instances, the tibial, peroneal, sural, and biceps branches of the sciatic nerve were all cut at the time of injection to prevent [^{125}I]NGF from reaching sensory axon terminals.

For intraspinal injections, laminectomies were performed with microsurgical technique at high cervical or high lumbar levels. After subdural injection of paraffin oil to prevent extravasation in the CSF, [^{125}I]NGF (or another ^{125}I-protein) was injected in two to four sites to a total volume of 2 to 4 μl.

Counting of gamma activity. Four to 24 hr after injection of [^{125}I]NGF, rats were anesthetized and perfused with 4% formaldehyde, 0.5% glutaraldehyde in phosphate buffer. The fourth and fifth lumbar dorsal root ganglia (L4 and L5 DRG), identified by reference to the sacrum, were removed, and their gamma emission was counted in an LKB-Wallac 1270 Rackgamma counter.

SDS-polyacrylamide gel electrophoresis. Twelve L4 or L5 DRG, collected 10 hr after intraneural administration of [^{125}I]NGF, were homogenized in an aqueous solution of 1% SDS and 2% β-mercaptoethanol. The homogenate was concentrated to 0.3 ml by evaporation, heated to 100°C for 5 min, and centrifuged. Fifty-microliter aliquots of the supernatant were electrophoresed with a discontinuous buffer system (Laemmli, 1970) and resolving gel containing 12% polyacrylamide and 0.1% SDS. Each lane of the gel was cut into 10-mm slices which were counted individually.

Radioautography. Selected DRG were fixed, osmicated, dehydrated, and embedded in plastic. Sections, 1 μm thick, were dipped in Kodak NTB-2 emulsion, stored in lightproof boxes for 1 month, developed with Kodak D-19 solution, stained with toluidine blue, and mounted in glycerine.

Results

One hour after injection of [^{125}I]NGF (1 μl, 8 ng) into the sciatic nerve, 97% of the activity within the nerve was contained in a segment 1 cm long; at 12 hr, 96% of the intraneural activity (35% of the injected activity) was recovered in a 3.5 cm segment of nerve (Fig. 1). These data delineate limits for diffusion of [^{125}I]NGF within the nerve.

Eight or more hours after injection of [^{125}I]NGF into the sciatic nerve, significant gamma activity was consistently detected in ipsilateral L4 and L5 DRG (Fig. 2*a*). Small and variable amounts of gamma activity were also counted in L3 and L6 ganglia, but none was found in the lumbar spinal cord. Neither crushing the nerve at the site of injection nor isolating the nerve from its peripheral connections by sectioning distal branches changed the accumulation of activity in L4 and L5 DRG. Nerve crush 1.5 to 2.0 cm proximal to the injection site completely prevented gamma activity from reaching lumbar DRG (Table I); crush 1.0 cm proximal blocked 90% of gamma activity from accumulating in L4 and L5 DRG. After injection of comparable amounts of [^{125}I]cytochrome C or [^{125}I]oxidized NGF, gamma activity in lumbar DRG was not significantly higher than background (Table I). These control experiments exclude diffusion along the nerve, hematogenous spread, and nonspecific uptake as spurious causes of labeling in DRG of experimental rats.

To determine the rate of transport of [^{125}I]NGF in the sciatic nerve, rats were sacrificed 4, 8, 12, 18, and 24 hr after intraneural injection in the thigh (Fig. 2*b*). No activity reached L4 and L5 DRG in 4 hr; counts were maximal at 12 to 18 hr and fell by 24 hr. Given that the injection site was 3.5 cm from the 14 ganglion and that [^{125}I]NGF diffused 0.5 to 1.5 cm proximally, the rate of transport was estimated at 2.5 to 7.5 mm/hr for the fastest particles.

In another group of rats, a dose-response curve was obtained by injecting different quantities (0.1 to 74 ng in 1 μl) of [^{125}I]NGF into the sciatic nerve and counting activity in L4 and L5 DRG after 11 hr (Fig. 2*c*). Double reciprocal analysis of data (inverse of accumulation versus inverse of injection) indicated a saturable process with maximal accumulation per DRG of 29 pg (1.1 fmol) and half-maximal uptake at 4 ng (0.2 pmol) (Fig. 2*d*). The true maximal accumulation is, perhaps, slightly higher because accumulation was 38 pg in one series of rats injected with freshly dialyzed [^{125}I]NGF. The amounts of NGF injected were insufficient to study probable additional uptake at lower affinity (Dumas et al., 1979).

1.

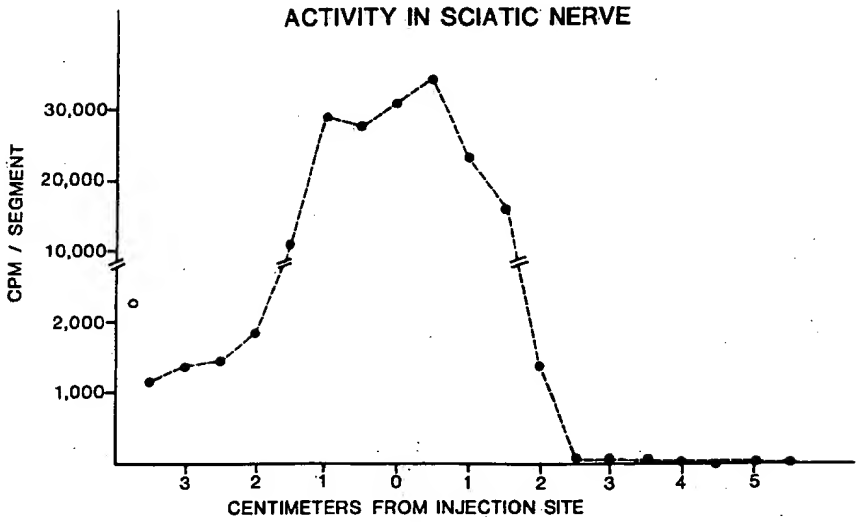

Figure 1. Activity in segments, 5 mm long, of the sciatic nerve 12 hr after injection of [^{125}I]NGF (1 μl, 8 ng, 500,000 cpm) into nerve in upper thigh. ●, mean value per segment in two injected nerves; O, mean total activity in L4 and L5 DRG. Thirty-seven percent of injected activity was recovered in the nerve and two DRG at 12 hr. Very high counts near the site of injection indicate the extent of diffusion; negligible counts in distal segments show lack of anterograde axonal transport; moderate counts in proximal segments and DRG are compatible with retrograde axonal transport.

After SDS-polyacrylamide gel electrophoresis, 77% of the recovered gamma activity migrated in the penultimate slice before the front as did a standard molecule of molecular weight = 14,400 (α-lactalbumin). This information is compatible with previous evidence that NGF is transported retrogradely in an intact form (Hendry et al., 1974; Stoeckel et al., 1975; Johnson et al., 1978; Dumas et al., 1979).

In radioautographs of L4 and L5 DRG, label was concentrated in neurons rather than non-neuronal cells or the extracellular space. Neurons of all sizes were labeled and, in some ganglia, more than a third of neurons contained 10 or more grains.

Uptake from lumbar spinal cord. Very little [^{125}I]NGF diffused into L4 and L5 spinal roots after lumbar intraspinal injection. In one such rat, 10 hr after injection, the total activity in a 1 cm segment of the spinal cord at the site of injection was 218,000 cpm, and the average activities in consecutive 5-mm segments of the L4 and L5 roots were 1721, 543, 240, 255, and 386 cpm. Thus, injection of [^{125}I]NGF into the lumbar spinal cord did not result in a large pool of activity in the lumbar spinal roots.

After intraspinal injection, as after intraneural injection, [^{125}I]NGF was consistently recovered from L4 and L5 DRG (Fig. 3*a*). In radioautographs, activity was concentrated in neurons. Accumulation was prevented if dorsal roots were crushed or avulsed at the time of injection (Table I). Twelve hours after injection of [^{125}I] cytochrome C, the mean activity in L4 and L5 DRG averaged 8 cpm above background.

The time course of accumulation of [^{125}I]NGF in lumbar DRG after injection into the lumbar spinal cord (Fig. 3*b*) showed insignificant activity at 4 hr, peak counts at 12 hr, and some loss from the ganglia by 24 hr. As the L4 and L5 dorsal roots are 2.5 to 3.0 cm long, these data are compatible with maximal retrograde axonal transport at 3.1 to 7.5 mm/hr.

A dose-response curve (Fig. 3*c*) and double reciprocal plotting of data (Fig. 3*d*) again suggested saturable uptake with maximal accumulation of 14 pg (0.5 fmol)/DRG and half-maximal uptake with 14 ng (0.5 pmol).

Uptake from high spinal levels. In a total of 11 rats (Table II), [^{125}I]NGF from four preparations was injected into the dorsal columns and dorsal column nuclei at the craniocervical junction. Subsequently, mean accumulation per lumbar DRG was 0.5 to 1.3 pg in the four groups. In radioautographs of DRG in one well labeled animal, approximately 6% of neurons were labeled (Fig. 4). Counts in lumbar DRG after cervical injection of [^{125}I] cytochrome C did not exceed background.

Following injection of [^{125}I]NGF into the midthoracic spinal cord (32 ng in 3 μl), the accumulation per lumbar DRG (0.8 ± 0.1 pg) was similar to that after cervical injection of the same batch of [^{125}I]NGF. The uptake was unchanged by deliberate injury to the spinal cord immediately rostral to the site of injection.

Discussion

NGF uptake by peripheral axons. NGF receptors are deduced to be present along the course of normal sensory axons in the sciatic nerve because the intraneuronal accumulation of [^{125}I]NGF injected into the endoneurium cannot be entirely explained by diffusion to peripheral

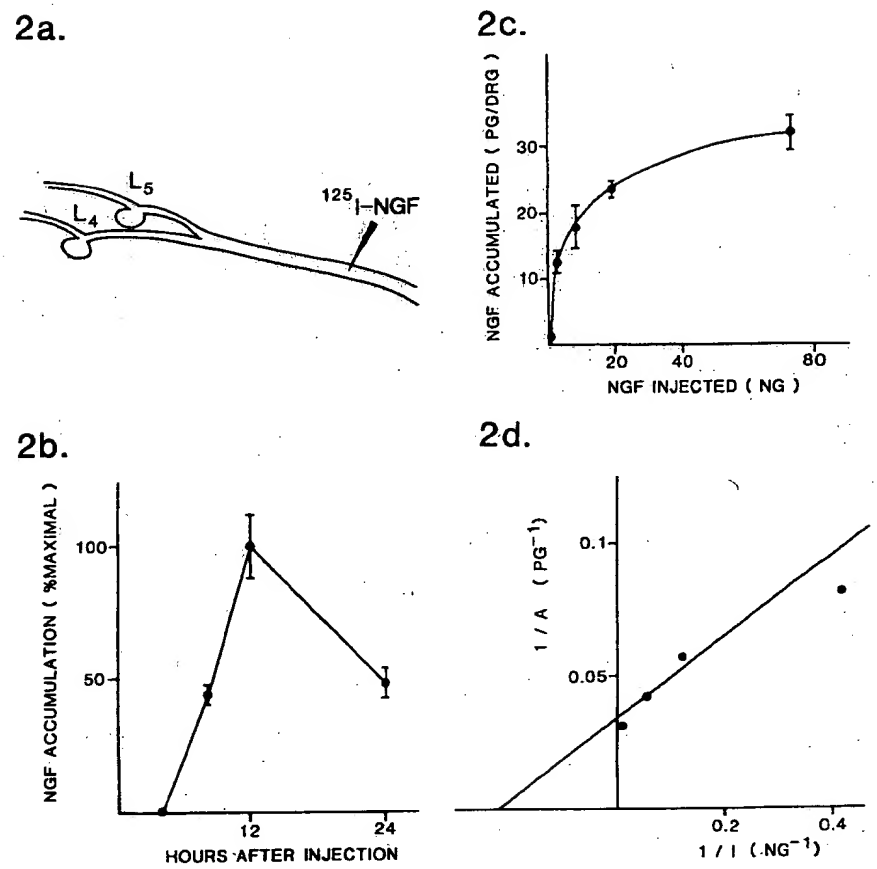

Figure 2. a, Diagram illustrating experiments in which [^{125}I]NGF was injected into the sciatic nerve in the upper thigh and gamma activity was subsequently counted in L4 and L5 DRG. *b*, Accumulation of NGF in L4 or L5 DRG of rats sacrificed 0 to 24 hr after injection of [^{125}I]NGF (1 μl, 11 ng) into sciatic nerve in upper thigh. The mean ± SEM for 12 ganglia (6 nerves) is expressed as a percentage of the accumulation at 12 hr. *c*, Accumulation of NGF in L4 or L5 DRG of rats sacrificed 11 hr after injection of 0.3 to 74 ng of [^{125}I]NGF (1 μl) into sciatic nerve in upper thigh. A mixture of labeled and unlabeled NGF was used for the highest concentration; serial dilutions of [^{125}I]NGF were used for all other points. Data are the mean ± SEM (picograms per DRG) for 12 to 16 ganglia and 6 to 8 nerves. *d*, Double reciprocal plot of data in *c*. The reciprocal of the *y* intercept = the maximal amount of [^{125}I]NGF accumulated per DRG by high affinity system = 29 pg (1.1 fmol). The reciprocal of the *x* intercept = the amount of injected [^{125}I]NGF yielding half-maximal saturation = 4 ng (0.2 pmol).

TABLE I

Comparison of mean accumulation per DRG in one experimental group and three control groups after intraneural injection, and in one experimental group and two control groups after intraspinal injection

Activity in L4 and L5 DRG was counted 12 to 24 hr after injection

	Injection into Sciatic Nerve		Injection into Lumbar Spinal Cord	
	Injection	Accumulation	Injection	Accumulation
	cpm	*cpm/DRG*	*cpm*	*cpm/DRG*
[^{125}I]NGF	500,000	1071	700,000	409
[^{125}I]NGF with nerve or root crush	500,000	3	1,800,000	6
[^{125}I]Cytochrome C	400,000	5	800,000	8
[^{125}I]Oxidized NGF	300,000	3		

receptors or by injury of axons at the time of injection. Indeed, it was originally reported (Hendry et al., 1974), although not subsequently emphasized, that intact terminals are not necessary for NGF internalization by sympathetic axons. NGF receptors were specific in their recognition of injected molecules and in their distribution among types of axons. [^{125}I]Cytochrome C and [^{125}I] oxidized NGF were not taken up at high affinity as was [^{125}I]NGF; somatic motor axons did not internalize and transport [^{125}I]NGF as did sensory axons (and, presumably, sympathetic axons). Although [^{125}I]NGF accumulated in large and small neurons in DRG, it is not known whether axonal membrane on all dorsal root ganglion neurons is equally responsive to NGF. The maximal rate of retrograde axonal transport of NGF in sensory axons was found to be slightly slower than previously calculated (Stoeckel et al., 1975) but similar to that for NGF in sympathetic axons (Hendry et al., 1974) and for other proteins in general (Grafstein and Forman, 1980).

Quantitative considerations. The amounts of NGF accumulating in sensory ganglia after intraneural injection and in sympathetic ganglia after intraocular injection are similar, as are the amounts of injected NGF necessary

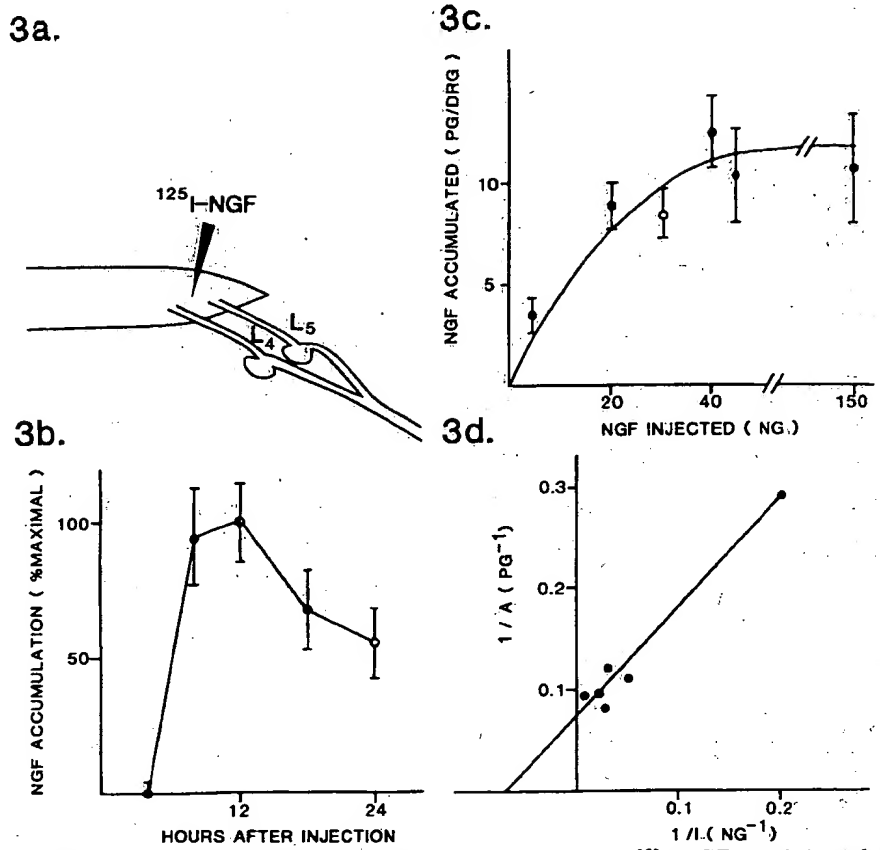

Figure 3. a, Diagram illustrating experiments in which [^{125}I]NGF was injected into lumbar spinal cord and gamma activity was subsequently counted in L4 and L5 DRG. *b*, Accumulation of NGF in L4 or L5 DRG in rats sacrificed 0 to 24 hr after injection of [^{125}I]NGF into the lumbar spinal cord. Two preparations of [^{125}I]NGF were injected: O, 40 ng in 4 μl; ●, 100 ng in 3 μl. The mean ± SEM for 16 ganglia (4 rats) is expressed as a percentage of the accumulation at 12 hr. *c*, Accumulation of NGF in L4 or L5 DRG in rats sacrificed 12 hr after injection of [^{125}I]NGF (4 μl) into the lumbar spinal cord. O, Three different batches of [^{125}I]NGF were used. Data are the mean ± SEM (picograms of [^{125}I]NGF per DRG) for 16 ganglia (4 rats). A mixture of labeled and unlabeled NGF was used for the highest concentration; serial dilutions of [^{125}I]NGF were used for all other points. *d*, Double reciprocal plot of data in *c*. The reciprocal of the *y* intercept = the maximal amount of [^{125}I]NGF accumulated per DRG by high affinity system = 14 pg (0.5 fmol). The reciprocal of the *x* intercept = the amount of injected [^{125}I]NGF yielding half-maximal saturation = 14 ng (0.5 pmol).

TABLE II

Cervical injection of [^{125}I]NGF

Results of four experiments (11 rats) in which [^{125}I]NGF was injected into the dorsal columns and dorsal column nuclei at the bulbospinal junction. Gamma activity in L4 and L5 was consistently above background levels.

Injection		Hours to Sacrifice	Accumulation
ng	*µl*		*pg/DRG ± SEM*
20	2	18	0.6 ± 0.1
32	3	24	0.6 ± 0.1
42	2	24	0.8 ± 0.1
53	2	24	1.3 ± 0.2

for half-maximal uptake (Johnson et al., 1978). The maximal accumulation and half-saturation point of the dose-response curve are assumed to reflect the density and affinity of axonal receptors for NGF (Dumas et al., 1979). The density of receptors in the sciatic nerve can be very approximately estimated at 10,000/mm length of each sensory axon if it is assumed that [^{125}I]NGF reaching the L4 or L5 DRG is taken up by 6000 axons over a 10-mm segment of nerve, that each receptor internalizes one molecule of NGF only, and that recycling of receptors is negligible during a few hours. The dissociation-equilibrium constant (K_d) of axonal receptors cannot be calculated precisely from these data because the concentration of [^{125}I]NGF at the axonal membrane after endoneurial injection is unknown. It remains to be proved that NGF receptors with K_d in the order of 10^{-11} M are present on adult rat axons as on embryonic chick neurons (Sutter et al., 1979; Riopelle et al., 1980).

The finding of NGF receptors along the course of peripheral sensory axons suggests that NGF released by endoneurial cells might have local paracrine effects. However, the amount of injected [^{125}I]NGF yielding half-saturable uptake in sensory axons (4 ng) is two orders of

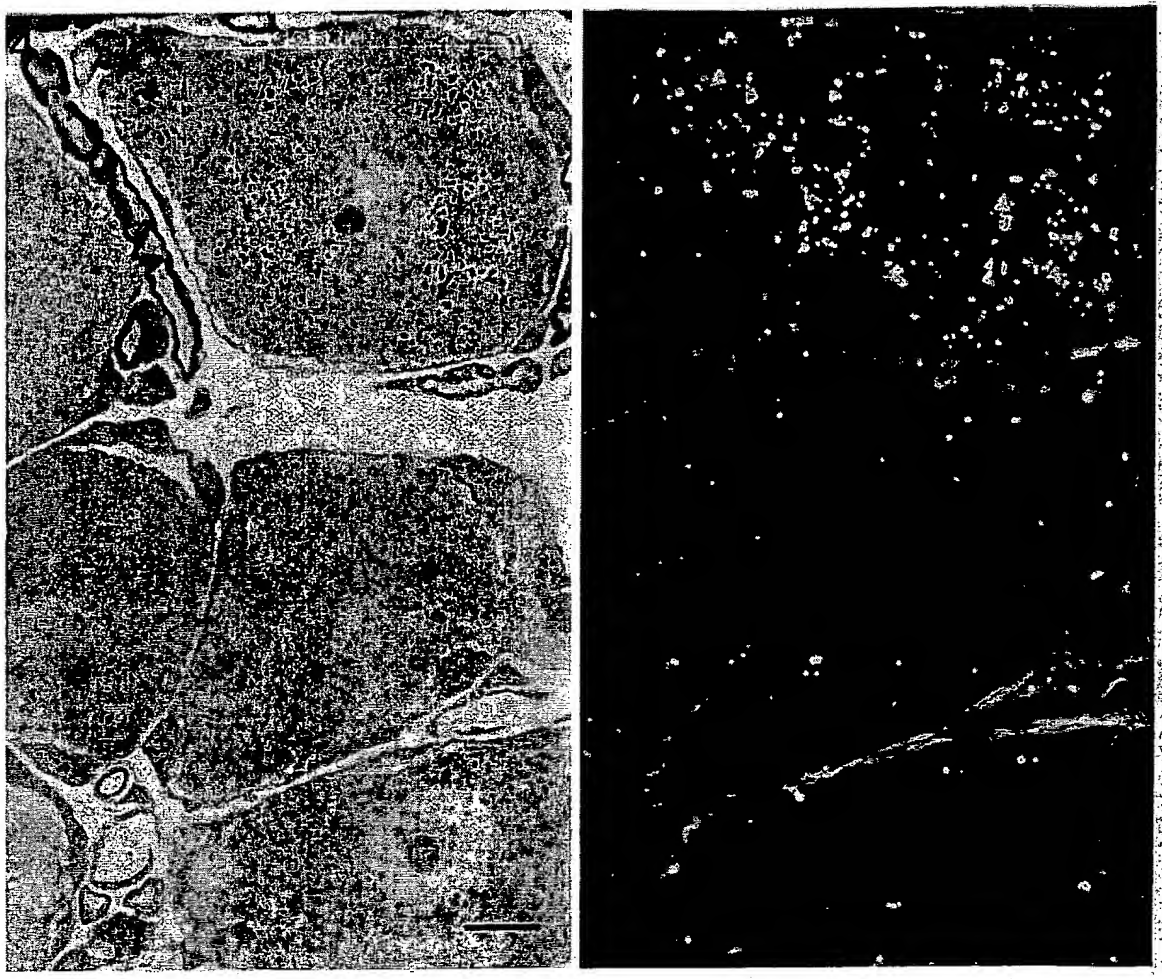

Figure 4. Light- and darkfield radioautographs of L5 DRG in a rat sacrificed 24 hr after injection of [^{125}I]NGF (2 μl, 53 ng, 4.5 × 10^6 cpm) into dorsal column nuclei and high cervical dorsal columns. Labeling in one neuron is well above background level (*scale bar* = 10 μm).

magnitude greater than the estimated content of NGF-like activity per centimeter length of normal rat sciatic nerve (Ebendal and Richardson, 1983). Quantitative analysis of endogenous ligand-receptor interactions awaits knowledge of the distribution of NGF-like activity within the endoneurium and the deployment of NGF receptors on axonal membrane of nodal and internodal segments.

NGF uptake by spinal axons. Previous evidence that receptors for NGF are present within the central nervous system (Frazier et al., 1974; Schwab et al., 1979) is corroborated by the finding of labeled neurons in radioautographs of lumbar DRG after cervical injection of [^{125}I]NGF (Fig. 4). In other words, ensheathment by Schwann cells is not a necessary condition for the manifestation of NGF receptors. The apparent difference in affinities of NGF uptake from the lumbar spinal cord and the sciatic nerve is probably due to a larger volume of diffusion in the spinal cord rather than to different dissociation equilibrium constants for spinal and peripheral receptors. Sites for NGF internalization could be on terminal or nonterminal regions of spinal axons, and their density per unit area of axon membrane in the spinal cord could be equal or less to that in peripheral nerves. The function of NGF receptors in the maintenance and regeneration (Richardson et al., 1982) of sensory axons in the spinal cord is unknown.

References

Beitz, A. J., and G. W. King (1976) An improved technique for the microinjection of horseradish peroxidase. Brain Res. *108:* 175–179.

Burnham, P., C. Raiborn, and S. Varon (1972) Replacement of nerve-growth factor by ganglionic non-neuronal cells for the survival *in vitro* of dissociated ganglionic neurons. Proc. Natl. Acad. Sci. U. S. A. *69:* 3556–3560.

Carbonetto, S., and R. W. Stach (1982) Localization of nerve growth factor bound to neurons growing nerve fibers in culture. Dev. Brain Res. *3:* 463–473.

Chapman, C. A., B. E. C. Banks, C. A. Vernon, and J. M. Walker (1981) The isolation and characterisation of nerve growth factor from the prostate gland of the guinea-pig. Eur. J. Biochem. *115:* 347–351.

Cohen, P., A. Sutter, G. Landreth, A. Zimmermann, and E. M. Shooter (1980) Oxidation of tryptophan-21 alters the biological activity and receptor binding characteristics of mouse nerve growth factor. J. Biol. Chem. *255:* 2949–2954.

Dumas, M., M. E. Schwab, and H. Thoenen (1979) Retrograde axonal transport of specific macromolecules as a tool for characterizing nerve terminal membranes. J. Neurobiol. *10:* 179–197.

Ebendal, T., and P. M. Richardson (1983) Bioassay and radioimmunoassay of NGF-like activity in rat peripheral nerve. Soc. Neurosci. Abstr. *9:* 839.

Frazier, W. A., L. F. Boyd, M. W. Pulliam, A. Szutowicz, and R. A. Bradshaw (1974) Properties and specificity of binding sites for ^{125}I-nerve growth factor in embryonic heart and brain. J. Biol. Chem. *249:* 5918–5923.

Goedert, M., K. Stoeckel, and U. Otten (1981) Biological importance of the retrograde axonal transport of nerve growth factor in sensory neurons. Proc. Natl. Acad. Sci. U. S. A. *78:* 5895–5898.

Gorin, P. D., and E. M. Johnson (1979) Experimental autoimmune model of nerve growth factor deprivation: Effects on developing peripheral sympathetic and sensory neurons. Proc. Natl. Acad. Sci. U. S. A. *76:* 5382–5386.

Gorin, P. D., and E. M. Johnson, Jr. (1980) Effects of long-term nerve growth factor deprivation on the nervous system of the adult rat: An experimental autoimmune approach. Brain Res. *198:* 27–42.

Grafstein, B., and D. S. Forman (1980) Intracellular transport in neurons. Physiol. Rev. *60:* 1167–1283.

Hendry, I. A., K. Stoeckel, H. Thoenen, and L. L. Iversen (1974) The retrograde axonal transport of nerve growth factor. Brain Res. *68:* 103–121.

Johnson, E. M., Jr., R. Y. Andres, and R. A. Bradshaw (1978) Characterization of the retrograde transport of nerve growth factor (NGF) using high specific activity ^{125}I-NGF. Brain Res. *150:* 319–331.

Kessler, J. A., and I. B. Black (1980) Nerve growth factor stimulates the development of substance P in sensory ganglia. Proc. Natl. Acad. Sci. U. S. A. *77:* 649–652.

Kim, S. U., R. Hogue-Angeletti, and N. K. Gonatas (1979) Localization of nerve growth factor receptors in sympathetic neurons cultured *in vitro.* Brain Res. *168:* 602–608.

Laemmli, U. K. (1970) Cleavage of structural proteins during the assembly of the head of bacteriophage T4. Nature *227:* 680–685.

Mobley, W. C., A. Schenker, and E. M. Shooter (1976) Characterization and isolation of proteolytically modified nerve growth factor. Biochemistry *15:* 5543–5551.

Otten, U., and H. P. Lorez (1983) Nerve growth factor increases substance P, cholecystokinin and vasoactive intestinal polypeptide immunoreactivities in primary sensory neurones of newborn rats. Neurosci. Lett. *34:* 153–158.

Richardson, P. M., and T. Ebendal (1982) Nerve growth activities in rat peripheral nerve. Brain Res. *246:* 57–64.

Richardson, P. M., U. M. McGuinness, and A. J. Aguayo (1982) Peripheral nerve autografts to the rat spinal cord: Studies with axonal tracing methods. Brain Res. *237:* 147–162.

Riopelle, R. J., and D. A. Cameron (1981) Neurite growth promoting factors of embryonic chick—ontogeny, regional distribution and characteristics. J. Neurobiol. *12:* 175–186.

Riopelle, R. J., M. Klearman, and A. Sutter (1980) Nerve growth factor receptors: Analysis of the interaction of βNGF with membranes of chick embryo dorsal root ganglia. Brain Res *199:* 63–77.

Riopelle, R. J., R. J. Boegman, and D. A. Cameron (1981) Peripheral nerve contains heterogeneous growth factors that support sensory neurons in vitro. Neurosci. Lett. *25:* 311–316.

Rohrer, H., and Y. -A. Barde (1982) Presence and disappearance of nerve growth factor receptors on sensory neurons in culture. Dev. Biol. *89:* 309–315.

Schwab, M. E., U. Otten, Y. Agid, and H. Thoenen (1979) Nerve growth factor (NGF) in the rat CNS: Absence of specific retrograde axonal transport and tyrosine hydroxylase induction in locus coeruleus and substantia nigra. Brain Res. *168:* 473–483.

Schwartz, J. P., J. Pearson, and E. M. Johnson (1982) Effect of exposure to anti-NGF on sensory neurons of adult rats and guinea pigs. Brain Res. *244:* 378–381.

Stoeckel, K., M. Schwab, and H. Thoenen (1975) Specificity of retrograde transport of nerve growth factor (NGF) in sensory neurons: A biochemical and morphological study. Brain Res. *89:* 1–14.

Sutter, A., R. J. Riopelle, R. M. Harris-Warrick, and E. M. Shooter (1979) Nerve growth factor receptors: Characterization of two distinct classes of binding sites on chick embryo sensory ganglia cells. J. Biol. Chem. *254:* 5972–5982.

Varon, S. S., and R. P. Bunge (1978) Trophic mechanisms in the peripheral nervous system. Annu. Rev. Neurosci. *1:* 327–361.

Journal of Neurochemistry
Lippincott–Raven Publishers, Philadelphia

Time-Resolved Signaling Pathways of Nerve Growth Factor Diverge Downstream of the p140trk Receptor Activation Between Chick Sympathetic and Dorsal Root Ganglion Sensory Neurons

Franz-Josef Klinz and Rolf Heumann

Department of Molecular Neurobiochemistry, Ruhr-Universität Bochum, Bochum, Germany

Abstract: We have recently shown that the small GTP binding protein p21ras is essential for nerve growth factor (NGF)-mediated survival of peripheral embryonic chick dorsal root ganglia (DRG) sensory but not sympathetic neurons. To investigate at which level of the signaling cascade the pathways diverge, we have studied the time-resolved pattern of NGF-stimulated tyrosine phosphorylation of proteins within 4 h after addition of the neurotrophin. In both chick sympathetic neurons [embryonic day (E) 12] and DRG sensory neurons (E9) NGF induces within 1 min the autophosphorylation of the receptor tyrosine kinase p140trk. However, the pattern of substrate protein tyrosine phosphorylation downstream of p140trk is distinctly different in both neuronal subtypes. In sympathetic neurons, we observe within 1 min the tyrosine phosphorylation of a new substrate protein, p105, reaching maximal levels at 3 min. Tyrosine phosphorylation of p105 remains elevated for up to 4 h. Subsequent to p105, NGF induces the tyrosine phosphorylation of p42, a protein belonging to the family of mitogen-activated protein (MAP) kinases. This stimulation is transient, reaching maximal levels at 10 min and returning to very low levels already after 2 h. In DRG sensory neurons, tyrosine phosphorylation of p105 is weak and very short lived, disappearing already after treatment with NGF for 10 min. In contrast, activation of MAP kinase p42 in DRG sensory neurons is more stable than in sympathetic neurons. All NGF-stimulated tyrosine phosphorylation events were inhibited by preincubation of neurons with the tropomyosin-related kinase (trk) inhibitor K252a. We suggest the working hypothesis that persistent tyrosine phosphorylation of p105 may play a role in the p21ras-independent NGF survival pathway of chick sympathetic neurons. **Key Words:** Chick sympathetic neurons—Chick dorsal root ganglia sensory neurons—Nerve growth factor signal transduction—Protein tyrosine phosphorylation—Tropomyosin-related kinase receptor—Mitogen-activated protein kinase.
J. Neurochem. **65,** 1046–1053 (1995).

Nerve growth factor (NGF) belongs to the family of neurotrophins specifically interacting with the receptor tyrosine kinase p140trk and with the low-affinity receptor p75 (see, for review, Meakin and Shooter, 1992; Chao, 1992; Barbacid, 1993). Recent gene knock-out experiments on NGF and on the tyrosine kinase domain of its p140trk receptor have confirmed that NGF activity is essential for the survival of peripheral sympathetic and certain types of sensory neurons involved in pain transmission (see, for review, Snider, 1994). The p75 low-affinity NGF receptor binds to all neurotrophins and appears to modulate the p140trk receptor activity at limiting concentrations of the NGF ligand (Barker and Shooter, 1994). In addition, an intrinsic p75 receptor signaling mechanism involving activation of the sphingomyelin cycle has been described recently (Dobrowsky et al., 1994).

As with other tyrosine kinase receptors, aggregation and tyrosine autophosphorylation of tropomyosin-related kinase (trk) receptor are essential to initiate the various signaling mechanisms of NGF (Jing et al., 1992; Clary et al., 1994). The subsequent steps of intracellular signaling events (see, for review, Heumann, 1994; Saltiel and Decker, 1994) have been extensively studied in transformed rat pheochromocytoma PC12 cells, which differentiate into sympathetic neuron-like cells on long-term exposure to NGF (Greene and Tischler, 1976). The autophosphorylation of the trk receptor opens binding sites for the src homology region 2 (SH2) domains of the SHC protein (Obermeier et al., 1994; Ohmichi et al., 1994; Stephens et al., 1994), the p85 regulatory subunit of phosphati-

Received December 19, 1994; revised manuscript received March 6, 1995; accepted March 14, 1995.

Address correspondence and reprint requests to Dr. F.-J. Klinz at Department of Molecular Neurobiochemistry, Ruhr-Universität Bochum, Universitätsstrasse 150, D-44780 Bochum, Germany.

Abbreviations used: DRG, dorsal root ganglia; E, embryonic day; ERK, extracellular signal-regulated kinase; MAP, mitogen-activated protein; MEK, mitogen-activated protein kinase kinase; NGF, nerve growth factor; PAGE, polyacrylamide gel electrophoresis; SDS, sodium dodecyl sulfate; trk, tropomyosin-related kinase.

dylinositol-3 kinase (Ohmichi et al., 1992*a*; Soltoff et al., 1992) and of phospholipase C-γ1 (Vetter et al., 1991; Obermeier et al., 1994; Stephens et al., 1994). During this process these proteins become phosphorylated on tyrosine residues themselves, and additional SH2 domain proteins are recruited to the membrane. After Grb2-mediated membrane recruitment (Hashimoto et al., 1993; Basu et al., 1994), the p21ras exchange factor mSOS is thought to activate in turn p21ras protein, an inner membrane-bound protein oscillating between the inactive GDP-bound and the signaling-competent GTP-bound conformation (see, for review, Boguski and McCormick, 1993). Other membrane-recruited proteins belong to the family of the raf serine/threonine kinases or mitogen-activated protein (MAP) kinase kinase (MEK) kinases (Oshima et al., 1991; Ohmichi et al., 1992*b*; Jaiswal et al., 1994; Lange-Carter and Johnson, 1994; Vaillancourt et al., 1994). Subsequently, these proteins induce the phosphorylation of MEK and finally MAP kinase (Boulton et al., 1991; Ahn et al., 1992; Lloyd and Wooten, 1992; Qiu et al., 1992; Thomas et al., 1992; Wood et al., 1992). p21ras activity and MEK1 activity have recently been shown to be essential for the induction of neurite outgrowth in PC12 cells (Hagag et al., 1986; Szeberenyi et al., 1990; Cowley et al., 1994).

Although the elucidation of the mechanisms leading to neurite outgrowth in PC12 cells is progressing well, surprisingly little is known about the sequence of events coupled to neurite outgrowth and survival in postmitotic neurons. As an initial approach we have shown previously that activated p21ras protein promotes neurite outgrowth and survival in embryonic chick dorsal root ganglia (DRG) sensory but not sympathetic neurons (Borasio et al., 1989, 1993). Measuring the time-resolved NGF-stimulated tyrosine phosphorylation of proteins in these peripheral neural crest-derived subtypes of neurons, we describe here the common activation of p140trk and divergent downstream signaling pathways.

MATERIALS AND METHODS

Materials

NGF from adult male mouse submaxillary glands was purified as described (Suda et al., 1978) and kindly provided by H. Rohrer (Frankfurt, Germany). Recombinant human NGF and NT3 were gifts of Genentech (San Francisco, CA, U.S.A.).

Plastic dishes were from Nunc (Wiesbaden, Germany). Ham's F14 medium and horse serum were obtained from GIBCO (Eggenstein, Germany). Nonidet P-40 was purchased from Boehringer (Mannheim, Germany). Sodium deoxycholate and sodium dodecyl sulfate (SDS) were obtained from Serva (Heidelberg, Germany). Anti-phosphotyrosine monoclonal antibody 4G10 and anti-MAP kinase R2 antiserum were purchased from UBI (Lake Placid, NY, U.S.A.). Anti-trk rabbit antiserum was purchased from Oncogene Science (Uniondale, NY, U.S.A.). The enhanced chemiluminescence detection system (ECL) and Hyperfilm-ECL were obtained from Amersham (Braunschweig, Germany). All other reagents were from Sigma (Deisenhofen, Germany).

Cell culture

Chick embryonic sensory DRG neurons [embryonic day (E) 9] and sympathetic neurons (E12) were isolated from the corresponding ganglia at the indicated ages and cultured using previously described methods (Lindsay et al., 1985). After trypsinization and dissociation, the cell suspension was preplated as described to remove fibroblasts and glial cells. The neuron-enriched cell suspension was plated at Nunc Petri dishes that had been coated with poly-L-lysine hydrobromide (70–150 kDa). The cultures were maintained with F14 medium containing 10% heat-inactivated horse serum at 37°C and 2.5% CO_2 in a humidified environment.

Two hours after plating NGF was added at a concentration of 10 ng/ml. For some experiments, neurons were preincubated for 10 min with the trk kinase inhibitor K252a at a concentration of 1 μM.

Cell lysis

Cells were washed two times with Ca^{2+}/Mg^{2+}-free phosphate-buffered saline and lysed in a small volume of lysis buffer [50 m*M* Tris-HCl (pH 7.4), 150 m*M* NaCl, 40 m*M* NaF, 5 m*M* EDTA, 5 m*M* EGTA, 1 m*M* sodium orthovanadate, 1% (vol/vol) Nonidet P-40, 0.1% (wt/vol) sodium deoxycholate, 0.1% (wt/vol) SDS, 1 m*M* phenylmethylsulfonyl fluoride, and 10 μg/ml of aprotinin] using a rubber policeman. Lysates were centrifuged for 5 min at 16,000 *g* and 4°C. The supernatant was immediately used for experiments or frozen at −80°C.

SDS-polyacrylamide gel electrophoresis (PAGE)

Three volumes of lysate were mixed with 1 volume of fourfold concentrated sample buffer according to the procedure of Laemmli (1970) and heated for 5 min at 95°C. Proteins in samples together with molecular mass marker proteins were separated on SDS-polyacrylamide gels prepared by the method of Laemmli (1970). If not otherwise indicated, the slab gels (1.5 mm thick) consisted of a 3% stacking gel (10 mm long) and an 8% separating gel (50 mm long).

To analyze the phosphorylation state of MAP kinase p42, we used low-cross-linker SDS-polyacrylamide gels (1.5 mm thick), consisting of a 5% stacking gel (15 mm long) and a 15% separating gel (120 mm long).

Immunoblot analysis

Subsequent to SDS-PAGE, proteins were electrotransferred onto nitrocellulose membranes for 2 h at 100 V in buffer containing 25 m*M* Tris, 192 m*M* glycine, 20% (vol/vol) methanol, and 0.01% (wt/vol) SDS. Proteins on blots were stained with Ponceau S (Nakamura et al., 1985) to ascertain that comparable amounts of protein were loaded in each lane. The nitrocellulose sheets were blocked with 1% (wt/vol) nonfat dry milk, reacted with the primary antibody followed by reaction with the second antibody coupled to horseradish peroxidase. Detection of proteins was performed using the ECL detection system.

Immunoprecipitation analysis

One volume of lysate was diluted with 3 volumes of washing buffer [50 m*M* Tris-HCl (pH 7.9), 137 m*M* NaCl, 1 m*M* sodium orthovanadate, 10% (vol/vol) glycerol, and 1% (vol/vol) Nonidet P-40]. Diluted lysates were incubated

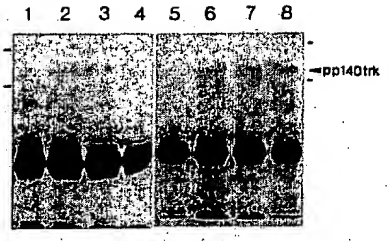

FIG. 1. Tyrosine phosphorylation of p140trk in NGF-treated sympathetic neurons: inhibition by the trk inhibitor K252a. Chick sympathetic neurons (E12) were not treated (lanes 1 and 5) or treated with 10 ng/ml of NGF for 1 (lane 2), 5 (lane 3), 3 (lane 6), 10 (lane 7), or 30 min (lane 8). For lane 4, sympathetic neurons were pretreated with 1 μM K252a for 10 min, followed by incubation with 10 ng/ml of NGF for 1 min. Lanes 1–4 and 5–8 were derived from two independent experiments. Cells were lysed, and trk proteins in the lysate were immunoprecipitated using anti-trk antiserum. Proteins in immunoprecipitates were subjected to SDS-PAGE. After transfer to nitrocellulose, blots were reacted with anti-phosphotyrosine monoclonal antibody. Horizontal upper and lower bars indicate the position of 205- and 116-kDa molecular mass standard proteins, respectively. The arrow on the right points to the position of tyrosine-phosphorylated protein p140trk. The broad bands represent antibody heavy chains in the immunoprecipitate.

with anti-trk antiserum for 4 h, followed by incubation with protein A-Sepharose CL-4B beads for 2 h. After centrifugation the beads were washed three times with washing buffer and heated for 5 min at 95°C in sample buffer according to the procedure of Laemmli (1970). Immunoprecipitated proteins were separated by SDS-PAGE, and immunoblot analysis with anti-phosphotyrosine monoclonal antibody was performed as described before. All experiments were repeated two or three times with similar results.

RESULTS

NGF-stimulated tyrosine phosphorylation of p140trk in cultured chick sympathetic and DRG sensory neurons

We used a combined immunoprecipitation–immunoblot approach to analyze the NGF-stimulated tyrosine phosphorylation of trk in primary neurons. Trk proteins were immunoprecipitated from lysates of NGF-treated sympathetic neurons followed by immunoblot analysis using an anti-phosphotyrosine monoclonal antibody. As can be seen in Fig. 1, tyrosine phosphorylation of p140trk was detectable after stimulation of sympathetic neurons with NGF for 1 min. Treatment with NGF for longer times (up to 30 min) resulted in similar levels of tyrosine phosphorylation of p140trk (see Fig. 1). As expected, NGF-stimulated tyrosine phosphorylation of p140trk could be prevented by preincubation of sympathetic neurons with the trk inhibitor K252a (see Fig. 1).

Similarly, tyrosine phosphorylation of p140trk was observed within 1 min after addition of NGF to chick DRG sensory neurons (Fig. 2). Tyrosine phosphorylation of p140trk could be inhibited by preincubation of DRG sensory neurons with the trk inhibitor K252a (see Fig. 2).

Time-resolved NGF-stimulated tyrosine phosphorylation of a novel protein p105 in cultured chick sympathetic and DRG sensory neurons

We have developed a sensitive method to analyze the tyrosine phosphorylation of proteins in ~50,000 cultured primary neurons. Cells were lysed in a small volume of lysis buffer, and soluble proteins were characterized by immunoblotting using a sensitive and specific monoclonal anti-phosphotyrosine antibody followed by a horseradish peroxidase-conjugated second antibody and an enhanced chemiluminescence detection system.

NGF induced the rapid tyrosine phosphorylation of two proteins in chick sympathetic neurons. A protein with an apparent molecular mass of 105 kDa (p105) became tyrosine-phosphorylated already within 1 min, with phosphorylation peaking at 3 min after exposure to NGF (Fig. 3). On prolonged treatment with NGF, tyrosine phosphorylation of p105 remained stable and declined moderately between 2 and 4 h, the longest interval measured (Fig. 4). Preincubation of sympathetic neurons with the trk inhibitor K252a (see, for review, Knüsel and Hefti, 1992) inhibited the tyrosine phosphorylation of p105 (see Fig. 3). Recombinant NGF stimulated the tyrosine phosphorylation of p105 at the same concentration as did NGF from mouse submaxillary glands (data not shown).

In DRG sensory neurons, NGF induced the weak and transient tyrosine phosphorylation of a protein with an apparent molecular mass of 105 kDa (Fig. 5). Maximal tyrosine phosphorylation of p105 was observed

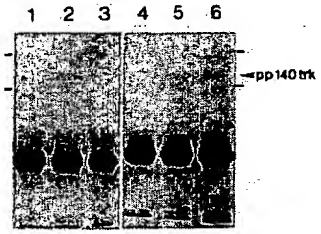

FIG. 2. Tyrosine phosphorylation of p140trk in NGF-treated DRG sensory neurons: inhibition by the trk inhibitor K252a. Chick DRG sensory neurons (E9) were not treated (lanes 1 and 4) or treated with 10 ng/ml of NGF for 1 (lanes 2 and 5) or 5 min (lane 6). For lane 3, DRG sensory neurons were pretreated with 1 μM K252a for 10 min, followed by incubation with 10 ng/ml of NGF for 1 min. Lanes 1–3 and 4–6 were derived from two independent experiments. Cells were lysed, and trk proteins in the lysate were immunoprecipitated using anti-trk antiserum. Proteins in immunoprecipitates were subjected to SDS-PAGE. After transfer to nitrocellulose, blots were reacted with anti-phosphotyrosine monoclonal antibody. Horizontal upper and lower bars indicate the position of 205- and 116-kDa molecular mass standard proteins, respectively. The arrow on the right points to the position of tyrosine-phosphorylated protein p140trk. The broad bands represent antibody heavy chains in the immunoprecipitate.

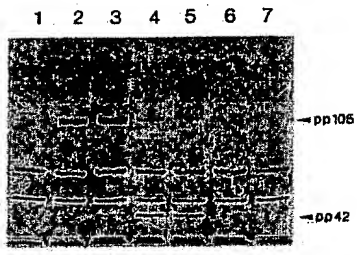

FIG. 3. Tyrosine phosphorylation of proteins in NGF-treated sympathetic neurons: short time course and inhibition by the trk inhibitor K252a. Chick sympathetic neurons (E12) were not treated (lanes 1 and 7) or treated with 10 ng/ml of NGF for 1 (lane 2), 3 (lane 3), 10 (lane 4), or 30 min (lane 5). For lane 6, sympathetic neurons were pretreated with 1 μM K252a for 10 min, followed by incubation with 10 ng/ml of NGF for 10 min. Cells were lysed, and proteins in the lysate were subjected to SDS-PAGE. After transfer to nitrocellulose, blots were reacted with anti-phosphotyrosine monoclonal antibody. Arrows on the right indicate the position of tyrosine-phosphorylated proteins p105 and p42.

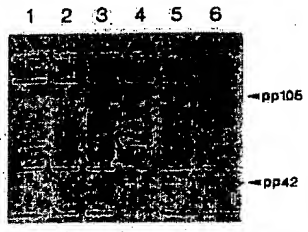

FIG. 5. Tyrosine phosphorylation of proteins in NGF-treated DRG sensory neurons: short time course and inhibition by the trk inhibitor K252a. Chick DRG sensory neurons (E9) were not treated (lane 1) or treated with 10 ng/ml of NGF for 1 min (lane 2), 3 min (lane 3), 10 min (lane 4), or 30 min (lane 5). For lane 6, DRG sensory neurons were pretreated with 1 μM K252a for 10 min, followed by incubation with 10 ng/ml of NGF for 10 min. Cells were lysed, and proteins in the lysate were subjected to SDS-PAGE. After transfer to nitrocellulose, blots were reacted with anti-phosphotyrosine monoclonal antibody. Arrows on the right indicate the position of tyrosine-phosphorylated proteins p105 and p42.

after treatment with NGF for 3 min. In contrast to sympathetic neurons, tyrosine phosphorylation of p105 was hardly detectable after treatment of DRG sensory neurons with NGF for 10 min (see Fig. 5).

Time-resolved NGF-stimulated tyrosine phosphorylation of protein p42 in sympathetic and DRG sensory neurons

After stimulation of sympathetic neurons with NGF for 3 min, we observed the tyrosine phosphorylation of a protein with an apparent molecular mass of 42 kDa (p42) (see Fig. 3). Tyrosine phosphorylation of p42 in sympathetic neurons was maximal after treatment with NGF for 10 min. Between 10 and 30 min after stimulation with NGF the amount of tyrosine-phosphorylated p42 started to decrease to barely detectable levels after 4 h (see Fig. 4). Preincubation of sympathetic neurons with the trk inhibitor K252a prevented the NGF-dependent tyrosine phosphorylation of p42 (see Fig. 3). Recombinant NGF stimulated the tyrosine phosphorylation of p42 at the same concentration as did NGF from mouse submaxillary glands (data not shown).

As in the case with sympathetic neurons, treatment of DRG sensory neurons with NGF for 3 min induced the tyrosine phosphorylation of a protein with a molecular mass of 42 kDa (p42) (see Fig. 5). Tyrosine phosphorylation of p42 was maximal after treatment with NGF for 10 min and remained constant for ~1 h. Longer incubation times of DRG sensory neurons resulted in a decrease in the tyrosine phosphorylation of p42, but the level was still elevated after treatment with NGF for 4 hours (Fig. 6). Preincubation of DRG sensory neurons with the trk kinase inhibitor K252a prevented the NGF-stimulated tyrosine phosphorylation of p42 (see Fig. 5).

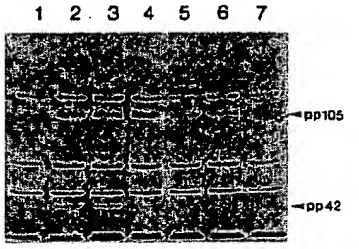

FIG. 4. Tyrosine phosphorylation of proteins in NGF-treated sympathetic neurons: long time course. Chick sympathetic neurons (E12) were not treated (lanes 1 and 7) or treated with 10 ng/ml of NGF for 10 min (lane 2), 30 min (lane 3), 1 h (lane 4), 2 h (lane 5), or 4 h (lane 6). Cells were lysed, and proteins in the lysate were subjected to SDS-PAGE. After transfer to nitrocellulose, blots were reacted with anti-phosphotyrosine monoclonal antibody. Arrows on the right indicate the position of tyrosine-phosphorylated proteins p105 and p42.

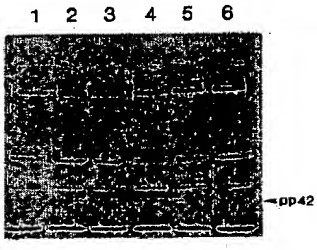

FIG. 6. Tyrosine phosphorylation of proteins in NGF-treated DRG sensory neurons: long time course. Chick DRG sensory neurons (E9) were not treated (lane 1) or treated with 10 ng/ml of NGF for 10 min (lane 2), 30 min (lane 3), 1 h (lane 4), 2 h (lane 5), or 4 h (lane 6). Cells were lysed, and proteins in the lysate were subjected to SDS-PAGE. After transfer to nitrocellulose, blots were reacted with anti-phosphotyrosine monoclonal antibody. The arrow on the right indicates the position of tyrosine-phosphorylated protein p42.

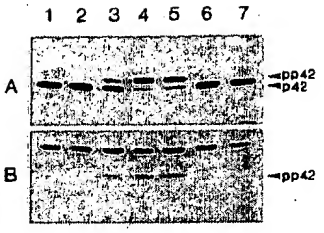

FIG. 7. Identification of pp42 as a tyrosine-phosphorylated MAP kinase in NGF-treated sympathetic neurons. Chick sympathetic neurons (E12) were not treated (lanes 1 and 7) or treated with 10 ng/ml of NGF for 1 (lane 2), 3 (lane 3), 10 (lane 4), or 30 min (lane 5). For lane 6, sympathetic neurons were pretreated with 1 μM K252a for 10 min, followed by incubation with 10 ng/ml of NGF for 10 min. Cells were lysed, and proteins in the lysate were subjected to SDS-PAGE on large low-cross-linker gels and transferred to nitrocellulose. **A:** The blot was incubated with anti-MAP kinase antiserum. **B:** After removal of bound antibodies the blot was reincubated with anti-phosphotyrosine monoclonal antibody. Arrows on the right indicate the position of shifted tyrosine-phosphorylated MAP kinase p42 (pp42) and the position of unshifted unphosphorylated MAP kinase p42 (p42).

Identification of p42 as a MAP kinase

Molecular mass and time kinetics of tyrosine phosphorylation of p42 in NGF-treated sympathetic neurons led us to the suggestion that p42 might belong to the family of MAP kinases. Further evidence for this hypothesis was obtained by the fact that, after removal of anti-phosphotyrosine monoclonal antibody from the immunoblot, reprobing with an antiserum directed against the MAP kinases extracellular signal-regulated kinase (ERK) 1 and ERK2 revealed a band with a molecular mass of 42 kDa (data not shown). To prove that p42 indeed belongs to the family of MAP kinases, we used a gel shift assay that discriminates between phosphorylated and unphosphorylated forms of the protein.

Proteins in lysates from untreated and NGF-treated chick sympathetic neurons were blotted from large SDS-polyacrylamide gels with low cross-linker, and blots were incubated with anti-MAPK antiserum. As can be seen in Fig. 7A, this antiserum detected a single protein species in untreated cells. Stimulation of sympathetic neurons with NGF for 3 min resulted in a shift of part of the MAP kinase to a higher apparent molecular mass (see Fig. 7A). Stimulation with NGF for 10 min was accompanied by a shift of most of the MAP kinase, whereas treatment with NGF for 30 min led to an increase in the amount of the unshifted form of MAP kinase. Preincubation of NGF-stimulated sympathetic neurons with K252a resulted in the appearance of the unshifted form of MAP kinase (see Fig. 7A).

To verify that the shifted species of MAP kinase was indeed tyrosine-phosphorylated, the blot was stripped and reincubated with anti-phosphotyrosine monoclonal antibody. As can be seen in Fig. 7B, only the shifted form of MAP kinase was stained with anti-phosphotyrosine monoclonal antibody, demonstrating that NGF treatment of sympathetic neurons resulted in a tyrosine-phosphorylated form of MAP kinase.

Other tyrosine-phosphorylated proteins

Several other tyrosine-phosphorylated proteins could be detected in unstimulated sympathetic and DRG sensory neurons. As expected, tyrosine phosphorylation of these proteins was not prevented by preincubation of neurons with the trk inhibitor K252a (see Figs. 3 and 5). Preincubation of anti-phosphotyrosine monoclonal antibody with phosphotyrosine inhibited the binding of the antibody to both basally and NGF-stimulated tyrosine-phosphorylated proteins in sympathetic and DRG sensory neurons (data not shown).

DISCUSSION

Although sympathetic and DRG sensory neurons derived from the chick PNS represent "classical" NGF-responsive systems, only limited information is available on the mechanism of NGF-mediated signal transduction beyond the trk receptor activation (Borasio et al., 1993; Clary et al., 1994). Specifically, the intracellular signaling cascade leading to neuronal survival is virtually unknown. As we have demonstrated previously, DRG sensory neurons are absolutely dependent on p21ras activity: Intracellular application of activated p21ras replaces the NGF requirement for survival (Borasio et al., 1989), and, conversely, intracellular application of function-blocking anti-p21ras Fab fragments inhibits the NGF signal pathway for survival (Borasio et al., 1993). Consistently, activation of p21ras by NGF has been shown recently in chick DRG sensory neurons (Ng and Shooter, 1993). However, no effect of activated p21ras was found in chick sympathetic neurons, and, correspondingly, the anti-p21ras Fab fragments could influence neither neurite outgrowth nor survival induced by NGF (Borasio et al., 1993). Accordingly, we present evidence here that the time-resolved tyrosine phosphorylation pattern of proteins is distinctly different between both neural crest-derived neuronal subtypes at a branchpoint downstream the p140trk receptor.

The action of NGF initiated by the aggregation of the p140trk receptor is followed by rapid cross-phosphorylation at defined tyrosine residues of the intracellular domain (Obermeier et al., 1994; Stephens et al., 1994). Here, maximal tyrosine phosphorylation of p140trk can be observed after treatment of sympathetic neurons with NGF for 1 min. In sympathetic neurons tyrosine phosphorylation persisted for up to 30 min, the longest interval measured. Consistently, it has been shown recently that persistent trkA receptor aggregation by antibodies against the extracellular portion of trkA is sufficient to cause its autophosphorylation leading to neurite outgrowth and survival (Clary et al., 1994). Moreover, in trkA tyrosine kinase mouse gene knock-out mutants the sympathetic ganglia were strik-

ingly affected (Smeyne et al., 1994), demonstrating that the tyrosine kinase activity of trkA is essential for survival.

Downstream to the activation of p140trk receptor, NGF induces the rapid and persistent tyrosine phosphorylation of an as yet uncharacterized protein, p105, selectively in chick sympathetic neurons. Tyrosine phosphorylation of p105 can be detected already 30 s after treatment with NGF (data not shown), indicating that this is an early step of NGF-induced signal transduction. However, activated p140trk and tyrosine-phosphorylated p105 may probably not interact directly because pp105 is not coprecipitated when using anti-trk antibodies (see Fig. 1).

Tyrosine-phosphorylated p105 undergoes a time-dependent progressive shift to higher apparent molecular masses after treatment of sympathetic neurons with NGF. Blots from enlarged SDS-polyacrylamide gels using low cross-linker indicate the presence of multiple species of pp105 (data not shown). Most likely, tyrosine-phosphorylated p105 is subjected to additional posttranslational modifications.

In contrast to sympathetic neurons, NGF-stimulated tyrosine phosphorylation of p105 is transient in DRG sensory neurons, showing a profound difference between both subtypes of neurons. As has been demonstrated previously, NGF induces the activation of p21ras in DRG sensory neurons (Ng and Shooter, 1993). The activation of p21ras has been shown in many systems to initiate a cascade of protein phosphorylation events, leading finally to the activation of MAP kinases. Consistent with this idea, NGF stimulates the rapid tyrosine phosphorylation of a single form of MAP kinase (p42) in both chick sympathetic and DRG sensory neurons. We have identified this protein as a MAP kinase using an anti-MAP kinase antiserum directed against the mammalian ERK1 and ERK2 proteins.

Unlike NGF-stimulated tyrosine phosphorylation of p105, similarities exist between sympathetic and DRG sensory neurons with respect to the onset of tyrosine phosphorylation of MAP kinase p42. Whereas in both subtypes of neurons tyrosine phosphorylation of MAP kinase p42 is induced after treatment with NGF for 3 min, the decrease in tyrosine phosphorylation is differentially regulated in these systems. In sympathetic neurons maximal tyrosine phosphorylation of MAP kinase p42 can be observed after treatment with NGF for 10–30 min, whereas in DRG sensory neurons maximal tyrosine phosphorylation of MAP kinase p42 is more long-lasting and decreases after stimulation with NGF for 1 h. The difference in the time course of NGF-stimulated tyrosine phosphorylation of MAP kinase p42 between sympathetic and DRG sensory neurons may be explained by either a different strength of signal input or different inactivation of tyrosine-phosphorylated MAP kinase p42 by tyrosine phosphatase(s) (Nebreda, 1994).

Using the gel shift assay for detection of phosphorylated proteins, we observed that the tyrosine-phosphorylated form of MAP kinase p42 shifts to a higher apparent molecular mass after treatment of sympathetic neurons with NGF. Because it has been shown that the more slowly migrating form of MAP kinase ERK2 corresponds to the activated phosphorylated species (Leevers and Marshall, 1992), we can estimate from our blots the percentage of MAP kinase that becomes activated by NGF. Treatment of sympathetic neurons for 10 min with 10 ng/ml of NGF activates ~90% of the MAP kinase p42, whereas only a smaller fraction of MAP kinase is activated after stimulation with NGF for 3 or 30 min.

As was recently shown, not only the function of p21ras but also the activity of MEK1 is essential for NGF-stimulated neurite outgrowth in PC12 cells (Cowley et al., 1994). However, because in sympathetic neurons p21ras activity does not influence survival (Borasio et al., 1993), its downstream effects are not necessarily coupled to prevent apoptosis. Thus, it is not surprising that the time course of NGF-stimulated tyrosine phosphorylation of MAP kinase p42 is different between chick DRG sensory and sympathetic neurons. It is unclear at the moment whether MAP kinase p42 is activated via a p21ras-independent pathway in chick sympathetic neurons. As was shown earlier, activation of p21ras is necessary for NGF-stimulated survival and neurite outgrowth of chick DRG sensory neurons but not sympathetic neurons. Our data provide evidence that in DRG sensory neurons NGF signal transduction proceeds via the activation of p21ras and subsequently MAP kinase p42.

In addition to the neurotrophins NGF and neurotrophin-3, survival of chick sympathetic neurons can be induced by treatment with ciliary neurotrophic factor (Barbin et al., 1984; Ernsberger et al., 1989), a high K^+ concentration (Wakade et al., 1983), or forskolin (Wakade et al., 1990). It is interesting that treatment with these agents does not stimulate the tyrosine phosphorylation of p105, whereas neurotrophin-3 does so (data not shown). Our results support the working hypothesis that variant signal pathways may exist for survival in sympathetic neurons and suggest that tyrosine phosphorylation of p105 is only involved in stimulation of survival via the neurotrophins NGF and neurotrophin-3.

Rat pheochromocytoma PC12 cells (Greene and Tischler, 1976) are commonly used as a model system for sympathetic neurons. Our study indicates that several differences exist in NGF-stimulated tyrosine phosphorylation of proteins between chick sympathetic neurons and transformed PC12 cells:

a. In chick sympathetic neurons maximal tyrosine phosphorylation of p140trk can be observed within 1 min after treatment with NGF and persists for up to 30 min. This time course is different from that observed for PC12 cells, where maximal tyrosine phosphorylation of p140trk was reported to occur after

treatment with NGF for 5 min and decreased thereafter (Kaplan et al., 1991).

b. In contrast to PC12 cells, where NGF induces the tyrosine phosphorylation of many proteins (Maher, 1988; Miyasaka et al., 1991; authors' unpublished data), NGF stimulates the rapid and reproducible tyrosine phosphorylation of two proteins in chick sympathetic and DRG sensory neurons. The observed difference in the number of tyrosine-phosphorylated proteins between NGF-treated primary neurons and PC12 cells may be due to the fact that PC12 cells are transformed and that these proteins may therefore be involved in signal transduction leading to mitosis.

c. In contrast to PC12 cells, where three types of MAP kinase (p43erk1, p41erk2, and p45erk4) become tyrosine-phosphorylated after treatment with NGF (Boulton et al., 1991; Ahn et al., 1992; Lloyd and Wooten, 1992), NGF stimulates the rapid tyrosine phosphorylation of a single form of MAP kinase (p42) in chick sympathetic and DRG sensory neurons.

Our results provide evidence that NGF signal transduction in primary neurons and transformed cells of neuronal origin is different at several steps. Because transformation and indefinite division of PC12 cells are in contrast to characteristics of postmitotic neurons, experiments with primary neurons may result in more valuable information regarding NGF signal transduction.

In conclusion, determination of the time-resolved protein tyrosine phosphorylation pattern shows that the signaling pathways of NGF diverge downstream the trk receptor level between sympathetic and DRG sensory neurons of the chick. We have used the chick sympathetic neurons as a model to establish p21ras-independent neurotrophin signaling pathways. The rapid and persistent tyrosine phosphorylation of a protein p105 with unknown biochemical function may imply that it plays an important role in this p21ras-independent NGF signaling pathway.

Acknowledgment: We thank D. Peter for expert technical assistance and K. Grabert for photographic work. This work was supported by a grant from the Deutsche Forschungsgemeinschaft.

REFERENCES

Ahn N. G., Robbins D. J., Haycock J. W., Seger R., Cobb M. H., and Krebs E. G. (1992) Identification of an activator of the microtubule-associated protein 2 kinases ERK1 and ERK2 in PC12 cells stimulated with nerve growth factor or bradykinin. *J. Neurochem.* **59,** 147–156.

Barbacid M. (1993) Nerve growth factor: a tale of two receptors. *Oncogene* **8,** 2033–2042.

Barbin G., Manthorpe M., and Varon S. (1984) Purification of the chick eye ciliary neuronotrophic factor. *J. Neurochem.* **43,** 1468–1478.

Barker P. A. and Shooter E. M. (1994) Disruption of NGF binding to the low affinity neurotrophin receptor $p75^{LNTR}$ reduces NGF binding to trkA on PC12 cells. *Neuron* **13,** 203–215.

Basu T., Warne P. H., and Downward J. (1994) Role of Shc in the activation of Ras in response to epidermal growth factor and nerve growth factor. *Oncogene* **9,** 3483–3491.

Boguski M. S. and McCormick F. (1993) Proteins regulating Ras and its relatives. *Nature* **366,** 643–654.

Borasio G. D., John J., Wittinghofer A., Barde Y.-A., Sendtner M., and Heumann R. (1989) ras p21 protein promotes survival and fiber outgrowth of cultured embryonic neurons. *Neuron* **2,** 1087–1096.

Borasio G. D., Markus A., Wittinghofer A., Barde Y.-A., and Heumann R. (1993) Involvement of ras p21 in neurotrophin-induced response of sensory, but not sympathetic neurons. *J. Cell Biol.* **121,** 665–672.

Boulton T. G., Nye S. H., Robbins D. J., Ip N. Y., Radziejewska E., Morgenbesser S. D., DePinho R. A., Panayotatos N., Cobb M. H., and Yancopoulos G. D. (1991) ERKs: a family of protein-serine/threonine kinases that are activated and tyrosine phosphorylated in response to insulin and NGF. *Cell* **65,** 663–675.

Chao M. V. (1992) Neurotrophin receptors: a window into neuronal differentiation. *Neuron* **9,** 583–593.

Clary D. O., Weskamp G., Austin L. R., and Reichardt L. F. (1994) trkA crosslinking mimics neuronal responses to nerve growth factor. *Mol. Biol. Cell* **5,** 549–563.

Cowley S., Paterson H., Kemp P., and Marshall C. J. (1994) Activation of MAP kinase is necessary and sufficient for PC12 differentiation and for transformation of NIH 3T3 cells. *Cell* **77,** 841–852.

Dobrowsky R. T., Werner M. H., Castellino A. M., Chao M. V., and Hannun Y. A. (1994) Activation of the sphingomyelin cycle through the low-affinity neurotrophin receptor. *Science* **265,** 1596–1599.

Ernsberger U., Sendtner M., and Rohrer H. (1989) Proliferation and differentiation of embryonic chick sympathetic neurons: effects of ciliary neurotrophic factor. *Neuron* **2,** 1275–1284.

Greene L. A. and Tischler A. S. (1976) Establishment of a noradrenergic clonal line of rat adrenal pheochromocytoma cells which respond to nerve growth factor. *Proc. Natl. Acad. Sci. USA* **73,** 2424–2428.

Hagag N., Halegoua S., and Viola M. (1986) Inhibition of growth factor-induced differentiation of PC12 cells by microinjection of antibody to ras p21. *Nature* **319,** 680–682.

Hashimoto Y., Matuoka K., Takenawa T., Muroya K., Hattori S., and Nakamura S. (1993) Different interactions of Grb2/Ash molecule with the NGF and EGF receptors in rat pheochromocytoma PC12 cells. *Oncogene* **9,** 869–875.

Heumann R. (1994) Neurotrophin signalling. *Curr. Opin. Neurobiol.* **4,** 668–679.

Jaiswal R. K., Moodie S. A., Wolfman A., and Landreth G. E. (1994) The mitogen-activated protein kinase cascade is activated by B-raf in response to nerve growth factor through interaction with $p21^{ras}$. *Mol. Cell. Biol.* **14,** 6944–6953.

Jing S., Tapley P., and Barbacid M. (1992) Nerve growth factor mediates signal transduction through trk homodimer receptors. *Neuron* **9,** 1067–1079.

Kaplan D. R., Martin-Zanca D., and Parada L. F. (1991) Tyrosine phosphorylation and tyrosine kinase activity of the trk proto-oncogene product induced by NGF. *Nature* **350,** 158–160.

Knüsel B. and Hefti F. (1992) K-252 compounds: modulators of neurotrophin signal transduction. *J. Neurochem.* **59,** 1987–1996.

Laemmli U. K. (1970) Cleavage of structural proteins during the assembly of the head of bacteriophage T4. *Nature* **227,** 680–685.

Lange-Carter C. A. and Johnson G. L. (1994) Ras-dependent growth factor regulation of MEK kinase in PC12 cells. *Science* **265,** 1458–1461.

Leevers S. J. and Marshall C. J. (1992) Activation of extracellular signal-regulated kinase, ERK2, by p21ras oncoprotein. *EMBO J.* **11,** 569–574.

Lindsay R. M., Thoenen H., and Barde Y.-A. (1985) Placode and neural crest-derived sensory neurons are responsive at early

developmental stages to brain-derived neurotrophic factor. *Dev. Biol.* **112,** 319–328.

Lloyd E. D. and Wooten M. W. (1992) $^{pp42/44}$MAP kinase is a component of the neurogenic pathway utilized by nerve growth factor in PC12 cells. *J. Neurochem.* **59,** 1099–1109.

Maher P. A. (1988) Nerve growth factor induces protein-tyrosine phosphorylation. *Proc. Natl. Acad. Sci. USA* **85,** 6788–6791.

Meakin S. O. and Shooter E. M. (1992) The nerve growth factor family of receptors. *Trends Neurosci.* **15,** 323–331.

Miyasaka T., Sternberg D. W., Miyasaka J., Sherline P., and Saltiel A. R. (1991) Nerve growth factor stimulates tyrosine phosphorylation in PC-12 pheochromocytoma cells. *Proc. Natl. Acad. Sci. USA* **88,** 2653–2657.

Nakamura K., Tanaka T., Kuwahara A., and Takeo K. (1985) Microassay for proteins on nitrocellulose filter using protein dye-staining procedure. *Anal. Biochem.* **148,** 311–319.

Nebreda A. R. (1994) Inactivation of MAP kinases. *Trends Biochem. Sci.* **19,** 1–2.

Ng F. L. and Shooter E. M. (1993) Activation of p21^{ras} by nerve growth factor in embryonic sensory neurons and PC12 cells. *J. Biol. Chem.* **268,** 25329–25333.

Obermeier A., Bradshaw R. A., Seedorf K., Choidas A., Schlessinger J., and Ullrich A. (1994) Neuronal differentiation signals are controlled by nerve growth factor receptor/Trk binding sites for SHC and PLCγ. *EMBO J.* **13,** 1585–1590.

Ohmichi M., Decker S. J., and Saltiel A. R. (1992*a*) Activation of phosphatidylinositol-3 kinase by nerve growth factor involves indirect coupling of the *trk* proto-oncogene with src homology 2 domains. *Neuron* **9,** 769–777.

Ohmichi M., Pang L., Decker S. J., and Saltiel A. R. (1992*b*) Nerve growth factor stimulates the activities of the raf-1 and the mitogen-activated protein kinases via the *trk* protooncogene. *J. Biol. Chem.* **267,** 14604–14610.

Ohmichi M., Matuoka K., Takenawa T., and Saltiel A. R. (1994) Growth factors differentially stimulate the phosphorylation of Shc proteins and their association with Grb2 in PC-12 pheochromocytoma cells. *J. Biol. Chem.* **269,** 1143–1148.

Oshima M., Sithanandam G., Rapp U. R., and Guroff G. (1991) The phosphorylation and activation of B-raf in PC12 cells stimulated by nerve growth factor. *J. Biol. Chem.* **266,** 23753–23760.

Qiu M.-S. and Green S. H. (1992) PC12 cell neuronal differentiation is associated with prolonged p21ras activity and consequent prolonged ERK activity. *Neuron* **9,** 705–717.

Saltiel A. R. and Decker S. J. (1994) Cellular mechanisms of signal transduction for neurotrophins. *Bioessays* **16,** 405–411.

Smeyne R. J., Klein R., Schnapp A., Long L. K., Bryant S., Lewin A., Lira S. A., and Barbacid M. (1994) Severe sensory and sympathetic neuropathies in mice carrying a disrupted trk/NGF receptor gene. *Nature* **368,** 246–249.

Snider W. D. (1994) Functions of the neurotrophins during nervous system development: what the knockouts are teaching us. *Cell* **77,** 627–638.

Soltoff S. P., Rabin S. L., Cantley L. C., and Kaplan D. R. (1992) Nerve growth factor promotes the activation of phosphatidylinositol 3-kinase and its association with the trk tyrosine kinase. *J. Biol. Chem.* **267,** 17472–17477.

Stephens R. M., Loeb D. M., Copeland T. D., Pawson T., Greene L. A., and Kaplan D. R. (1994) Trk receptors use redundant signal transduction pathways involving SHC and PLC-γ1 to mediate NGF responses. *Neuron* **12,** 691–705.

Suda K., Barde Y. A., and Thoenen H. (1978) Nerve growth factor in mouse and rat serum: correlation between bioassay and radioimmunoassay determination. *Proc. Natl. Acad. Sci. USA* **75,** 4042–4046.

Szeberenyi J., Cai H., and Cooper G. M. (1990) Effect of a dominant inhibitory Ha-*ras* mutation on neuronal differentiation of PC12 cells. *Mol. Cell. Biol.* **10,** 5324–5332.

Thomas S. M., DeMarco M., D'Arcangelo G., Halegoua S., and Brugge J. S. (1992) Ras is essential for nerve growth factor- and phorbol ester-induced tyrosine phosphorylation of MAP kinases. *Cell* **68,** 1031–1040.

Vaillancourt R. R., Gardner A. M., and Johnson G. L. (1994) B-Raf-dependent regulation of the MEK-1/mitogen-activated protein kinase pathway in PC12 cells and regulation by cAMP. *Mol. Cell. Biol.* **14,** 6522–6530.

Vetter M. L., Martin-Zanca D., Parada L. F., Bishop J. M., and Kaplan D. R. (1991) Nerve growth factor stimulates tyrosine phosphorylation of phospholipase C-γ1 by a kinase activity associated with the product of the *trk* protooncogene. *Proc. Natl. Acad. Sci. USA* **88,** 5650–5654.

Wakade A. R., Edgar D., and Thoenen H. (1983) Both nerve growth factor and high K^+ concentrations support the survival of chick embryo sympathetic neurons: evidence for a common mechanism of action. *Exp. Cell Res.* **144,** 377–384.

Wakade A. R., Bhave S. V., Malhotra R. K., and Wakade T. D. (1990) Forskolin mediates the survival of nerve growth factor-dependent sympathetic neurons of chick embryo by a cyclic AMP-independent mechanism. *J. Neurochem.* **54,** 1281–1287.

Wood K. W., Sarnecki C., Roberts T. M., and Blenis J. (1992) ras mediates nerve growth factor receptor modulation of three signal-transducing protein kinases: MAP kinase, raf-1, and RSK. *Cell* **68,** 1041–1050.

ELSEVIER

Molecular Brain Research 29 (1995) 147–156

MOLECULAR BRAIN RESEARCH

Research report

Regulation of mRNA expression involved in Ras and PKA signal pathways during rat hypoglossal nerve regeneration

Sumiko Kiryu, Naonori Morita, Kohji Ohno, Hiroshi Maeno, Hiroshi Kiyama *

Department of Neuroanatomy, Biomedical Research Center, Osaka University Medical School, 2-2 Yamadaoka, Suita, Osaka 565, Japan

Accepted 11 October 1994

Abstract

Using in situ hybridization histochemistry and immunohistochemistry, the present study examines the cooperative regulation of transcription of molecules involved in the Ras-signal and the cAMP dependent protein kinase (PKA) pathways during peripheral nerve regeneration in rats. Injury to hypoglossal motor neurons resulted in an increase in extracellular regulated kinase (ERK, or MAP kinase) and ERK kinase (MEK, or MAP kinase kinase) mRNAs, but in a decrease in the expression of the catalytic subunits of PKA (Cα and Cβ) mRNAs. These results show the importance of the Ras-signal pathway in the nerve regeneration process and extend recent observation which suggested a cross-talk between the Ras and PKA pathways in vitro. The down-regulation of PKA may facilitate the activation of the Ras pathway which is located downstream of the growth factor receptor. The present study may suggest a possibility of regulatory talk between these two major signal transduction pathways.

Keywords: MAP kinase; ERK; MEK; PKA; MAPKK; Axotomy; Injury

1. Introduction

Recently the possibility of cross-talk between the two major signal transduction pathways namely, the Ras and cAMP dependent protein kinase (PKA) pathways, has been demonstrated in some mammalian cell lines [7,10,16,38,45]. The Ras pathway is a downstream effector pathway following growth factor receptor activation [13]. A receptor tyrosine kinase, which is common among the growth factor receptors, conveys information from the extracellular signal mediator to the extracellular signal regulated kinase (ERK or MAP kinase) through Grb2-SOS, Ras-GTP, Raf-1 and MAP kinase kinase (MAPKK or MEK) cascade to transcription factors [31,39,44]. Among implicated cross-talk points, inhibition of Raf-1 by PKA could be a major element. In addition, phosphorylation of Rap and SOS by PKA has also been suggested to inhibit Ras signal transduction [7,10,16,38,45].

Recently we have focused our attention on the expression of genes associated with nerve regeneration in particular the cytoplasmic membrane associated enzymes phospholipase C (PLC), PKC isozymes and phosphatidylinositol kinase isozymes (PI3K and PI4K). We have reported previously the regulation characteristics of PLC isozymes [34]; the down-regulation of PLCβ and PI4K mRNAs following nerve injury suggested that the signal transduction pathway involving a G-linked receptor was perturbed following damage. However, expression of PLCα, whose structure is different from the other PLC isozymes, was up-regulated, whilst expression of PLCγ and PI3K were unaffected. As PLCγ and PI3K are associated the receptor tyrosine kinase, we then expected an importance of remaining major pathway downstream of the receptor tyrosine kinase namely, the Ras-pathway to see whether it is activated or not following peripheral nerve injury. In addition, we also examined the expression of the PKA genes, catalytic subunits of PKA (PKAC) and regulatory subunits of PKA (PKAR), to determine how these are influenced by damage and regeneration, as the PKA could influence the Ras-signal pathway. A PKA molecule consists of two catalytic (C) and two regulatory (R) subunits. When the catalytic subunits are bound to the regulatory subunit, the enzyme is silent, whereas cAMP can dissociate the C and R subunits' complex and activate the enzyme [37]. Fur-

* Corresponding author. Fax: (81) (6) 879-3589.

SSDI 0169-328X(94)00241-X

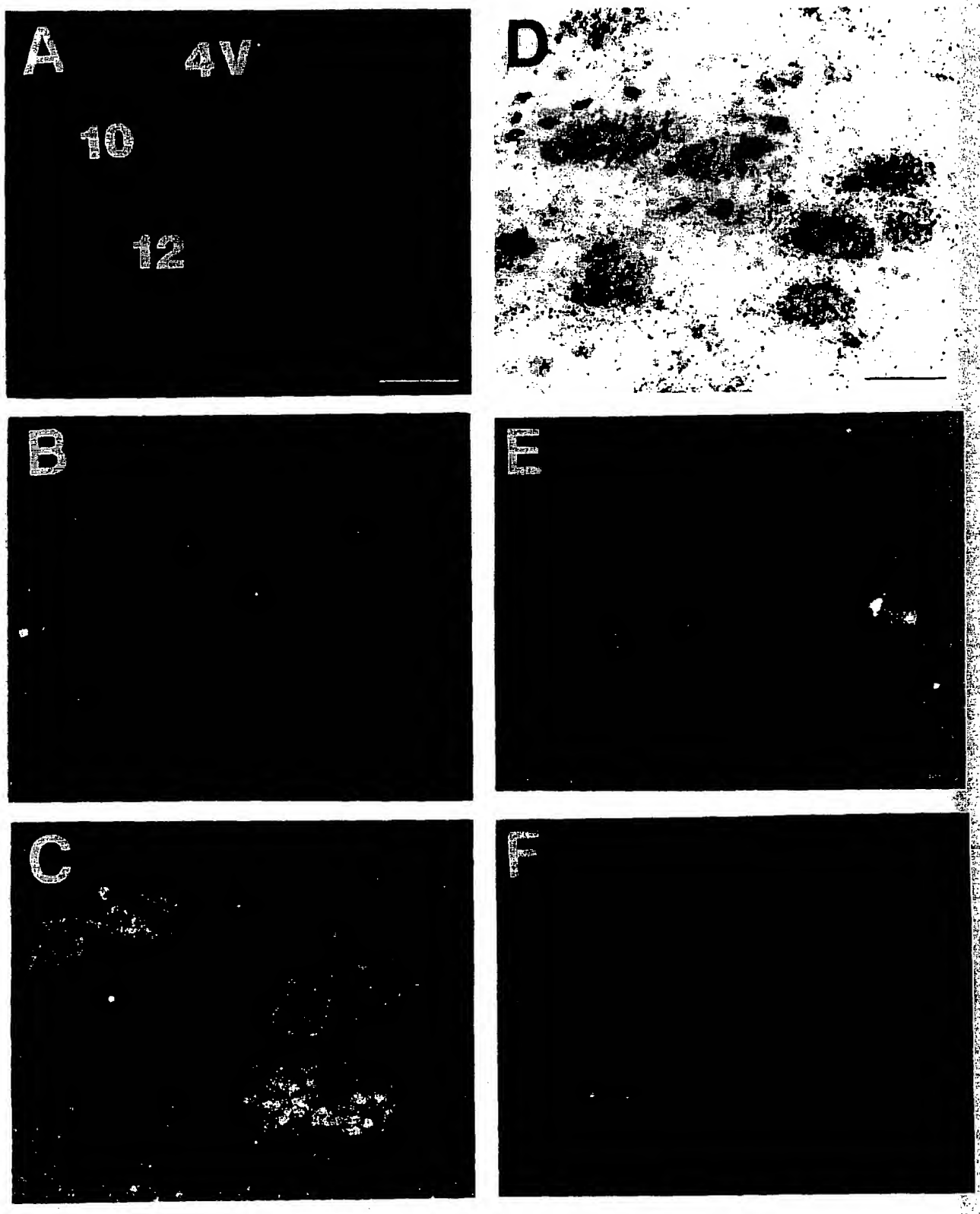
A
4V
10
12
D
B
E
C
F

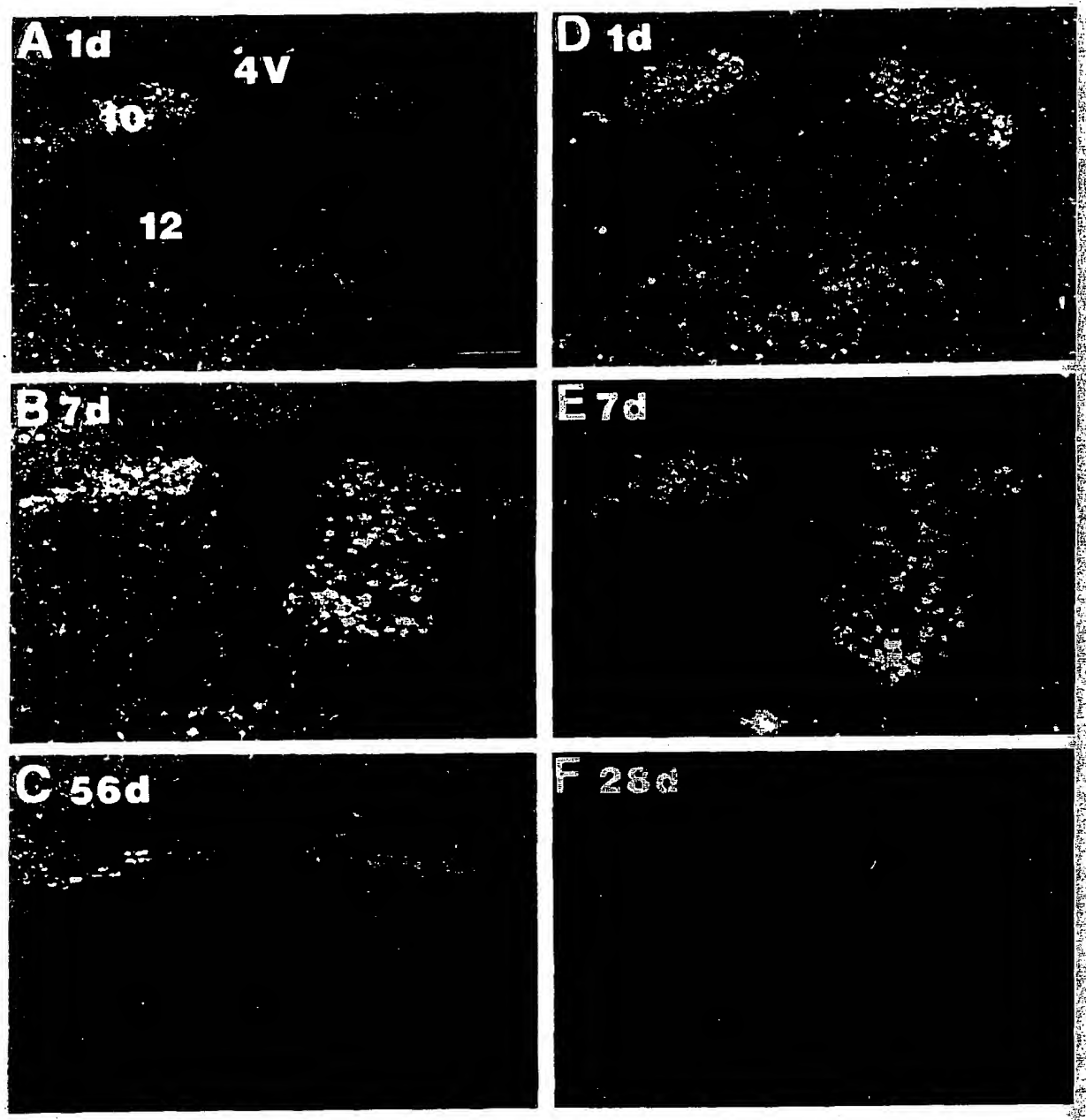

Fig. 2. Expression of ERK1 mRNA in the hypoglossal nucleus 1 day (A), 7 days (B), and 56 days (C) after unilateral hypoglossal nerve resection (right side), and 1 (D), 7 (E), and 28 (F) days after nerve crush (right side). 4V, fourth ventricle; 10, dorsal nucleus of vagus nerve; 12, hypoglossal nucleus. Bar = 200 μm.

thermore, PKA can be classified into two subsets (type I and type II) according to structural difference of regulatory subunits (RI and RII). So far two distinct forms (α and β) of each R subunit have been cloned, and also two isoforms of C subunits (α and β) are known to be expressed in the brain. Thus, at least two

Fig. 1. Histological control experiment demonstrating the specificity of the ERK1 probe and photomicrographs showing mRNA for ERK1, ERK2 and ERK3. A series of three adjacent sections were obtained from unilaterally resected animals 3 days after surgery (right side is the resected side). A: is derived from pre-RNase A treatment; and B: shows the results of the competition test derived from hybridization with an excess amount of unlabeled probe. C: shows the normal reaction. D: shows bright-field photomicrographs of ERK1 mRNA in the ipsilateral hypoglossal nucleus 7 days after axotomy. Sections are counterstained with thionin. E,F: show dark-field photomicrographs for ERK2 (E) and ERK3(F) mRNAs, 3 days after unilateral resection. 4V, fourth ventricle; 10, dorsal nucleus of vagus; 12, hypoglossal nucleus. Bar = 200 μm (A,B,C,E,F); Bar = 30 μm (D).

C subunits (Cα and Cβ) and four R subunits (RIα, RIβ, RIIα, and RIIβ) are thought to exist in the brain [8]. In the present study we examined the regulation of gene transcription in all these six subunits (Cα, Cβ, RIα, RIβ, RIIα, and RIIβ) after hypoglossal nerve axotomy.

2. Materials and methods

2.1. Animals

Male Wistar rats weighing about 100 g were anesthetized with pentobarbital (45 mg/kg), positioned supine and their right hypoglossal nerve carefully exposed. The nerve was then either crushed with a pair of fine forceps for 30 s or resected with a pair of scissors and the distal nerve segment (5 mm) removed.

2.2. In situ hybridization

Animals were decapitated at 1, 3, 5, 7, 14, 21, 35, 49, and 56 days after surgery. Their brains were removed quickly and frozen in powdered dry-ice. Twenty micrometer thick sections were cut on a cryostat, thaw-mounted onto 3-aminopropyltriethoxysilane coated slides, and stored at −80°C until used. Sections were fixed in 4% paraformaldehyde in 0.1 M phosphate buffer for 15 min at room temperature, rinsed three times in 1×SSC, acetylated in freshly made 100 mM triethanolamine, pH 7, 0.25% acetic anhydride and then dehydrated in a graded ethanol series. Sections were treated with chloroform for 10 min to remove fat from tissue, and immersed in 100% ethanol twice before hybridization. Hybridization was carried out at 42°C overnight. The composition of the hybridization buffer was as follows: 50% deionized formamide, 4×NaCl-sodium citrate buffer, 1×Denhardt's solution, 0.12 M phosphate buffer (pH 7.2), 2.5% tRNA, 10% dextran sulfate, 50 mM dithiothreitol and labeled probes ($6–9\times10^8$ dpm/ml). Hybridized sections were rinsed briefly in 1×SSC to remove hybridization mixture at room temperature, and washed in 1×SSC at 60°C. Sections were then dehydrated in a graded series of ethanol and air-dried prior to exposure to autoradiography film cassette for 1 week, whereafter sections were dipped in Ilford K-5 photoemulsion (Ilford, UK) diluted 6:4 in water. Sections were then exposed for 7 weeks at 4°C, developed in Kodak D19 developer, counterstained with thionin, dehydrated in a graded series of ethanol to xylene, and covershipped before microscopic observation.

2.3. Oligonucleotides

The oligonucleotide probes for ERK1, ERK2 and ERK3 were synthesized complementary to bases (ERK1: 862–903, ERK2: 557–597, ERK3: 1086–1127) of the rat ERK1,2,3 cDNAs [4–6] and (Cα, 151–190; Cβ, 158–196; RIα, 280–327; RIβ, 32–79; RIIα, 1131–1178; RIIβ, 1341–1380) for rat PKA subunits [20,24,27,28,35,36,43]. These probes were labelled with (α-^{35}S)dATP using terminal deoxynucleotidyl transferase, giving a specific activity of 23–28 MBq/mg. Specificity of the ERK1 hybridization signals was confirmed as follows: (1) no appreciable hybridization signal was detected in a competition experiment involving prehybridization of sections with 100-fold unlabelled probe; (2) prior to in situ hybridization, sections were incubated for 1 h at 37°C with a buffer containing 10 mM Tris-HCl (pH 7.5), 1 mM EDTA and pancreatic RNase A (10 mg/ml, Sigma). No hybridization signal was detected under such conditions (Fig. 1). Specificity against PKA RIα, RIβ and RIIα subunit hybridization signals have already been examined in other reports [27]. The sequences of specific probes to RIIβ, Cα, Cβ mRNAs were carefully chosen to rule out the possibility of cross-reaction against mRNAs presently identified for other proteins using computer analysis.

2.4. Relative quantification of ERK1 mRNA

The number of grains resulting from in situ hybridization was counted by image analysis. The relative area occupied by autoradiographic grains in the hypoglossal nuclei was measured bilaterally on the X-ray film using a computerized image analysis system (MCID; Image Res. Inc., Ontario, Canada). In the same section, we calculated the difference in the optical density between the right (ipsilateral side) and the left (contralateral side) hypoglossal nuclei. For statistical analysis, at least four sections from three rats per time point were studied during same post operative interval. The *t*-test was done when necessary.

2.5. Immunohistochemistry

Animals were perfused 1, 2, 3, 5, 7, 14 days postoperatively with saline followed by 4% paraformaldehyde containing 14% of a saturated picric acid solution in phosphate buffer. Brains were postfixed in the same fixative for 1–2 days, and then immersed in phosphate buffered saline (PBS) containing 20% sucrose, before being sectioned (20 μm) on a cryostat. Sections were processed with a Vectastain ABC kit (Vector, USA). The primary antisera against ERK1 and MEK1 were obtained from Santa Cruz (California, USA) and UBI (NY, USA), and used at a dilution of 1:1000 and 1:2000, respectively. After overnight incubation in the diluted antisera, sections were then incubated in biotinylated anti rabbit immunoglobulin G followed by an avidin-biotin-horseradish peroxidase complex and rinsed after both incubations in 0.02 M phosphate buffer and finally reacted with 3,3'-diaminobenzidine tetrahydrochloride and hydrogen peroxide to reveal a brown reaction product.

3. Results

3.1. ERKs

ERK2 and ERK3 mRNAs were not changed following hypoglossal nerve injury, while only ERK1 mRNA

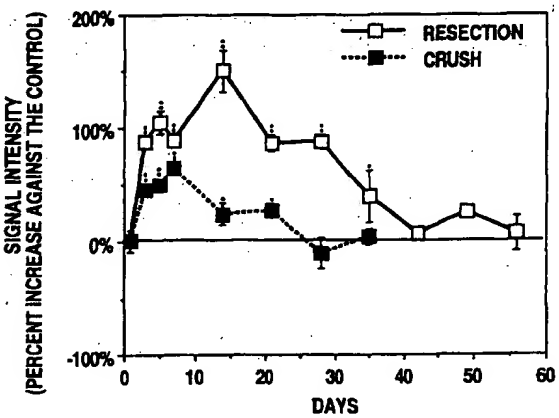

Fig. 3. Changes in ERK1 mRNA levels after hypoglossal nerve resection (open square) and nerve crush (black square). Each point shows the average and standard deviation of the relative signal increases seen in the ipsilateral nucleus when compared to the contralateral side.

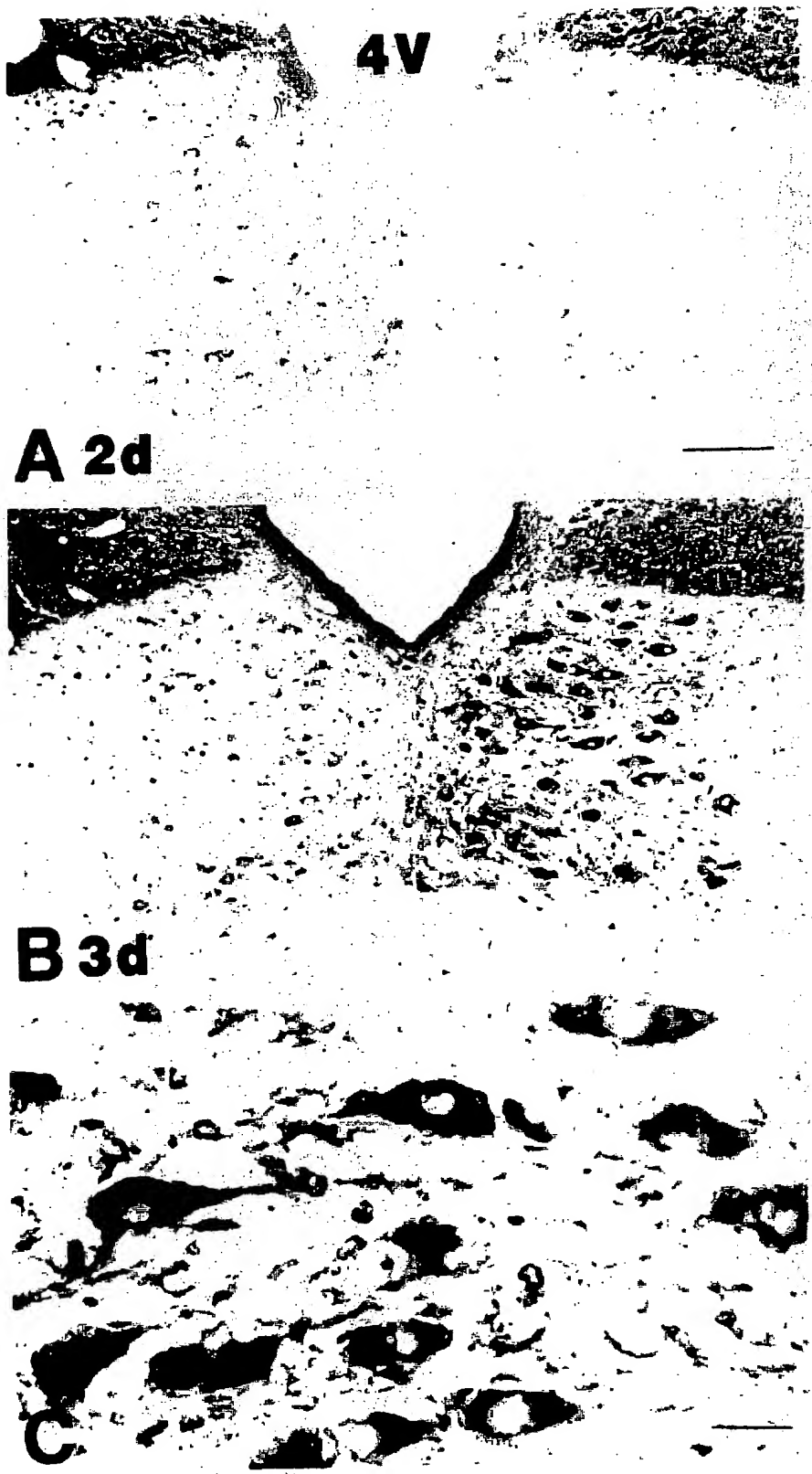

Fig. 4. Bright-field photomicrographs showing ERK1-like immunoreactivity in the hypoglossal nucleus unilaterally operated (right is the operated side) 2 days (A) and 3 days (B) after hypoglossal nerve resection. C: shows higher magnification of the ipsilateral hypoglossal nucleus 3 days after operation. 4V, fourth ventricle. Bar = 120 μm (A,B); Bar = 27 μm (C).

Table 1
Expression profile of MEK1, ERK1, PKA-Cα and PKA-Cβ after the motor nerve resection

	1 day	2 days	3 days	5 days	7 days	14 days	28 days	35 days
MEK1	+/−	+	++	++	++	++	+	+
ERK1	−	−	+	+++	+++	+++	+++	++
ERK1(mRNA)	−	+	++	+++	+++	+++	+++	++
PKACα(mRNA)	+++	nd	+	+	+	+	++	+++
PKACα(mRNA)	+++	nd	+	+	+	+	++	+++

The number of + indicates the extent of MEK1, ERK1, PKA Cα and Cβ mRNA expression on ipsilateral hypoglossal nucleus, compared with background level. − shows that the mRNA level is almost the background level. nd, not determined.

was found to be up-regulated in the hypoglossal motor neurons but not in glia (Figs. 1 and 2). ERK1 mRNA transiently increased after both nerve resection and crush. The increase in ERK1 hybridization signal was detected initially in the ipsilateral hypoglossal nucleus 2 days after either surgical procedure, however, the intensity of the hybridization signal markedly increased to a peak level during the following 3 days and persisted at this level for 14 days for the resection rats and 7 days for the nerve crushed rats. Thereafter, the hybridization signal gradually decreased until control levels were reached during the following 6 weeks for the resection group and 3 weeks for the nerve crush group (Figs. 2 and 3). The increase in ERK1 mRNA was greater following nerve resection (Fig. 3). A similar expression profile was seen for ERK1 protein; the increase in ERK1 mRNA was paralleled by an increase in ERK1 like immunoreactivity (Fig. 4). The increase in ERK1-like immunoreactivity was first detected in injured motoneurons 3 days after surgery; that is one day after the initial increase in ERK1 mRNA (Table 1). While ERK has been detected previously in both the cytoplasm and nucleus in some cell lines, in this study ERK1 was observed mainly in the cytoplasm after nerve injury.

3.2. MEK

MEK is a kinase which is located upstream of ERK in the Ras signal transduction cascade. Expression of this molecule after nerve injury was examined by immunohistochemistry. An increase in the intensity of MEK-like immunoreactivity was detected in the ipsilateral motoneurons 2 days after nerve transection (Fig. 5). Appearance of MEK immunoreactivity was detected one day earlier than the downstream protein, ERK (Table 1). The quicker increase of MEK immunoreactivity than ERK-1 immunoreactivity is probably reasonable for the facilitation of the signal cascade, and also implies that MEK up-regulation was not due to the up-regulation of ERK which can phosphorylate MEK.

3.3. PKA

In the hypoglossal nucleus of normal rats, the PKA Cα and Cβ subunit mRNAs are expressed in abundance, while a moderate level of RIα, β and RIIα, β subunit mRNAs are detected. After resection of the hypoglossal nerve, no dramatic change was seen for either of PKA regulatory subunits; rather a slight increase in the RIIα and RIIβ subunit mRNAs was observed in the ipsilateral hypoglossal motor neurons, and expression of RIα and RIβ remained unchanged following nerve injury. In contrast, a marked decrease in Cα and Cβ mRNAs was observed (Fig. 6). The decrease in these mRNAs was detected initially 3 days after surgery, with a plateau being reached about 5–7 days after the operation. Recovery of Cα and Cβ mRNA levels to control levels was seen 4–5 weeks after the operation. The duration of Cα and Cβ down-regulation was shorter than that observed for ERK and MEK. The time of on-set of this decreased gene expression was similar to that of ERK1.

4. Discussion

The present study demonstrates that during hypoglossal nerve regeneration, ERK1 mRNA and immunoreactivity, which is a pivotal enzyme in the Ras-signal pathway, are up-regulated. Further, an earlier up-regulation of MEK, which is a ERK regulating enzyme, was also found. It is feasible to expect that the up-regulation of this pathway is important for peripheral nerve regeneration which can be effected by some growth factors. In addition, the down-regulation of the PKA system may facilitate the up-regulation of MEK and ERK activity.

Several lines of studies have reported the up-regulation of ERK activity after stimulation of various kinds of growth factors [1,2,4–6,9,15,21,26,30,32,33,40,42]. Two kinds of activation profiles have been described among growth factors: the EGF type which shows an early transient up-regulation, and the

Fig. 5. Bright-field photomicrographs showing MEK-like immunoreactivity in the hypoglossal nucleus 1 day (A), 2 days (B), and 3 days (C) after hypoglossal nerve resection (right hand side is the operated side). 4V, fourth ventricle. Bar = 120 μm.

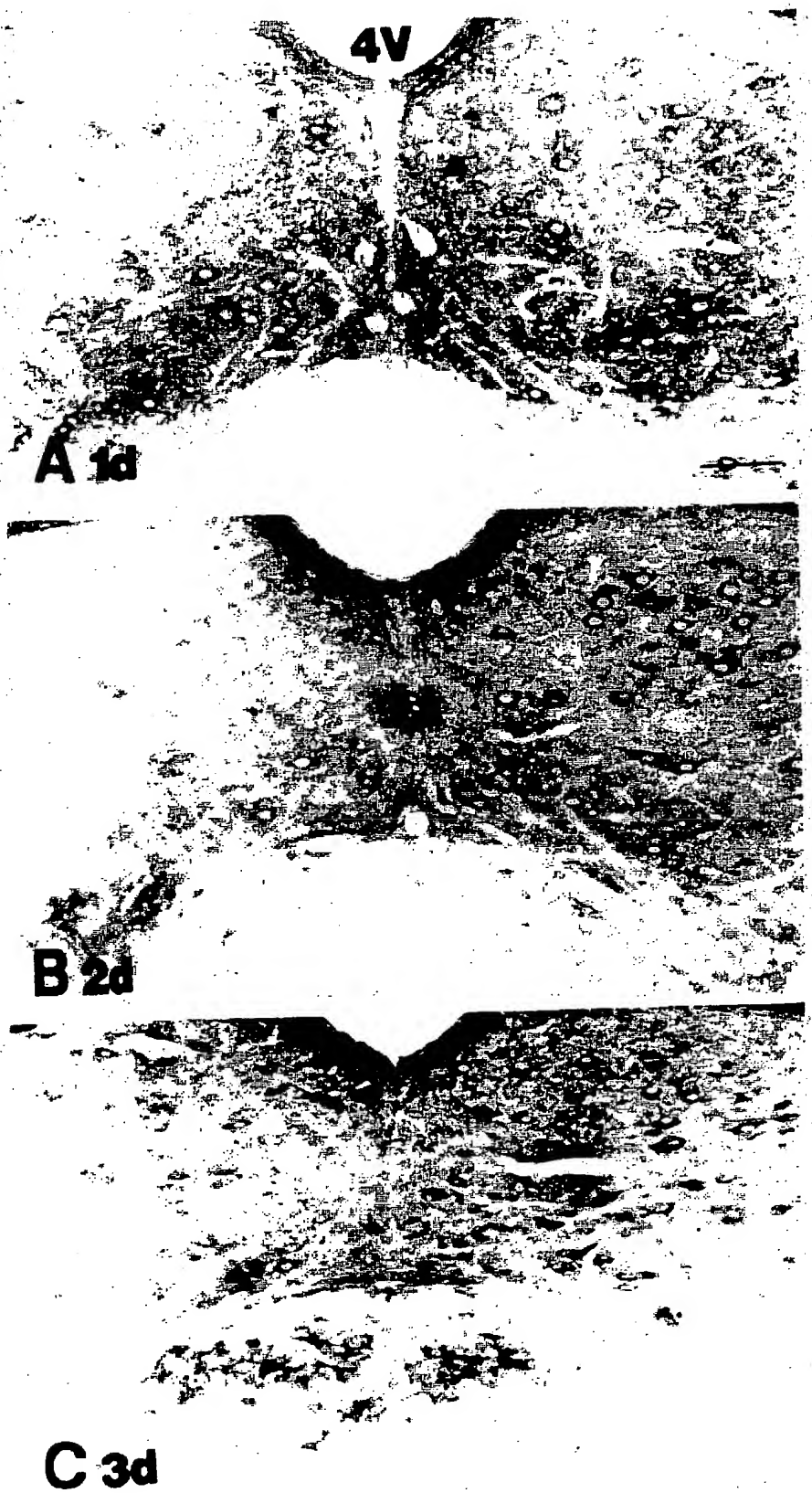
4V
A 1d
B 2d
C 3d

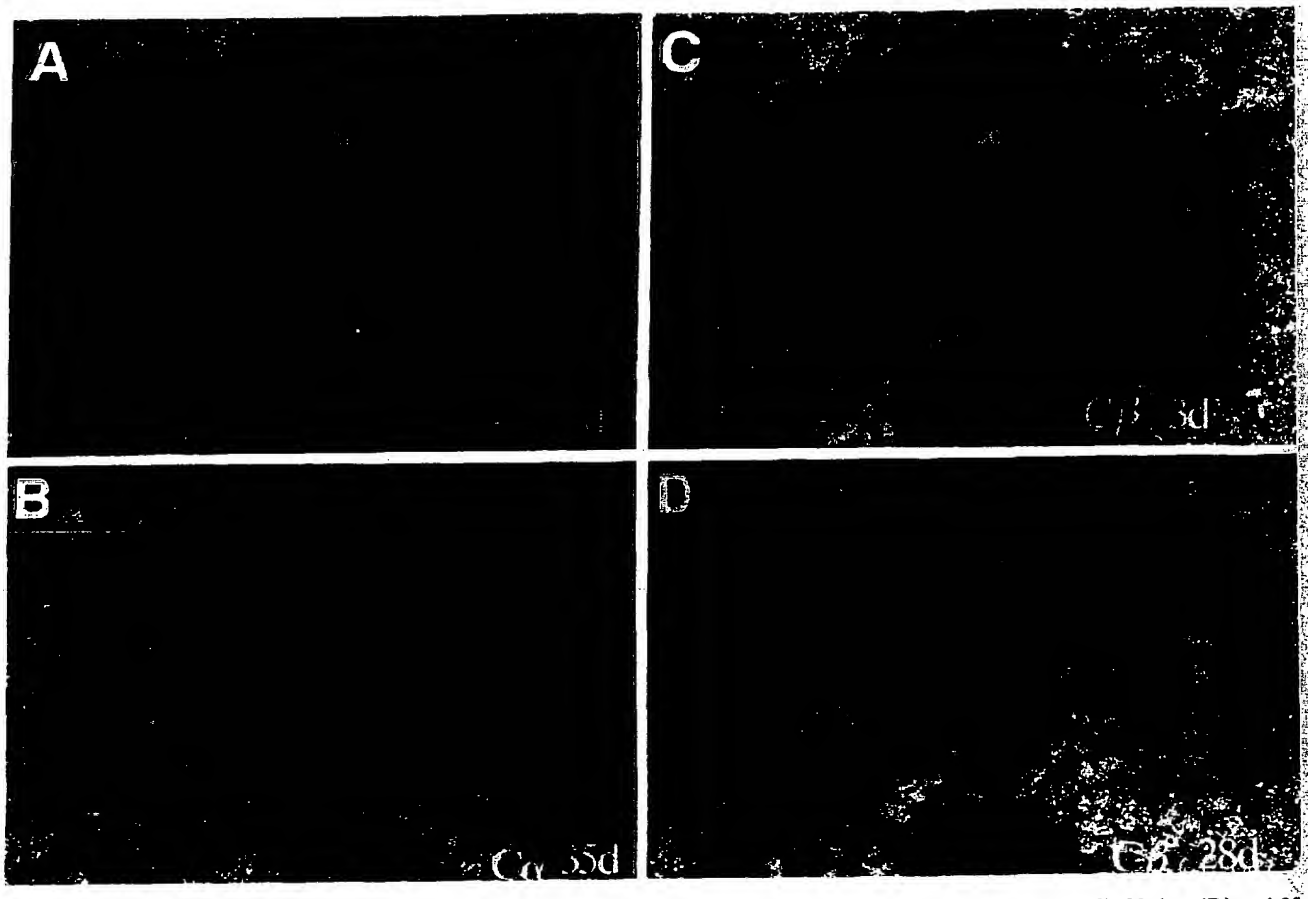

Fig. 6. Dark-field photomicrographs showing mRNA for Cα and Cβ subunit of PKA in hypoglossal nucleus 3 days (A,C), 28 days (D) and 35 days (B) after axotomy. Both Cα and Cβ mRNA levels in the ipsilateral side (right) decrease 3 days after operation, and recover to the normal level around 28 days (crush, D) and 35 days (resection B) after operation. cc; central canal.

NGF/FGF type which shows biphasic activation comprising of an early and a late component [9,15,21,29, 30,33]. The late component is supposed to be due to newly synthesized protein. Therefore, the NGF/FGF type of growth factors may promote ERK transcription. Indeed, cranial and spinal motor neurons express numerous growth factor receptors including FGFR1 (flg, FGF receptor), TrkB (high affinity BDNF receptor), $p75^{NGFR}$ (low affinity component of NGF/BDNF/NT-3) [12,14,19,22,41]. Among these receptors, Trk B and $p75^{NGFR}$ have been demonstrated to be up-regulated after nerve injury. As for TrkB, this receptor is known to have two distinct forms, one is so-called the truncated type which does not have an intracellular tyrosine kinase domain, and the other is the non-truncated type which contains full length of the molecules including the tyrosine kinase domain. Interestingly, transcription of the truncated type of the receptor was down-regulated after motor nerve injury, whereas expression of the non-truncated type of the receptor was up-regulated [14]. This opposing regulation of TrkB can lead to an increase in the strength of the signal transduction pathway initiated by activation of the TrkB receptor by BDNF. As for the growth factors themselves, up-regulation of the synthesis of NGF and BDNF has been shown in lesioned motoneurons and/or Schwann cells [11,17,18,22]. Furthermore, exogenous application of BDNF to motor nerve lesion increased the survival of the motor neurons [19,23]. Taking these evidence into account, it is likely that BDNF is probably released from both the injured motor neurons and surrounding Schwann cells, binds to its receptor (non-truncated TrkB) in an autocrine manner and up-regulates the transcription of MEK and ERK to accelerate the following Ras signaling pathway. This series of events involving growth factors, their receptors and intracellular signaling molecules along the Ras signal transduction pathway, might be crucial in facilitating neuronal regeneration.

In addition to growth factors, some factors from other signal pathways have been suggested to activate ERK, for example G protein coupled PLC. Recent studies by Meloche et al. and L'Allemain et al. [25,29,30] reported that pertussis toxin inhibited the α-thrombin induced activation of both ERK1 ($p44^{mapk}$) and ERK2 ($p42^{mapk}$). α-Thrombin is known to activate

PLC by interacting with pertussis toxin-sensitive and -insensitive G proteins and to inhibit adenylyl cyclase through pertussis toxin-sensitive Gi proteins [42]. This suggests that the activation of the adenylyl cyclase may lead to an inhibition of ERK1 probably via activation of a PKA, as recent reports have suggested that the implied and the PKA pathways may cross-talk. PKA has been shown to inhibit Raf-1 activity which is located up-stream of the MEK. In addition, PKA was also shown to phosphorylate SOS and Rap. The phosphorylation of SOS inhibits the signal pathway between Grb2 and Ras-GTP, while Rap phosphorylation causes a competition between Ras-GTP and Rap-GTP leading to inhibition of Raf-1 activation which is adjacent to Ras-GTP in the Ras pathway [3]. At all junctures in the pathway, PKA seems to have an inhibitory influence on the various components of the Ras-signal pathway. The results detailed above were derived from in vitro studies using selective mammalian cell lines, and so the functional significance of these interactions in vivo has been unknown. In the present study, we have suggested that the down-regulation of the PKA catalytic subunits (Cα and Cβ) possibly disinhibited the PKA inhibition of Ras-signal pathway leading to a facilitation of the Ras-signal pathway. Therefore, at least some of the molecules involved in these two major signal pathways are thought to be regulated cooperatively during the peripheral nerve regeneration process. These findings may suggest that linkage between the Ras-signal pathway and the PKA pathway is of importance for the facilitation of the Ras-signaling pathway during nerve regeneration.

Acknowledgements

We are grateful to Dr. Masaya Tohyama (Osaka University Medical School, Japan.) for support and encouragement, and Drs. P.C. Emson and S.J. Augood (MRC, Babraham, Cambridge, UK) for critical reading and English correction. This work was supported by Senri Life Science Foundation (Osaka, Japan), Brain Science Foundation (Tokyo, Japan) and Grant-in-Aid for Scientific Research from the Ministry of Education, Science and Culture, Japan.

References

[1] Ahn, N.G. and Krebs, E.G., Evidence for an epidermal growth factor-stimulated protein kinase cascade in swiss 3T3 cells, *J. Biol. Chem.*, 265 (1990) 11495–11501.

[2] Ahn, N.G., Weiel, J.E., Chan, C.P. and Krebs, E.G., Identification of multiple epidermal growth factor-stimulated protein serine/threonine kinases from swiss 3T3 cells, *J. Biol. Chem.*, 265 (1990) 11487–11494.

[3] Bokoch, G.M., Biology of the Rap proteins, members of the *ras* superfamily of GTP-binding proteins, *Biochem. J.*, 289 (1993) 17–24.

[4] Boulton, T.G. and Cobb, M.H., Identification of multiple extracellular signal-regulated kinases (ERKs) with antipeptide antibodies, *Cell Regul.*, 2 (1991) 357–371.

[5] Boulton, T.G., Nye, S.H., Robbins, D.J., Ip, N.Y., Radziejewska, E., Morgenbesser, S.D., DePinho, R.A., Panayotatos, N., Cobb, M.H. and Yancopoulos, G.D., ERKs: a family of protein-serine/threonine kinases that are activated and tyrosine phosphorylated in response to insulin and NGF, *Cell*, 65 (1991) 663–675.

[6] Boulton, T.G., Yancopoulous, G.D., Gregory, J.S., Slaughter, C., Moomaw, C., Hsu, J. and Cobb, M.H., An insulin-stimulated protein kinase similar to yeast kinases involved in cell cycle control, *Science*, 249 (1990) 64–67.

[7] Burgering, B.M., Pronk, G.J., Weeren, P.C.v., Chardin, P. and Bos, J.L., cAMP antagonizes p21ras-directed activation of extracellular signal-regulated kinases 2 and phosphorylation of mSos nucleotide exchange factor, *EMBO J.*, 12 (1993) 4211–4220.

[8] Cadd, G. and McNight, S., Distinct patterns of cAMP-dependent protein kinase gene expression in mouse brain, *Neuron*, 3 (1989) 71–79.

[9] Chao, M.V., Growth factor signaling: where is the specificity?, *Cell*, 68 (1992) 995–997.

[10] Cook, S.J. and McCormick, F., Inhibition by cAMP of Ras-dependent activation of Raf, *Science*, 262 (1993) 1069–1072.

[11] Eckenstein, F.P., Shipley, G.D. and Nishi, R., Acidic and basic fibroblast growth factors in the nervous system: distribution and differential alternation of levels after injury of central versus peripheral nerve, *J. Neurosci.*, 11 (1991) 412–419.

[12] Ernfors, P., Rosario, C.M., Merlio, J.-P., Grant, G., Aldskogius, H. and Persson, H., Expression of mRNAs for neurotrophin receptors in the dorsal root ganglion and spinal cord during development and following peripheral or central axotomy, *Mol. Brain Res.*, 17 (1993) 217–226.

[13] Feig, L.A., The many roads that lead to Ras, *Science*, 260 (1993) 767–768.

[14] Frisen, J., Verge, V.M.K., Fried, K., Risling, M., Persson, H., Trotter, J., Hökfelt, T. and Lindholm, D., Characterization of glial trkB receptors: differential responses to injury in the central and peripheral nervous systems, *Proc. Natl. Acad. Sci. USA*, 90 (1993) 4971–4975.

[15] Gotoh, Y., Nishida, E., Yamashita, T., Hoshi, M., Kawakami, M. and Sakai, H., Microtubule-associated-protein(MAP) kinase activated by nerve growth factor and epidermal growth factor in PC12 cells, *Eur. J. Biochem.*, 193 (1990) 661–669.

[16] Graves, L.M., Bornfeldt, K.E., Raines, E.W. and Potts, B.C., Protein kinase A antagonizes platelet-derived growth factor-induced signaling by mitogen-activated protein kinase in human arterial smooth muscle cells, *Proc. Natl. Acad. Sci. USA*, 90 (1993) 10300–10304.

[17] Heumann, R., Korsching, S., Bandtlow, C. and Thoenen, H., Changes of nerve growth factor synthesis in nonneuronal cells in response to sciatic nerve transection, *J. Cell Biol.*, 104 (1987) 1623–1631.

[18] Heumann, R., Lindholm, D., Meyer, M., Radeke, M., MIsko, T., Shooter, E. and Thoenen, H., Differential regulation of mRNA encoding nerve growth factor and its receptor in rat sciatic nerve during development, degeneration, and regeneration: role of macrophages, *Proc. Natl. Acad. Sci. USA*, 84 (1987) 8735–8739.

[19] Hughes, R.A., Sendtner, M. and Thoenen, H., Members of several gene families influence survival of rat motoneurons in vitro and in vivo, *J. Neurosci. Res.*, 36 (1993) 663–671.

[20] Jahnsen, T., Hedin, L., Kidd, V.J., Beattie, W.G., Lohmann, S.M., Walter, U., Durica, J., Schiltz, T.Z., Browner, M., Lowrence, C.B., Goldman, D., Ratoosh, S.L. and Richards, J.S.,

Molecular cloning, cDNA structure and regulation of the regulatory subunit (RII51) of type I cAMP-dependent protein kinase from rat granulosa cells, *J. Biol. Chem.*, 261 (1986) 12352–12361.

[21] Kahan, C., Seuwen, K., Meloche, S. and Pouyssegur, J., Coordinate, biphasic activation of p44 mitogen-activated protein kinase and S6 kinase by growth factors in hamster fibroblasts, *J. Biol. Chem.*, 267 (1992) 13369–13375.

[22] Kobayashi, N.R., Bedard, A.M. and Tetzlaff, W., Increased expression of trkB and BDNF mRNA in rat facial motoneurons after axotomy, *Soc. Neurosci. Abstr.*, 19 (1993) 110.10.

[23] Koliatsos, V., Clatterbuck, R.E., Winslow, J.W., Cayouette, M.H. and Price, D.L., Evidence that brain-derived neurotrophic factor is a trophic factor for motor neurons in vivo, *Neuron*, 10 (1993) 359–367.

[24] Kuno, T., Ono, Y., Hirai, M., Hashimoto, S., Shuntoh, H. and Tanaka, C., Molecular cloning and cDNA structure of the regulatory subunit of type I cAMP-dependent protein kinase from rat brain, *BBRC*, 146 (1987) 878–883.

[25] L'Allemain, G., Pouysségur, J. and Weber, M.J., p42/mitogen-activated protein kinase as a converging target for different growth factor signaling pathways: use of pertussis toxin as a discrimination factor, *Cell Regul.*, 2 (1991) 675–684.

[26] Loeb, D.M., Tsao, H., Cobb, M.H. and Greene, L.A., NGF and other growth factors induce an association between ERK1 and the NGF receptor, gp140^{protoTrk}, *Neuron*, 9 (1992) 1053–1065.

[27] Lonnerberg, P., Parvinen, M., Jahnsen, T., Hansson, V. and Persson, H., Stage- and cell-specific expression of cyclic adenosine 3',5'-monophosphate-dependent protein kinases in rat seminiferous epithelium, *Biol. Reprod.*, 46 (1992) 1057–1068.

[28] Massa, J., Fellow, R. and Maurer, R., Rat RIβ isoform of type I regulatory subunit of cyclic adenosine monophosphate-dependent protein kinase: cDNA sequence analysis, mRNA tissue specificity, and rat/mouse difference in expression in testis, *Mol. Reprod. Dev.*, 26 (1990) 129–133.

[29] Meloche, S., Pagés, G. and Pouysségur, J., Functional expression and growth factor activation of an epitope-tagged p44 mitogen-activated protein kinase, p44^{mapk}, *Mol. Biol. Cell*, 3 (1992) 63–71.

[30] Meloche, S., Seuwen, K., Pagés, G. and Pouysségur, J., Biphasic and synergistic activation of p44^{mapk} (ERK1) by growth factors: activation and mitogenicity, *Mol. Endo.*, 6 (1992) 845–854.

[31] Moodie, S.A., Willumsen, B.M., Weber, M.J. and Wolfman, A., Complexes of Ras·GTP with Raf-1 and mitogen-activated protein kinase kinase, *Science*, 260 (1993) 1658–1661.

[32] Peraldi, P., Scimeca, J.C., Filloux, C. and Van, O.E., Regulation of extracellular signal-regulated protein kinase-1 (ERK-1; pp44/mitogen-activated protein kinase) by epidermal growth factor and nerve growth factor in PC12 cells: implication of ERK1 inhibitory activities, *Endocrinology*, 132 (1993) 2578–85.

[33] Qiu, M.-S. and Green, S.H., PC12 cell neuronal differentiation is associated and consequent prolonged ERK activity, *Neuron*, 9 (1992) 705–717.

[34] Saika, T., Kiyama, H., Matsunaga, T. and Tohyama, M., Differential regulation of phospholipase C isozymes in the rat facial nucleus following axotomy, *Neuroscience*, 59 (1994) 121–129.

[35] Sandberg, M., Levy, F.O., Oyen, O., Hansson, V. and Jahnsen, T., Molecular cloning, cDNA structure and deduced amino acid sequence for the hormone-induced regulatory subunit (RII β) of cAMP-dependent protein kinase from rat ovarian granulosa cells, *BBRC*, 154 (1988) 705–711.

[36] Scott, D.J., Glaccum, M.B., Zoller, M.J., Uhler, M.D., Helfman, O.M., McNight, G.S. and Krebs, E.G., The molecular cloning of a type II regulatory subunit of the cAMP dependent protein kinase from rat skeltal muscle and mouse brain, *Proc. Natl. Acad. Sci. USA*, 84 (1987) 5192–5196.

[37] Scott, J.D., Cyclic nucleotide-dependent protein kinases, *Pharmacol. Ther.*, 50 (1991) 123–145.

[38] Sevetson, B.R., Kong, X., John, J. and Lawrence, C., Increasing cAMP attenuates activation of mitogen-activated protein kinase, *Proc. Natl. Acad. Sci. USA*, 90 (1993) 10305–10309.

[39] Thomas, S.M., DeMarco, M., D'Arcangelo, G., Halegoua, S. and Brugge, J.S., Ras is essential for nerve growth factor- and phorbol ester-induced tyrosine phosphorylation of MAP kinases, *Cell*, 68 (1992) 1031–1040.

[40] Traverse, S., Gomez, N., Paterson, H., Marshall, C. and Cohen, P., Sustained activation of the mitogen-activated protein (MAP) kinase cascade may be required for differentiation of PC12 cells. Comparison of the effects of nerve growth factor and epidermal growth factor, *Biochem. J.*, 288 (1992) 351–355.

[41] Verge, V.M.K., Merlio, J., Grondin, J., Ernfors, P., Persson, H., Riopelle, R.J., Hökfelt, T. and Richardson, P.M., Colocalization of NGF binding sites, trk mRNA, and low-affinity NGF receptor mRNA in primary sensory neurons: responses to injury and infusion of NGF, *J. Neurosci.*, 12 (1992) 4011–4022.

[42] Vouret, C.V., Van, O.S.E., Scimeca, J.C., Van, O.E. and Pouyssegur, J., Differential activation of p44^{mapk} (ERK1) by α-thrombin and thrombin-receptor peptide agonist, *Biochem. J.*, 289 (1993) 209–214.

[43] Wiemann, S., Voß, H., Kinzel, V. and Pyerin, W., Rat Cα catalytic subunit of the cAMP-dependent protein kinase: cDNA sequence and evidence that it is the only isoform expressed in myoblasts, *Biochem. Biophys. Acta*, 1089 (1991) 254–256.

[44] Wood, K.W., Sarnecki, C., Roberts, T.M. and Blenis, J., ras mediates nerve growth factor receptor modulation of three signal-transducing protein kinases: MAP kinase, Raf-1, and RSK, *Cell*, 68 (1992) 1041–50.

[45] Wu, J., Inhibition of the EGF-activated MAP kinase signaling pathway by adenosine 3',5'-monophosphate, *Science*, 262 (1993) 1065–1068.

Journal of Neurocytology **15**, 789–798 (1986)

Comparative dynamics of retrograde transport of nerve growth factor and horseradish peroxidase in rat lumbar dorsal root ganglia

HENRY K. YIP and EUGENE M. JOHNSON, JR

Department of Pharmacology, Washington University School of Medicine, St. Louis, Missouri 63110, USA

Received 14 May 1986; accepted 17 June 1986

Summary

The dynamics of the retrograde transport of [^{125}I] nerve growth factor (NGF) and horseradish peroxidase (HRP) in dorsal root ganglion (DRG) neurons were studied in rats. After injection of [^{125}I]NGF or HRP into crushed sciatic nerve, labelling was examined in spinal nerves, dorsal root ganglia, dorsal roots and spinal cord. Retrograde transport of either [^{125}I]NGF or HRP was first observed in DRG neurons 6 h after injection: The maximal rate of transport (7 mm h^{-1}) was similar for both proteins. Significant differences in the sizes of DRG neurons labelled by [^{125}I]NGF were observed and were dependent upon survival time. No such difference was seen in HRP-injected animals. At 6 h after injection, 60% of all the HRP-labelled cells had a diameter of more than 25 μm, whereas 90% of all the [^{125}I]NGF-labelled neurons had a diameter of less than 25 μm. With increasing survival times there was a gradual shift in the size of [^{125}I]NGF-labelled neurons towards larger diameters. Thus, 24 h after the [^{125}I]NGF injection, 83% of the labelled cells had a diameter greater than 25 μm. The data suggest that small diameter neurons retrogradely transport and turnover NGF faster than larger diameter neurons. There was a preferential accumulation of silver grains in small DRG neurons (mean diameter 25 μm) at early survival times (4 and 8 h); at the later survival time (24 h) the reverse was observed, i.e. larger neurons (mean diameter 42 μm) were labelled. In contrast, the mean diameter of HRP-labelled neurons remained constant (30 μm) at all times after injection. The total number of neurons ultimately labelled (~ 80–85%) appeared to be the same with both tracers. In addition, the lack of transganglionic transport of NGF into the spinal cord and the short time span of the observable accumulated radioactivity in DRG neurons suggest the rate of degradation of transported NGF seems to be faster than HRP. As a practical matter, these data indicate that observing cells within DRG which accumulate retrogradely transported [^{125}I]NGF at any one time gives an inaccurate picture of the size properties of cells capable of transporting the ligand.

Introduction

Neurons take up macromolecular substances at the nerve terminals and transport then intra-axonally in a retrograde direction (i.e. towards the cell body). Certain toxins and viruses were among the first molecules or particles for which such retrograde transport was demonstrated (Kristensson, 1975). The retrograde transport of horseradish peroxidase (HRP) has been an invaluable tool for tracing neuronal pathways in both central and peripheral nervous systems (Nauta *et al.*, 1974; LaVail, 1975). However, the physiological importance and mechanism of the retrograde transport of these exogenous macromolecular substances remain uncertain. It is a mechanism whereby the terminals of nerve fibres may sample and transport information from their local surroundings back to the perikarya. Thus, a retrograde axonal transport system fulfils the regulatory role of conveying chemical messages from end organs back to the innervating nerve cells (Cragg, 1970; Hendry & Iversen, 1973; Hamburger, 1975). Studies performed during the last decade with radiolabelled nerve growth factor (NGF) have provided strong evidence in favour of this hypothesis and, at the same time, have indicated that NGF is a trophic factor released by the target organs to be taken up selectively by the sympathetic and sensory nerve endings (see review by Thoenen & Barde, 1980).

The selectivity of the uptake and retrograde axonal transport of labelled NGF, in contrast to HRP, depends on the binding of NGF to specific receptors on the surface of the nerve terminals (Hendry, 1975; Stöckel *et al.*, 1975). Other protein molecules which share many similar physiochemical properties with NGF, but do not display any biological function on the sympathetic and sensory neurons, are not

0300-4864/86 $03.00 + .12

retrogradely transported to the cell bodies. The high selectivity and specificity of the NGF binding sites can also be demonstrated by the fact that a minor chemical modification of NGF molecules results in both a loss of biological activity and of NGF retrograde transport (Stöckel *et al.*, 1974). Moreover, not all macromolecules are transported in all neurons; for example, HRP is taken up and transported by almost all neurons, while NGF is taken up by sympathetic and sensory dorsal root ganglion (DRG) neurons but not by motor neurons.

It has been previously reported that, after injection of [^{125}I]NGF into the rat forepaw, the accumulation of retrogradely transported NGF in sensory neurons is observed in the population of large neurons (> 25 μm) in the DRG (Stöckel *et al.*, 1975). Since there is a heterogeneous population of neurons in the mammalian DRG which can be distinguished from each other by morphological (Parfianowicz *et al.*, 1971), histochemical (Kalina & Wolman, 1970) and biochemical (Harmar & Keen, 1981) characteristics, and since the small neurons (< 25 μm) have been shown to be responsive to NGF (Kessler & Black, 1980; Kornblum & Johnson, 1982) and to NGF deprivation (Johnson *et al.*, 1980), the failure to demonstrate retrograde transport of [^{125}I]NGF by small neurons is puzzling.

One of the objectives of the present study was to determine what population of DRG neurons retrogradely transport [^{125}I]NGF by comparing the number of neurons accumulating radiolabelled NGF to the number accumulating HRP injected similarly. In addition, we wished to determine if there were any differences in the time course of appearance or accumulation of [^{125}I]NGF or HRP within the heterogeneous populations of neurons in the sensory ganglia. This was accomplished by injecting [^{125}I]NGF or HRP into a crush site in the sciatic nerve. Previously, we have found that 85% of the neurons in the L5 DRG were retrogradely labelled by this protocol (Yip *et al.*, 1984) and that efficient receptor-mediated retrograde transport of [^{125}I]NGF was also observed from such a crush site (Yip & Johnson, 1983). The results show that all DRG neurons retrogradely transport [^{125}I]NGF; surprisingly, and in contrast to HRP, different sizes of DRG neurons have different time courses of appearance and accumulation of [^{125}I]NGF.

Methods and materials

PREPARATION OF [^{125}I]NGF

The 2.5S mouse NGF was prepared from submaxillary glands of adult male mice as described by Bocchini & Angeletti (1969). For radioiodination (Marchalonis, 1969), a mixture of NGF (10 μg), Na^{125}I (1 mCi, Amersham), hydrogen peroxide (0.08 M) and phosphate buffer (0.2 M, pH 6.8) to a total volume of 50 μl was incubated for 15 min at room temperature. A total of 150 μl of phosphate buffer (0.05 M, pH 7.5) with bovine serum albumin (0.2%) and protamine sulphate (0.1%) was then added and the mixture was dialysed overnight against two changes of 0.1 M phosphate buffer (pH 7.4). The efficiency of labelling was 70–90%; after dialysis, incorporation of greater than 96% was determined by thin layer chromatography. Final concentration of NGF was 25 ng μl^{-1} with specific activities of ~ 80 μCi μg^{-1}. Bioactivity of [^{125}I]NGF was verified by the accumulation of radioactivity in the ipsilateral superior cervical ganglia (SCG) of the rat after injection of 2 μl of radiolabelled NGF into the anterior eye chamber. Iodinated NGF was used within a week of preparation.

INJECTIONS

Sprague–Dawley rats weighing 250–300 g (Chappel, St. Louis) were anaesthetized with chloral hydrate (350 mg per 1000 g body weight). The sciatic nerve was exposed in midthigh and crushed with jeweller's forceps at the tendon of *obturator internus*. A total of 2 μl of [^{125}I]NGF or 30% aqueous HRP (Sigma VI) solution was injected into the crush site through a glass micropipette connected to a 10 μl Hamilton syringe.

DETERMINATION OF RADIOACTIVITY

Between 4 and 96 h after injection of [^{125}I]NGF, rats were anaesthetized and perfused with 10% formalin in phosphate buffer. The L5 DRG were dissected out and their gamma emission was determined in a Beckman γ-counter.

AUTORADIOGRAPHY

L5 DRG with attached stumps of spinal nerves, as well as dorsal roots and corresponding spinal cord segments, were postfixed, dehydrated and embedded in paraffin. Serial sections, 8 μm thick, were dewaxed and dipped in Kodak NTB-2 emulsion, then stored in desiccated, lightproof boxes for a week. The slides were developed with Kodak D-19 solution, stained with toluidine blue and mounted in Permount. Cells with more than seven grains (background level) over the cytoplasm were designated as labelled.

HRP HISTOCHEMISTRY

The rats were sacrificed after various survival times and fixed by transcardial perfusion with a mixture of 2.5% glutaraldehyde and 1% paraformaldehyde in 0.1 M sodium phosphate buffer at pH 7.4. Samples of L5 DRG with the attached spinal nerves and dorsal roots, as well as the L5 segments of the spinal cord, were postfixed in the same fixative for several hours, transferred into 0.1 M sodium phosphate buffer containing 30% sucrose and stored overnight at 4°C. Serial sections, 30 μm thick, were cut on a freezing microtome in longitudinal or transverse planes. HRP histochemistry was performed by using the tetramethylbenzidine procedure as described by Mesulam (1978). Sections were counterstained with 1% Neutral Red.

MORPHOMETRIC ANALYSIS

Cell counting

Cell number and size were determined from coded slides of three or four animals for each of the five time points studied (6, 8, 16, 24 and 96 h). The sample consisted of three separate histological sections, approximately five to seven sections apart, which were chosen to represent the maximum longitudinal sections of each ganglion. These sections were examined in the light microscope using brightfield and/or darkfield illumination for the presence of HRP-labelled or [^{125}I]NGF-labelled cells. These were counted at a magnification of × 200, no correction being made for double counting except for the omission of obvious offcuts (profiles < 5–6 μm in diameter). This might have resulted in slight over-estimation of total cell numbers, although, as most sections (longitudinal) were aligned with the shortest axis of the majority of cells, the error would be expected to be small (< 10%). Both the HRP-labelled or [^{125}I]NGF-labelled neurons and the remaining non-labelled neurons in the L5 DRG were counted. A minimum of 1000–1500 cells were counted in each ganglion for each injection time.

Cell size

Measurements of cell size were made on the same sections as the neuronal counts. Size measurements were made on all cell profiles that contained nuclei. Two methods were used to measure perikaryal diameters. For the initial screening (see Figs 2, 3), measurements were made through a light microscope equipped with an eyepiece micrometer at a magnification of × 200. The cell diameter was calculated as the mean of the longest axis and the axis perpendicular to it at its middle. Since sensory neurons within the DRG have been divided into two classes on the basis of perikaryal size (Lieberman, 1976; Lawson, 1979; Lawson & Nickels, 1980), neurons of less than 25 μm in diameter were defined as small cells and those with a diameter greater than 25 μm were defined as large cells. For more detailed analysis of cell size distribution (see Fig. 4), frequency histograms of mean diameters were generated by tracing the perikarya of all labelled neurons onto a sheet of paper with the use of a Zeiss Camera lucida attached to the microscope (final magnification × 470). The drawings of neuronal perikarya were then traced with a stylus onto a Summagraphics Tablet and entered into a PDP 11/44 computer. With computer analysis the cell size histograms were generated for each section, each ganglion and the entire neuronal sample studied (Yip *et al.*, 1984).

Results

Retrograde transport of [^{125}I]NGF in L5 DRG

The time course of accumulation of radioactivity in L5 DRG after injection of [^{125}I]NGF at the crush site is shown in Fig. 1A. No radioactivity was seen at 4 h, but then radioactivity appeared rapidly, reaching a maximum at 8 h. This time course is the same as we have seen in previous studies (Yip & Johnson, 1983). Radioactivity declined rapidly thereafter with a 90% reduction by 96 h. Light microscopic autoradiography of the L5 DRG of the injected side revealed that the increase in the total percentage of cells in the ganglion which were labelled correlated well with the increase in the radioactivity accumulated in the ganglia (Fig. 1B). No labelling (above background) had accumulated in the neuronal cell bodies of the ipsilateral DRG at 4 h after injection of [^{125}I]NGF into the crushed sciatic nerve. After 6 h, however, 28% of the cells in L5 DRG contained labelling. The majority (57%) of the neurons were labelled after 8 h. The percentage of labelled cells dropped sharply after 16 h and continued to decline through 24 h (Fig. 2A). By 96 h after injection, there was little labelling in L5 DRG.

A gradient of labelling in terms of neuronal size is observed over the 6 to 96 h time course. Examples of [^{125}I]NGF-labelled neurons of different sizes after 6 and 24 h are shown in Fig. 3. Small neurons are labelled first, followed progressively by larger neurons (Figs 2B, 3, 4A). Fig. 2A shows that radioactively labelled small neurons (< 25 μm) occur primarily after 6 and 8 h, with a maximum after 8 h followed by a sharp decline after 16 h and beyond. Heavy labelling of small cells (indicated by S) 6 h after the injection of [^{125}I]NGF is shown in Fig. 3A and B, while absence of labelling of large cells (indicated by L) is also seen. Concurrent with the decline of

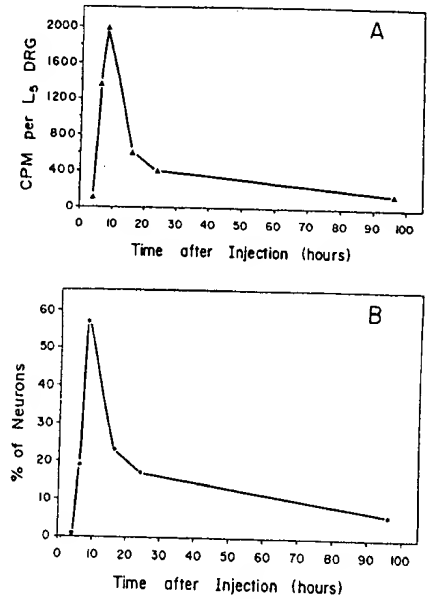

Fig. 1. Correlation between the amount of radioactivity accumulated in L5 DRG after injection of [^{125}I]NGF into a crushed sciatic nerve and the percentage of labelled cells in the same ganglion. (A) Amounts of radioactivity accumulated at various times after injections. (B) Percentage of labelled neurons at corresponding time points.

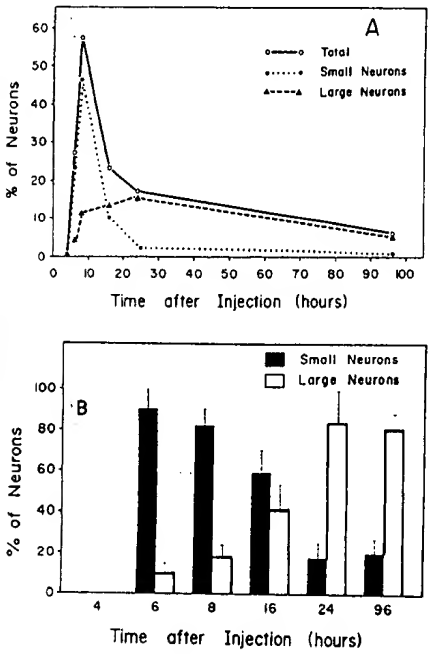

Fig. 2. Percentage of labelled neurons in L5 DRG at various times after injection of [^{125}I]NGF into a crushed sciatic nerve. (A) Percentage of labelled cells in the total population of neurons in L5 DRG. (B) Comparison between the percentage of labelled cells which were small (< 25 μm) or large (> 25 μm) at various times. Note a significant amount of small neurons are labelled at earlier time points than at later time points. The reverse is true for the large, labelled neurons.

heavily labelled small neurons after 8 h, an increase in both the intensity and percentage of labelling of large neurons occurs in the period between 8 and 24 h (Figs 2B, 3C, D, 4). There is, therefore, minimal overlap in the labelling of small and large cells in both early (6 and 8 h) and late (24 and 96 h) time points. At 16 h, similar percentages of both small (59%) and large (41%) neurons are labelled with [^{125}I]NGF (Fig. 2B).

The size distribution of the entire population of neurons was determined by a computer-assisted quantitative analysis of between 200 and 700 labelled neurons from three or four animals. The mean diameter of all [^{125}I]NGF-labelled cells after 6 and 24 h are plotted in 4-μm bins against frequency (Fig. 4A). At 6 h after [^{125}I]NGF injection there is a continuum of cell sizes extending over a range from 9 to 44 μm, with a mean diameter of 22 μm (Fig. 4). At 24 h after the injection, the size frequency spectrum is much broader with an upper boundary of cell size distribution of 48 μm and a mean diameter of [^{125}I]NGF-labelled neurons of 32 μm (Fig. 4). Examination of individual histograms at each time point studied (6, 8, 16, 24 and 96 h) demonstrated a gradual shift toward larger sizes (data not shown). There is also a progressive labelling shift from smaller to larger neurons labelled up to 24 h shown by plotting the mean neuronal size as a function of time after injection (Fig. 5). Thus, the temporal distribution of [^{125}I]NGF-labelled neurons in L5 DRG shows clear evidence for consistent gradients in selective sizes of these cells.

As early as 6 h after injection, rows of labelling were found distributed along the longitudinal sections of the nerve fibres within the sensory branches of the spinal nerves, indicating individual fibres containing high amounts of radioactivity. At no time during the course of the experiment was labelling observed in the dorsal roots, ventral roots, or within the spinal cord. A comparison of the localization and staining intensity of labelled structures after injection of [^{125}I]NGF or HRP into crushed sciatic nerves at different survival times is shown in Table 1.

Retrograde transport of HRP in L5 DRG

HRP labelling in L5 DRG is observed in 57% of all neurons after 6 h, 75% after 8 h, 87% after 18 and 24 h, and 57% after 96 h of administration (Fig. 6A). The time course of HRP-labelling in L5 DRG (Fig. 6A) shows that there is a sharp increase followed by a slow decrease of labelling in DRG neurons. This indicates that the HRP which accumulates in the cell body must require considerable time to be either transported out of or broken down by the perikarya.

In contrast to the selective retrograde labelling of DRG neurons by [^{125}I]NGF, there was no clear gradient of HRP labelling in terms of neuronal size in L5 DRG. The labelling of small neurons by HRP overlapped the labelling of large neurons in the 9–96 h period. Fig. 7 demonstrates some examples of HRP-labelled neurons after 6 and 24 h. There is no clear preference in the sequence of labelling of either small or large neurons. The percentage of HRP-labelled neurons greater or smaller than 25 μm does not change significantly at all time points examined (Fig. 6B). Thus, 6 h after the injection, 40% of the labelled cells were small and 60% of labelled cells were large. At 24 h, the percentages were 45 and 55% for small and large cells, respectively. An examination of the size distribution of cells labelled with HRP (approximately 10 000 neurons from a total of three or four animals) after 6 and 24 h does not indicate a shift (Fig. 4b). These histograms completely overlap each other. The mean diameter of labelled neurons was and 29 μm at 6 and 24 h, respectively. Clearly, bo

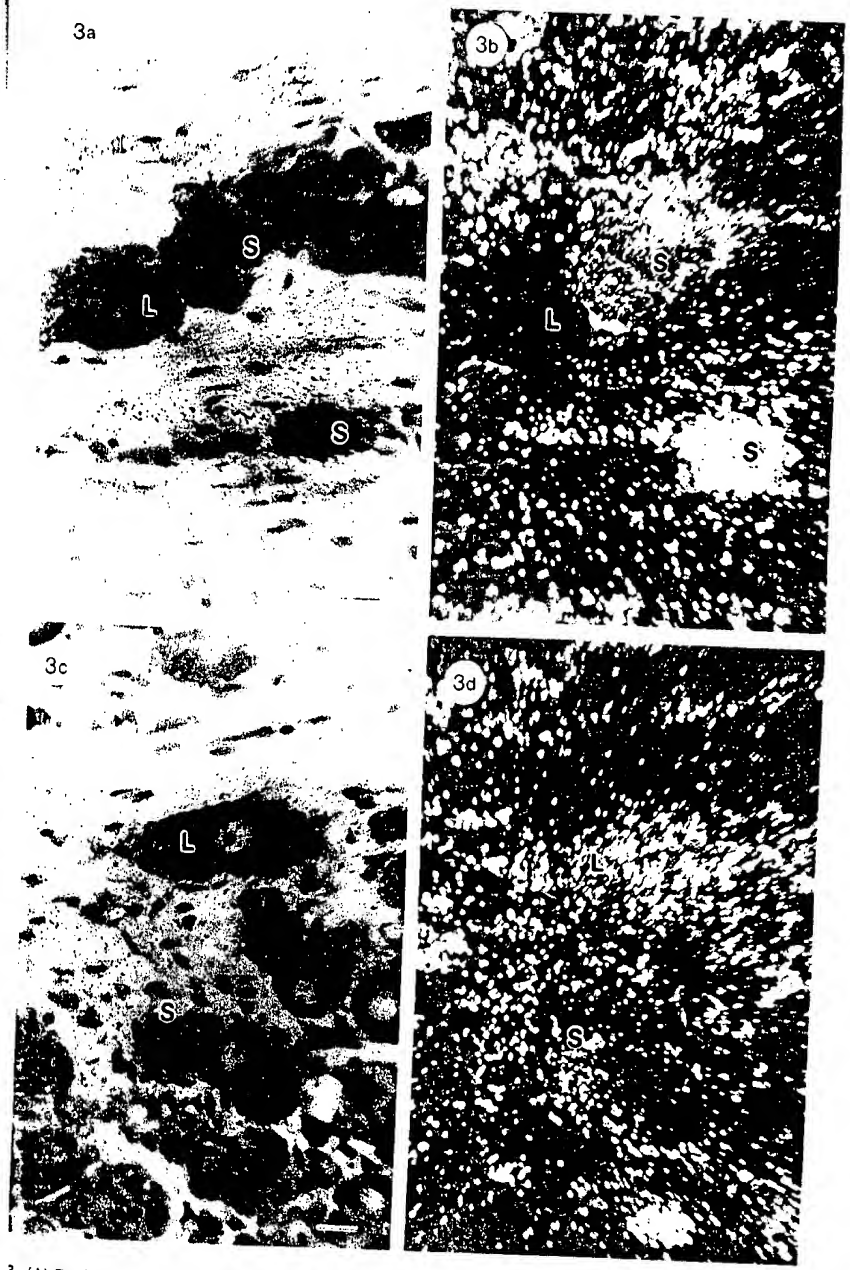

Fig. 3. (A) Brightfield autoradiograph of [^{125}I]NGF-labelled neurons 6 h after the injection which shows that small cells (indicated by S) are labelled and large cells (indicated by L) are not labelled. (B) Darkfield autoradiograph of the same section as in (A). (C) Brightfield autoradiograph of [^{125}I]NGF-labelled neurons 24 h after the injection which shows large cells also labelled. (D) Darkfield autoradiograph of the same section as in (C). Scale bars: 10 μm.

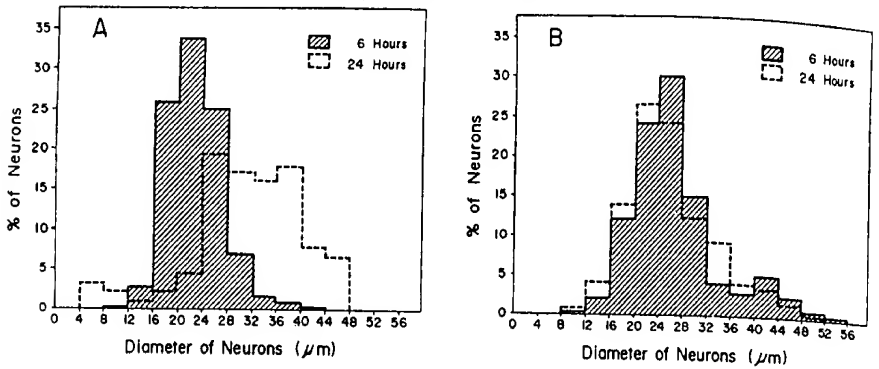

Fig. 4. (A) Histogram illustrating the size spectra of neuronal diameters in L5 DRG 6 h and 24 h after a [^{125}I]NGF injection into a crushed sciatic nerve. Note the histogram shifts to the right at 24 h which indicates an increase in the cell size of labelled neurons. (B) Histogram illustrating HRP injection into a crushed sciatic nerve. No shift in the histogram is observed in the HRP-injected ganglia.

Table 1. Comparison of differential labelling in L5 DRG with [^{125}I]NGF or HRP over time.

Survival time (h)	*Spinal nerve*	*Cell bodies DRG*	*Dorsal root*	*Ventral root*	*Axons or terminals in dorsal horn*	*Motor neuron cell bodies in ventral horn*
[^{125}I]NGF						
4	–	–	–	–	–	–
6	++	+	–	–	–	–
8	+++	+++	–	–	–	–
16	++	++	–	–	–	–
24	+	+	–	–	–	–
HRP						
4	–	–	–	–	–	–
6	+	+	–	–	–	–
8	++	++	–	–	–	–
16	+++	+++	+	+	+	++
24	+++	+++	++	++	+++	+++
96	+	++	+	+	++	+

– Indicates absence of labelling.
+ Indicates presence of labelling. Number of + represents the intensity of labelling: + means minimal but significant labelling; +++ means maximal labelling.

small and large neurons were equally well labelled after 6 and 24 h, respectively. Individual histograms of HRP-labelled neurons at each time point (6, 8, 16, 24 and 96 h) were remarkably similar to each other (data not shown), indicating that there was relatively little variability between time points. Further analysis of the relation of time of labelling to cell size shows that there is no change in the mean neuronal diameter over the period examined (Fig. 5).

At 4 h after the injection of HRP into the crushed sciatic nerve, no reaction product was observed in either dorsal and ventral roots or in any part of the corresponding spinal cord segments. At 8 h, labelled axons in the corresponding spinal nerves were seen. After 16 h, the intensity of the labelling was increased. Within the DRG, small neurons (10–25 μm) generally displayed a more intense labelling. However, some cells of this size were labelled rather

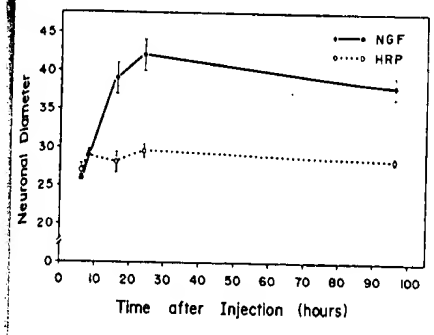

Fig. 5. The mean diameters of [^{125}I]NGF-labelled neurons and HRP-labelled neurons in L5 DRG at various times after the injection. Note the mean diameter of HRP-labelled neurons remains constant (30 μm) at all times after injection.

faintly, similar to larger neuronal cell bodies (25–45 μm). In addition to the increased labelling of DRG neuronal cell bodies and spinal nerve axons, a number of dorsal and ventral root axons showed traces of the label; labelling of the motor neurons was more distinct. The dorsal regions of the spinal cord did not show labelling until 16 h. At this time, labelling in Lissauer's tract and in the medial parts of the superficial laminae of the dorsal horn was evident. At 24 h after administration of HRP there was an intense labelling of DRG neurons and of their peripheral process, whereas a moderate staining was seen in axons of dorsal roots. Generally, the number of labelled fibres in the dorsal roots appeared definitely smaller than in the peripheral nerves and there was more reaction product in the peripheral than in the central process. At 24 h the majority of the dorsal and ventral root axons appeared labelled. Within the spinal cord, the number of labelled axons and terminals was increased in the first three laminae of the dorsal horn as well as in the tract of Lissauer. The motor neuron cell bodies and their dendrites and axons displayed a distinct labelling.

After a survival time of 96 h the number of labelled perikarya and axons in the DRG was significantly diminished; the intensity of the labelled structures was also decreased. Accordingly, fewer labelled fibres were observed in the dorsal roots and in spinal nerves. Labelling in the dorsal horn of the spinal cord was limited to the Lissauer's tract and the medial part of the dorsal horn. The intensity of labelling in motor neurons was also distinctly decreased. A summary of HRP-labelled structures at different survival times is shown in Table 1.

Discussion

The aim of the present study was, first, to determine whether the high selectivity of retrograde transport of NGF in sensory neurons is confined exclusively to a specific population of DRG neurons or is a property common to all neurons in the DRG. Second, we wished to compare the dynamics of retrograde transport and accumulation of NGF to HRP, a protein which has no biological effect but is, nevertheless, also retrogradely transported in sensory neurons.

Our results showed, in accordance with previous observations (Kristensson & Olsson, 1974; Yip &

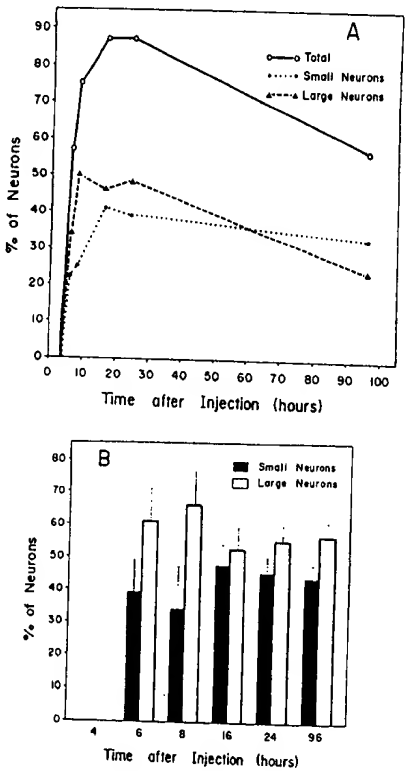

Fig. 6. Percentage of labelled neurons in L5 DRG at various times after injection of HRP into a crushed sciatic nerve. (A) Percentage of labelled cells in the total population of neurons in L5 DRG. (B) Comparison between the percentage of small (< 25 μm) labelled neurons and the percentage of large (> 25 μm) labelled neurons. There is no significant difference between the percentage of small labelled neurons and the percentage of large labelled neurons at all times observed.

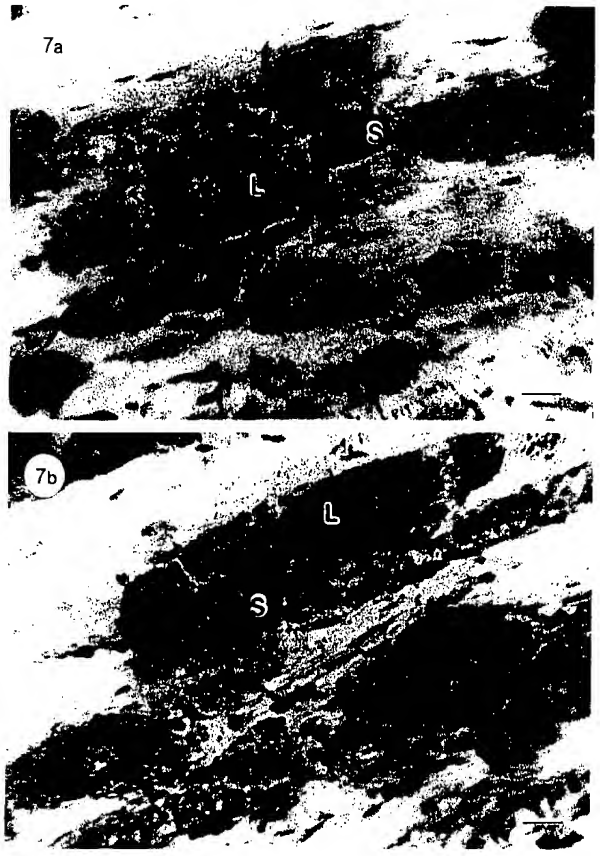

Fig. 7. Brightfield photomicrographs of HRP-positive labelled neurons at (A) 6 h and (B) 24 h after the injection. No observable difference in the labelling pattern of small (S) and large (L) neurons is demonstrated at either time point. Scale bars: 10 μm.

Johnson, 1983; Richardson & Riopelle, 1984), that application of either NGF or HRP to axotomized axons of peripheral nerves is followed by labelling of their perikarya. This suggests that much of the NGF or HRP is rapidly incorporated into organelles or bound to the receptors inside the crushed nerve. It is apparent from these experiments that the axon terminals are not essential for the uptake and retrograde transport of these macromolecules by peripheral nerves. This observation deserves some attention in the light of our previous finding which shows that uptake and retrograde transport of [^{125}I]NGF in axotomized sensory axons is specific and receptor-mediated (Yip & Johnson, 1983). It may, therefore, be suggested that NGF receptors are also present along the length of peripheral sensory axons or, alternatively, that NGF receptors are also retrogradely transported. In view of this observation and our recent observations (unpublished) which show that NGF receptors are retrogradely transported in sciatic nerves, the latter interpretation seems more likely. Previous experiments have shown that NGF is transported retrogradely and selectively accumulated in the population of large neurons in the DRG between 18 and 20 h after injection of [^{125}I]NGF into the forepaw (Stöckel *et al.*, 1975). Since it has been reported that retrograde transport of macromolecules can occur at several different rates (Kristensson *et al.*, 1971; Lubińska & Niemierko, 1971) and since it is known that the neurons of dorsal root ganglia are heterogeneous, it seemed possible that there is a difference in the labelling of neurons as a function of survival time. To test this hypothesis we studied the retrograde transport of [^{125}I]NGF in DRG neurons at various times after injection into crushed sciatic nerves. We found that the uptake and transport of NGF by DRG neurons (~ 4.5 cm from the crush site) proceeded generally in three phases that were dependent upon different survival times. (1) NGF was accumulated almost entirely (90%) in small neurons (25 μm or less) 6 and 8 h after the injection. (2) At 16 h after the injection of NGF into the crushed sciatic nerves, a more even distribution of large and small neurons contained NGF. (3) Subsequently, at 24 h after the injection, NGF was observed predominantly (83%) in large neurons (> 25 μm) and concomittantly there was a drastic decrease in the number of labelled small cells that were observed. The mean diameter of NGF-labelled neurons increased with longer survival time (from 22 μm at 6 h to 42 μm at 24 h). These results suggest that DRG neurons of different sizes transport or turnover [^{125}I]NGF at different rates. Ultimately, a similar percentage (~ 80%) of all cells in DRG at some time became labelled by both[^{125}I]NGF and HRP. This result is consistent with the observation that NGF deprivation during foetal development results in the death of the vast majority of DRG neurons and that the neurons are lost throughout the whole size spectrum (Johnson *et al.*, 1980). It remains to be seen whether the diversity in the NGF transport of different neurons is caused by varying transport capacities, by modified uptake rates of NGF at the crush site, by different turnover rates within the neuronal soma, or by some combination of these factors. There did not appear to be such a time-selective labelling of DRG with HRP. In our experiments, no clear trend of differential labelling of DRG neurons of different sizes by HRP was demonstrated. The mean diameter of HRP-labelled neurons (~ 30 μm) during the whole time course did not change. In general, small perikarya showed more intense labelling at an earlier stage than large perikarya. Similar observations have been demonstrated previously (Kristensson & Olsson, 1975; Grant *et al.*, 1979). This is probably because of a difference in the concentration of HRP accumulated in the small and large neurons. This finding, however, does not indicate that the small neurons are preferentially labelled at earlier survival times.

The concentration of tracer products observed in the DRG neuronal perikarya, at any of the time intervals, must reflect a balance of the rate of uptake of marker at the periphery, its rate of transport toward the cell body, its rate of degradation, and its possible anterograde transport back along the axons from the cell body. Therefore, the difference in labelling of neurons by different markers may be attributed to one or more of the factors mentioned. Labelling of perikarya of L5 DRG first appeared 6 h after injection of either [^{125}I]NGF or HRP to the sciatic nerve at the same distance (crushed at the tendon of *obturator internus*) to the ganglion. Thus, the fastest retrograde transport of [^{125}I]NGF and HRP occurred at a similar rate (~ 7.5 mm h^{-1}). However, the time span of the accumulated HRP in the neurons was much longer than that of [^{125}I]NGF. Transganglionic transport of HRP was observed in the dorsal horn. Similar findings have been reported in primary sensory neurons in rats (Grant *et al.*, 1979). There was no such labelling in the dorsal spinal cord after injection of [^{125}I]NGF. Since the apparent rate of degradation of the transported NGF seemed to be faster than HRP, this may contribute to the lack of transganglionic movement of NGF. Alternatively, the difference may result from a qualitative difference in the processing of ligands bound to the NGF receptors compared to agents transported by non-receptor-mediated processes.

In summary, this study has shown that different populations (in terms of sizes) of DRG neurons were retrogradely labelled by [^{125}I]NGF at different survival times. No such differences were seen in the labelling of neurons after injection of HRP. HRP also labelled motor neurons in the ventral horn and central terminals of DRG neurons by transganglionic transport. No transganglionic transport of [^{125}I]NGF was observed. The total number of DRG neurons which became labelled at some time with [^{125}I]NGF appeared to be the same as the number which became labelled by HRP, indicating that all DRG neurons retrogradely transport NGF. As a practical matter, in which retrograde labelling is used to define populations of neurons bearing NGF receptors, it is clear that observing retrogradely labelled DRG neurons at any given time after [^{125}I]NGF injection is not representative of the whole population of neurons capable of such transport. Whether this will be ultimately shown to be a consistent difference between specific 'receptor-mediated' transport and 'non-specific' transport is not known.

Acknowledgements

The authors thank Ms Patricia Lampe, Ms Patricia Osborne and Dr Arthur D. Loewy for their excellent assistance. We also thank Dr David McDougal for his helpful suggestions. This work was supported by NIH grants HL 20604 and NS 18071.

References

BOCCHINI, F & ANGELETTI, P. U. (1969) The nerve growth factor: purification as a 30,000 molecular weight protein. *Proceedings of National Academy of Sciences USA* **64**, 787–94.

CRAGG, B. G. (1970) What is the signal for chromatolysis? *Brain Research* **23**, 1–21.

GRANT, G., ARVIDSSON, J., ROBERTSON, B. & YGGE, J. (1979) Transganglionic transport of horseradish peroxidase in primary sensory neurons. *Neuroscience Letters* **12**, 23–8.

HAMBURGER, V. (1975) Cell death in the development of the lateral motor column of the chick embryo. *Journal of Comparative Neurology* **160**, 535–46.

HARMAR, A. J. & KEEN, P. (1981) Peptide biosynthesis in sensory ganglia. In *Neuropeptides: Basic and Clinical Aspects* (edited by FINK, G. & WHALLEY, L. J.), pp. 259–71. Edinburgh: Churchill Livingstone.

HENDRY, I. A. (1975) The retrograde axonal transport of nerve growth factor. *Brain Research* **94**, 87–97.

HENDRY, I. A. & IVERSEN, L. L. (1973) Changes in tissue and plasma concentration of nerve growth factor following removal of submaxillary glands in adult mice and the effects on the sympathetic nervous system. *Nature* **243**, 500–4.

JOHNSON, E. M., GORIN, P. D., BRANDIES, L. D. & PEARSON, J. (1980) Dorsal root ganglion neurons are destroyed by exposure *in utero* to maternal antibody to nerve growth factor. *Science* **210**, 916–18.

KALINA, M. & WOLMAN, M. (1970) Correlative histochemical and morphological study on the maturation of sensory ganglion cells in the rat. *Histochemie* **22**, 100–8.

KESSLER, J. A. & BLACK, I. B. (1980) Nerve growth factor stimulates the development of substance P in sensory ganglia. *Proceedings of the National Academy of Sciences USA* **77**, 649–52.

KORNBLUM, H. I. & JOHNSON, E. M., Jr (1982) Time and dose dependence of effects of nerve growth factor on sympathetic and sensory neurons in neonatal rats. *Brain Research* **234**, 41–51.

KRISTENSSON, K. (1975) Retrograde axonal transport of protein tracers. In *The Use of Axonal Transport for Studies of Neuronal Connectivity* (edited by COWAN, W. M. & CUÉNOD, M.), pp. 69–82. Amsterdam: Elsevier.

KRISTENSSON, K. & OLSSON, Y. (1974) Retrograde transport of horseradish peroxidase in transected axons. I. Time relationships between transport and induction of chromatolysis. *Brain Research* **79**, 101–10.

KRISTENSSON, K. & OLSSON, Y. (1975) Retrograde transport of horseradish peroxidase in transected axon. II. Relationship between rate of transfer from the site of injury to the perikaryon and onset of chromatolysis. *Journal of Neurocytology* **4**, 653–61.

KRISTENSSON, K., OLSSON, Y. & SJÖSTRAUD, J. (1971) Axonal uptake and retrograde transport of exogenous proteins in the hypoglossal nerve. *Brain Research* **32**, 399–406.

LaVAIL, J. H. (1975) The retrograde transport method. *Federation Proceedings* **34**, 1618–24.

LAWSON, S. N. (1979) The postnatal development of large light and small dark neurons in the mouse dorsal root ganglia: a statistical analysis of cell number and sign. *Journal of Neurocytology* **8**, 275–94.

LAWSON, S. N. & NICKELS, S. M. (1980) The use of morphometric techniques to analyze the effect of neonatal capsaicin treatment on rat dorsal root ganglia and dorsal roots. *Journal of Physiology* **303**, 12P.

LIEBERMAN, A. R. (1976) Sensory ganglia. In *The Peripheral Nerve* (edited by LANDON, D. N.), pp. 188–278, London: Chapman and Hall.

LUBÍNSKA, L. & NIEMIERKO, S. (1971) Velocity and intensity of bidirectional migration of AChE in transected nerves. *Brain Research* **27**, 329–42.

MARCHALONIS, J. J. (1969) An enzyme method for the trace iodination of immunoglobulins and other proteins. *Biochemical Journal* **113**, 229–305.

MESULAM, M. M. (1978) Tetramethylbenzidine for horseradish peroxidase neurochemistry. A non-carcinogenic blue reaction product with superior sensitivity for visualizing neural afferent and efferents. *Journal of Histochemistry and Cytochemistry* **26**, 106–17.

NAUTA, H. J. W., PRITZ, M. B. & LASEK, R. J. (1974) Afferents to the cat caudoputamen studied with horseradish peroxidase. An evaluation of a retrograde neuroanatomical research method. *Brain Research* **67**, 219–38.

PARFIANOWICZ, J., HAWRYLKO, S., PIETRZAK, J. & KMIEC, B. (1971) Morphology and cytochemistry of the nerve cells of the spinal ganglia. *Folia Morphologica* (Warsaw) **30**, 423–31.

RICHARDSON, P. M. & RIOPELLE, R. J. (1984) Uptake of nerve growth factor along peripheral and spinal axons of primary sensory neurons. *Journal of Neuroscience* **4**, 1683–9.

STÖCKEL, K., PARAVICINI, U. & THOENEN, H. (1974) Specificity of the retrograde axonal transport of nerve growth factor. *Brain Research* **76**, 413–21.

STÖCKEL, K., SCHWAB, M. E. & THOENEN, H. (1975) Specificity of retrograde transport of nerve growth factor (NGF) in sensory neurons: a biochemical and morphological study. *Brain Research* **89**, 1–14.

THOENEN, H. & BARDE, Y.-A. (1980) Physiology of nerve growth factor. *Physiological Review* **60**, 1285–335.

YIP, H. K. & JOHNSON, E. M., Jr (1983) Retrograde transport of nerve growth factor in lesioned goldfish retinal ganglion cells. *Journal of Neuroscience* **3**, 2172–82.

YIP, H. K., RICH, K. M., LAMPE, P. A. & JOHNSON, E. M., Jr (1984) The effects of nerve growth factor and its antiserum on the postnatal development and survival after injury of sensory neurons in rat dorsal root ganglia. *Journal of Neuroscience* **4**, 2986–92.

Journal of Neurocytology **15**, 799–815 (1986)

Distribution of the adhesion molecules N-CAM and L1 on peripheral neurons and glia in adult rats

RHONA MIRSKY[1], KRISTJÁN R. JESSEN[1], MELITTA SCHACHNER[2] and CHRISTO GORIDIS[3]

[1]*Department of Anatomy and Embryology, University College London, Gower Street, London WC1E 6BT, UK*
[2]*Department of Neurobiology, University of Heidelberg, Im Neuenheimer Feld 504, 6900, Heidelberg, FRG*
[3]*Centre d'Immunologie, INSERM–CNRS de Marseille-Luminy, 13288 Marseille Cedex 9, France*

Received 29 April 1986; revised 2 June 1986; accepted 9 June 1986

Summary

There is considerable evidence that the cell surface glycoproteins N-CAM and L1 are important mediators of cell–cell adhesion in the nervous system, at least during development. Numerous studies have been devoted to the molecular properties of these proteins and their adhesion role in embryonic and early postnatal development. Much less is known about their importance in mature tissues. A rigorous and comprehensive description of the cell distribution of these molecules in the adult nervous system would clearly form a useful baseline for functional and biochemical studies. In the present work we have addressed this issue and studied the distribution of N-CAM and L1 throughout adult, as opposed to developing, rat peripheral nervous tissue. Particular attention was paid to the ganglia of the enteric nervous system, since adhesion mechanisms within these ganglia are likely to be placed under unusual demands.

We report, for the first time, the presence of N-CAM and L1 on mature sensory, sympathetic and enteric neurons in adult rats. Thus, immunostaining of cell suspensions or short-term cultures showed N-CAM and L1 surface labelling on sympathetic and both large and small dorsal root sensory neurons. Both antigens were also present on the surface of enteric neurons in cultures prepared from 10-day-old rats and neonatal guinea pigs. Immunostaining of sections of enteric ganglia from adults indicated that both molecules were also expressed by mature enteric neurons. In sections of mature sciatic nerve neither N-CAM nor L1 immunoreactivity were detected at the site where the plasma membrane of myelinated axons meets the ad-axonal plasma membrane of the myelin-forming Schwann cell. Thus, both N-CAM and L1 were detected on all major classes of peripheral neurons, while their levels in the plasma membrane of myelinated axons may be significantly down-regulated.

Similarly, both N-CAM and L1 were present on all major classes of non-myelin-forming peripheral glia in adult rats. This includes the enteric glial cells of the myenteric ganglia, non-myelin-forming Schwann cells in the sciatic nerve, sympathetic trunk and fine autonomic nerves in the gut wall, and the satellite glial cells of sympathetic and dorsal root sensory ganglia. In contrast, myelin-forming Schwann cells did not express detectable levels of N-CAM and only very low levels of L1, which was mainly located near the nodes of Ranvier.

On the basis of these findings the prediction would be that, with the exception of myelinated fibres, N-CAM and L1 operate in parallel to link neurons and glia throughout the adult rat PNS. It remains to be seen whether myenteric ganglia, a part of the nervous system exposed to an unusual degree of mechanical stress, possess additional adhesive mechanisms. Myelin-forming Schwann cells appear to differ from other peripheral glia in their adhesive interactions with neuronal membranes since they do not express detectable levels of N-CAM and and show only low levels of L1.

Introduction

The evidence that the membrane glycoproteins N-CAM and L1 play a crucial role in the mechanical adhesion between neural cells derives from many biochemical, immunochemical and immunohistochemical studies, the majority of which have focused on embryonic or early postnatal tissue (e.g. Goridis *et al.*, 1983; Lindner *et al.*, 1983; Edelman, 1984; Rutishauser, 1984). Much less is known about their functional importance in the adult nervous system. Interestingly, recent studies suggest that the N-CAM present in mature tissues is more adhesive than the N-CAM present in early development, indicating that these adhesion molecules may be at least as important in adult animals (Edelman, 1985; Rutishauser *et al.*, 1985). A rigorous and comprehensive description of the localization of these molecules on different cell types in the adult nervous system would clearly form a useful baseline for further biochemical and functional studies. In this paper we have addressed this issue by studying the distribution of N-CAM and L1

0300-4864/86 $03.00 + .12